Examensarbete
Civilingenjörsprogrammet i energisystem

Torrefaction of biomass

– a comparative and kinetic study of thermal decomposition for Norway spruce stump, poplar and fuel tree chips

Xun Luo

SLU, Institutionen för energi och teknik
Swedish University of Agricultural Sciences
Department of Energy and Technology

Examensarbete 2011:09
ISSN 1654-9392
Uppsala 2011

SLU, Swedish University of Agricultural Sciences
Faculty of Natural Resources and Agricultural Sciences
Department of Energy and Technology

Xun Luo

Torrefaction of biomass – a comparative and kinetic study of thermal decomposition for Norway spruce stump, poplar and fuel tree chips

Supervisor: Khanh-Quang Tran, Department of Energy and Technology, SLU
Assistant examiner: Raida Jirjis, Department of Energy and Technology, SLU
Examiner: Tord Johansson, Department of Energy and Technology, SLU
EX0269, Degree project, 30 credits, Technology, Advanced E
Master Programme in Energy Systems Engineering (Civilingenjörsprogrammet i energisystem)

Examensarbete (Institutionen för energi och teknik, SLU)
ISSN 1654-9392
2011:09

Uppsala 2011

Keywords: torrefaction, biomass, poplar, Fuel Tree Chips (FTC), stump, heating value, grindability, Kinetic study, activation energy, pre-exponential factor, reaction order, Scanning Electric Microscope(SEM)

Online publication: http://stud.epsilon.slu.se

Cover: Lab view of the experimental set-up for biomass torrefaction, photo by author.

Abstract

Stump biomass is energy rich and stump harvesting for use as fuel become more and more interesting in Sweden. Swedish Forest Agency (2009) has estimated that stump harvesting in Sweden would respond to an annual energy supply of 57 TWh/year. However, stump has not been recognized as a bioenergy resource in Sweden. Suitable methods for pre-treatment of stump are probably of great importance to make it accepted as fuel. It is therefore rewarding to carry out an investigation in this area for stump.

This report represents results from a diploma project, which was aimed to develop a fixed bed reactor for experimental study of biomass torrefaction, followed by TG analysis and kinetic modelling employing Ozawa method and different kinetic models including one-step and three-pseudo-component models. The focus was on Norway spruce stump. Two other types of biomass, poplar and fuel tree chips were also included in the study for comparison.

The study has demonstrated that fuel properties, including heating values and grindability of the investigated biomasses, were improved by torrefaction. The heating rate affects the thermal decomposition process. In addition, SEM analysis indicated that the wood surface structure was broken and destroyed by torrefaction process. Activation energy of untreated and torrefied biomass were determined, being in good agreement with data in the literature. Among the kinetic models tested, three-pseudo-components model with reaction order $n \neq 1$ appears to be the best for simulating pyrolysis of untreated and torrefied biomass.

Sammanfattning

Biomassa, som är en förnyelsebar energikälla, är CO_2-neutral. Till en viss del kan fossila bränslen ersättas med denna energikälla och därmed minska CO_2-utsläppen. Bränslen från biomassa har dock, jämfört med fossila bränslen, lägre bränslekvalitetsegenskaper såsom t.ex. högre fukthalt, lägre värmevärde och sämre sönderdelningsbarhet. För att förbättra kvalitetsegenskaperna på rå biomassa kan torrefiering användas som en förbehandlingsteknik. Torrefiering är en termisk nedbrytningsprocess och kallas också för en mild pyrolysprocess, vilket innebär att reaktionstemperaturen är relativt låg (från 200^{o}C till 300^{o}C) under den ca 30 minuter långa reaktionstiden, som sker under inert atmosfär. Torrefieringsprocessen förbättrar den råa biomassans kvalitet, minskar kostnaderna för transporter av biomassa samt gör det enklare att lagra biomassa under längre tidsperioder.

Stubbar är energirika och intresset för att använda dessa som bränsle har ökat under senare år. Skogsstyrelsen (2009) har uppskattat att stubbskörd skulle kunna ge en årlig energitillförsel på 20,7 TWh då hänsyn även tas för gällande miljörestriktionen och ekonomiska intressen. Tyvärr har stubbar ännu inte erkänts som en bioenergiresurs pga att miljökonsekvenserna med storskalig stubbskörd inte är fastställda. Ur ett bränslekvalitetsperspektiv är lämpliga metoder för förbehandling av stubbar av stor betydelse för att öka acceptansen, då kvaliteten på detta sortiment är mycket varierande. På grund av detta är det givande att genomföra en undersökning inom detta område för stubbar.

I detta examensarbete presenteras resultat som syftar till utveckling av en fastbäddsreaktor för experimentell studie av torrefiering av biomassa. Den torrefierade biomassan har därefter även studerats genom, termogravimetrisk (TG) analys, kinetisk modellering med Ozawa metod och olika kinetiska modeller såsom one-step och three-pseudo-component modeller. Huvuddelen av biomassaproverna utgjordes av granstubbar (Norway spruce), men även två andra typer av biomassa, stamved av poppel och bränsle av träflis har studerats.

Studien har visat att bränslets egenskaper, inklusive värmevärde och sönderdelningsbarhet, hos de undersökta biomassorna har förbättrats genom torrefieringsprocessen. Det visades också att uppvärmningshastigeten påverkar den termiska nedbrytningsprocessen. Dessutom visade SEM-analys att ytstrukturen på trä bröts och förstördes av torrefieringsprocessen. Aktiveringsenergi av obehandlad och torrefierad biomassa bestämdes vilken väl stämde överens med data från litteraturen. Efter tester med olika kinetiska modeller, visade det sig att three-pesudo-components modellen med reaktionsordning $n \neq 1$ ger bäst resultat för simulering av pyrolys av obehandlad och torrefierad biomassa.

Nomenclature

P Poplar	FTC Fuel Tree Chips
S spruce stump	MC Moister content (%)
AC Ash content (%)	HV Heating Value (MJ/kg)
$E_{torrefied}$ the Energy of torrefied biomass	$E_{untreated}$ Energy of untreated biomass
$m_{torrefied}$ the mass of torrefied biomass	$m_{untreated}$ the initial mass of untreated biomass
E_d Energy desification	
TGA Thermogravimetric analyzer	SEM scanning electric microscope

TGA-curve: the thermogravimetric analysis which presents the change of conversion with temperature

DTG-curve: the derivative thermogravimetic analysis which presents the decomposition rate during pyrolysis

Ea activation energy (kJ/mol)	A pre-exponential factor (s^{-1})
α conversion	β heating rate(K/s)
M_i the initial mass	M_∞ the residual mass
M_t the mass of the sample at time t	n reaction order
R gas constant (8.314 J/mol/K)	T temperature (K or ^oC)
t time (s)	C dimensionless factor

Contents

1 Introduction

The use of biomass for heat and power generation contribute is CO_2-neutral, considering that CO_2 emission from combustion of biomass is just equal to that taken up by the plant during its growing. However, biomass fuel has inferior fuel properties, including for example low bulk density, high moisture content and low heating value compared to fossil fuels. These make bioenergy alternative technically difficult and economically less competitive. It is therefore a common practice to apply pre-treatment for biomass fuel.

According to the report made by Erik A. (2010) [8] the use of Norway spruce stump as fuel resource become more and more interesting in Sweden. It was reported that stump is energy rich and the Swedish Forest Agency (2009) has estimated that stump harvesting would respond to an annual energy supply of 57 TWh/year in Sweden. However, stump has not been recognized as a bioenergy resource. Suitable methods for pre-treatment of stump are probably of great importance to make it accepted as fuel. It is therefore rewarding to carry out an investigation in this area for stump.

This project was aimed to develop a fixed bed reactor for experimental study of biomass torrefaction, followed by thermogravity analysis and kinetic modelling. The focus was on Norway spruce stump. Two other types of biomass, poplar and Fuel Tree Chips (logging residues) were also included in the study for comparison. Poplar sample was taken from Helendala in southern Sweden [10]. Fuel Tree Chips (FTC) were received from Vattenfall AB which collected from the local Swedish sawmill industry and paper industry. The FTC was fresh and consisted of different types of clean chips with dimension of 20x40x3 (mm) approximately. [11]

2. Background

2.1 Biomass fuel

Using renewable energy resources is increasingly necessary to solve the world energy demand and reduce the greenhouse emission. Biomass as one of the renewable energy resources can be utilized as fuel for energy production. Currently, the definition of biomass fuel is very broad, but usually the major type of biomass fuel could consider as forest biomass, residues of the forest industries, recycled wood, energy crops.

Hemicelluloses, celluloses and lignin are the main components of lignocellulosic plant biomass. Hemicelluloses are formed by chain of mono-sugars, mainly xylose and comprise 25% to 35% of the dry weight of plant biomass [8,12]. Cellulose is a polymer composed of glucose chain and constitutes about 40% to 50% of woody plant mass [8,12]. Lignin is a phenylpropane polymer that gives a very strong strength to hold together the cellulose and hemicelluloses components of woody biomass. It makes up 15% to 25% of the weight of wood biomass. [8,12]

Compared with coal, untreated biomass fuels have high moisture contents, relatively low heating values, inhomogeneous and relatively low bulk density, and poor grindability. Due to these inferior fuel properties, using raw woody biomass material as a fuel entails many problems for combustion and gasification. During gasification for example hemicelluloses in biomass produces tar which may consequently poison catalyst used for Fischer-Tropsch (FT) synthesis of liquid fuel. In addition, the low bulk density of biomass makes it expensive to transport and difficult to feed into utilisation system, considering the level of atomization of the hydraulic feeding systems. For these reasons, pre-treatments are usually applied for biomass in order to improve its fuel properties for combustion and co-firing with coal. Torrefaction is one of emerging technology for this purpose, which is believed to have a high level of feasibility, both technically and economically.[14-17]

2.2 Biomass torrefaction for energy application

Torrefaction is a thermochemical treatment of biomass and may be defined as a mild pyrolysis process, which involves heating of the feedstock at moderate temperatures under an

inert atmosphere [2,3]. Figure 1 shows a typical torrefaction batch process. The total torrefaction process consists of drying, torrefaction and cooling. At beginning of the process the moisture in the biomass is released by drying. When the temperature of biomass ranges between 200^{o}C to 300^{o}C, only in this temperature range, the torrefaction decomposition reactions occur.

Three time temperature phases are recognised in torrefaction window. The reaction time of torrefaction is defined as the sum of heating time from 200^{o}C to desired temperature plus reaction time /holding time at desired torrefaction temperature ($t_{tor,h}$ + t_{tor}) and the duration of the torrefaction stage is around 30 minutes. After torrefaction, the last stage is cooling the biomass from 200^{o}C to the ambient temperature.

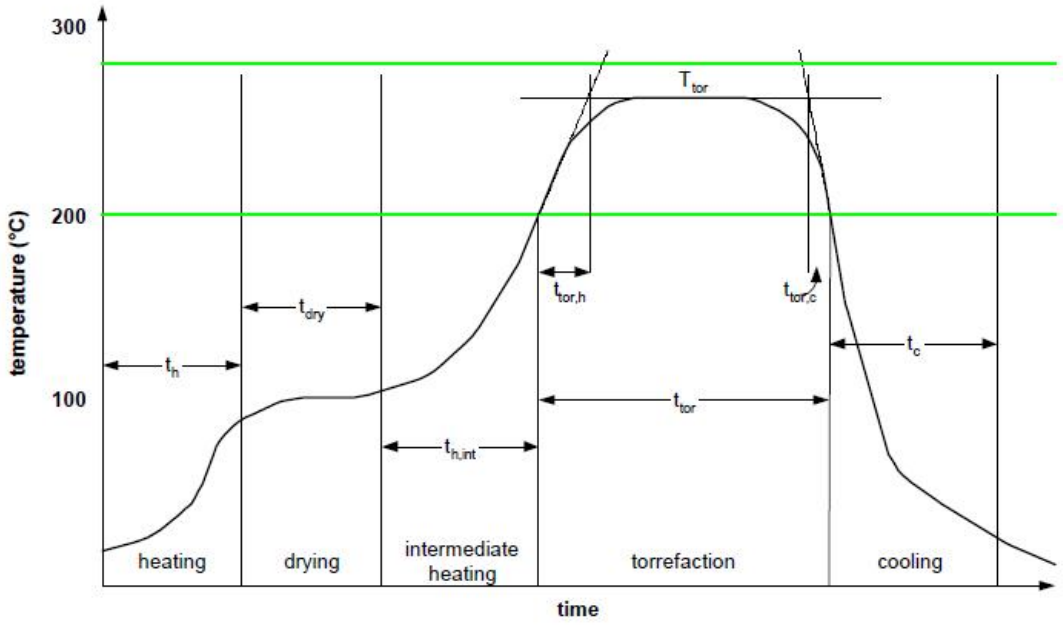

Figure 1: Heating stage of drying biomass during a typical torrefaction batch process.[2]

Explanation: T_{tor}: Torrefaction temperature. t_h: heating time to drying. t_{dry}: drying time. $t_{h.int}$: intermediate heating time to torrefaction. t_{tor} : Reaction time/holding time at desired torrefaction temperature (T_{tor}). $t_{tor.h}$: Heating time from 200^{o}C to desired temperature T_{tor}. $t_{tor.c}$: Cooling time from T_{tor} to 200^{o}C. t_c: cooling time to ambient temperature.

Figure 2 shows a decomposition regime of biomass torrefaction [2,3]. During torrefaction of lignocellulosic biomass, mainly hemicelluloses are decomposed, corresponding to the scarlet colour and orange colour regions. Lignin and cellulose may also be partly decomposed at

relatively higher temperatures within the temperature range for biomass torrefaction, but to a less degree as showed in Figure 2.

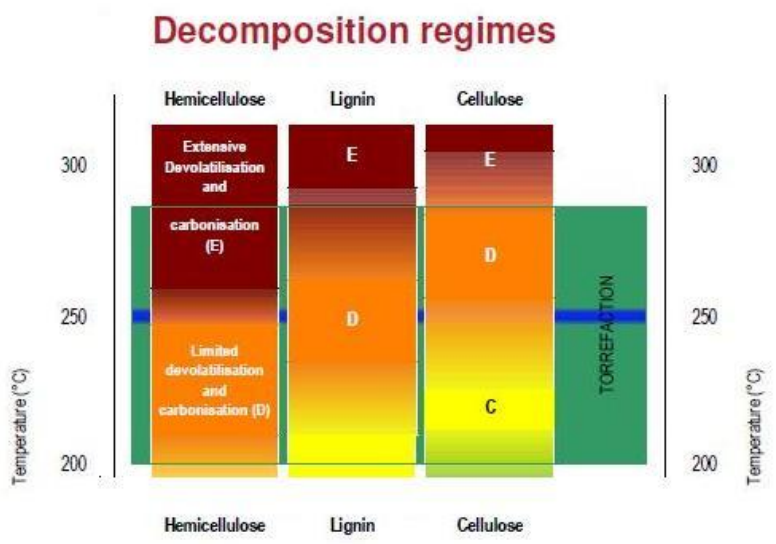

Figure 2: Decomposition regimes are based on Koukios et, Al. 1982 [4]. The Scarlet colour region (E): carbonisation and extensive devolatilization. The orange colour region (D): limited devolatilization and carbonisation. The yellow colour region(C): depolymerisation commences

Similar to pyrolysis, the chemical structure of plant biomass is changed during the torrefaction. Biomass torrefaction results in products found in three phases: solid, liquid, and gas. The solid is the main product of biomass torrefaction and also called torrefied biomass which has very low moisture contents and high caloric values. By cooling the exhaust gas from biomass torrefaction, liquid of yellowish colour is obtained from condensable gases. Non-condensable gases leave the process in the gas phase, which include carbon monoxide, carbon dioxide and little amount of methane.[2-4]

Figure 3 explains the concept of energy densification of biomass fuel by torrefaction. [2] Typically, 70% of the feed mass is retained after torrefaction as solid products (torrefied biomass) which contained 90% of initial energy. The rest of 30% of the feed mass is converted to the gas products, but the energy contains only 10% of the initial energy. The energy densification E_d could be used to prove the energy density of torrefied solid product is

increased by torrefaction; in this case the energy density of torrefied biomass increases by factor 1.3.

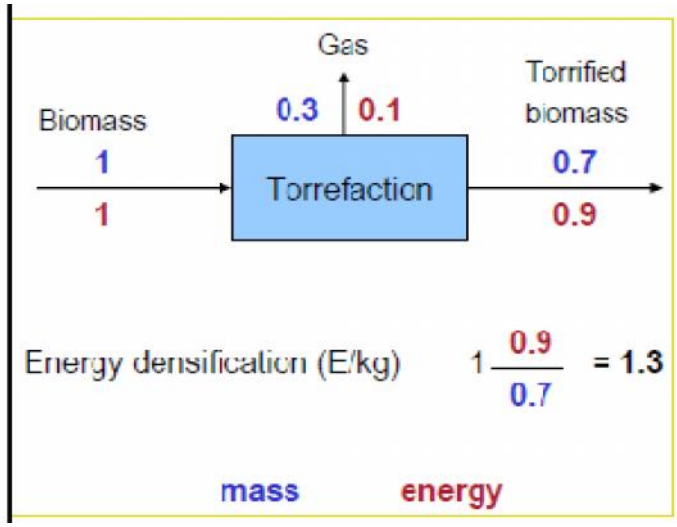

Figure 3: Typical mass and energy balance of torrefaction process [2]

Energy densification could be expressed as Equation (1)

$$E_d = \frac{\eta_{torr}}{M_{torr}} \quad (1)$$

where η_{torr}: energy of the torrefied biomass in percentage of initial energy

M_{torr} : mass of torrefied biomass in percentage of feed biomass

Energy of the torrefied biomass in percentage of initial energy could express as Equation (2)

$$\eta_{torr} = \frac{E_{torrified}}{E_{untreated}} \quad (2)$$

where $E_{torrefied}$ is the energy of torrefied biomass and $E_{untreated}$ is the energy of feed biomass which could be calculated by Equations (3) and (4)

$$E_{torrefied} = HHV_{torrefied} * m_{torrefied} \quad (3)$$

$$E_{untreated} = HHV_{untreated} * m_{untreated} \quad (4)$$

where $HHV_{untreated}$ is high heating value of untreated biomass and $HHV_{torrefied}$ is high heating value of torrefied biomass. Both are determined by bomb calorimeter 6300 Oxygen.

The mass of torrefied biomass in percentage of initial mass could express as Equation (5):

$$M_{torr} = \frac{m_{torrefied}}{m_{untreated}} \quad (5)$$

2.3 Determination of activation energy (Ozawa method)

Ozawa method is one of the several methods for extraction of the kinetic parameters from TGA data. The advantage is that it is a very simple method to calculate the activation energy without knowing the information about the reaction mechanism, but it can be only used for one-step reaction. [31]

Basically, the function of the rate of decomposition during a reaction can be expressed as following as equation (6), which depends on the temperature and conversion [31-34]:

$$\frac{d\alpha}{dt} = \Phi(T,\alpha) \quad (6)$$

where t is the time. T is absolute temperature and α is conversion.

The iso-conversional method [18-21,23,24] is used and assumed that the function in equation (6) can be rewrite by two functions, which are independent of each other.

$$\frac{d\alpha}{dt} = k(T) * f(\alpha) \quad (7)$$

where the first function $k(T)$ is dependent on the absolute temperature and the second function $f(\alpha)$ is dependent on the conversion α.

The first function $k(T)$ in equation (7) can be expressed by Arrhenius equation:

$$k(T) = Ae^{-\left(\frac{Ea}{RT}\right)} \quad (8)$$

where E_a is the activation energy. A is the pre-exponential factor. R stands for the gas constant and T is the absolute temperature.

The second function $f(\alpha)$ in equation (7) can be expressed by various possibilities. For this study the form in $f(\alpha)$ is used as following Equation (9)

$$f(\alpha) = (1-\alpha)^n \quad (9)$$

where $f(\alpha)$ is conversion function and depends on the reaction mechanism, n is reaction order and α is the conversion, define as

$$\alpha = \frac{(M_i - M_t)}{(M_i - M_{ash})} \quad (10)$$

Combining (7) and (8) gives

$$\frac{d\alpha}{dt} = Ae^{-\left(\frac{Ea}{RT}\right)} * f(\alpha) \quad (11)$$

Equation (11) can be rewritten as

$$\frac{d\alpha}{f(\alpha)} = Ae^{-\left(\frac{Ea}{RT}\right)} * dt \quad (12)$$

Equation (12) can be solved by integrating its both sides

$$\int_{\alpha 0}^{\alpha} \frac{d\alpha}{f(\alpha)} = A \int_{t0}^{t} exp\left(-\left(\frac{Ea}{RT}\right)\right) dt \quad (13)$$

where α_0 is the value of α at $t = t_0$

If the heating rate β is constant, the relation between temperature and time could be written as

$$T = T_0 + \beta t \rightarrow dT = \beta dt \rightarrow dt = \frac{dT}{\beta} \quad (14)$$

The change in α is given by equation (14)

$$\int_{\alpha 0}^{\alpha} \frac{d\alpha}{f(\alpha)} = \frac{A}{\beta} \int_{T0}^{T} exp\left(-\frac{Ea}{RT}\right) dT \quad (15)$$

where T_0 is the value of T at $t=t_0$

The left side in equation (13) can be rewritten

$$F_{(\alpha)} = \int_{\alpha 0}^{\alpha} \frac{d\alpha}{f_{(\alpha)}} = \frac{A}{\beta} \int_{T0}^{T} exp\left(-\frac{Ea}{RT}\right) dT \qquad (16)$$

The rate of reaction is very low at low temperature which means the lower limit of the temperature may be ignored if T_0 is well below the temperature at which the rate of reaction becomes measurable. [31,35,36]

The right side in equation (13) can be rewritten as

$$\int_{T0}^{T} exp\left(-\frac{Ea}{RT}\right) dT = \int_{0}^{T} exp\left(-\frac{Ea}{RT}\right) dT \qquad (17)$$

The value of the right side in Equation (17) can be expressed by C. Dolye's linear approximations [36] as the following function (18)

$$\frac{Ea}{R} p\left(\frac{Ea}{RT}\right) = \int_{0}^{T} exp\left(-\frac{Ea}{RT}\right) dT \qquad (18)$$

So if the E_a/RT is bigger than 20[36], the $p\left(\frac{Ea}{RT}\right)$ can be approximated by the following formula

$$\log p\left(\frac{Ea}{RT}\right) \cong -2{,}315 - 0{,}4567\frac{Ea}{RT} \qquad (19)$$

Combining Equations (16) and (18) gives

$$F_{(\alpha)} = \int_{\alpha 0}^{\alpha} \frac{d\alpha}{f_{(\alpha)}} = \frac{A}{\beta} \int_{T0}^{T} exp\left(-\frac{Ea}{RT}\right) dT = \left(\frac{AE_a}{\beta R}\right) P\left(\frac{Ea}{RT}\right) \qquad (20)$$

By the integral iso-conversional method and Dolye's linear approximations Equation (20) can be rewritten

$$\log F(\alpha) \cong \log\frac{AEa}{R} - \log\beta - 2{,}315 - 0{,}4567\frac{Ea}{RT} \qquad (21)$$

The Ozawa proved if the value of α and single value of f(α) are given, the left side of equation (21) which is F(α) will give a constant value which does not depend on the heating rate. [27]

Thus from Equation (16) gives

$$F_{(\alpha)} = \int_{\alpha 0}^{\alpha} \frac{d\alpha}{f_{(\alpha)}} = A \int_{t0}^{t} exp\left(-\frac{Ea}{RT}\right) dt \Rightarrow F(\alpha) - \int_{0}^{\alpha} \frac{d\alpha}{f(\alpha)} = A \int_{0}^{t\alpha} exp\left(-\frac{Ea}{RT}\right) dt = 1$$

$$\log F(\alpha) \cong 0$$

Then Equation (21) can be rewritten to obtain Equation (22)

$$\log \beta \cong \log \frac{AEa}{R} - 2{,}315 - 0{,}4567 \frac{Ea}{RT} \qquad (22)$$

It has been proved that for a constant degree of conversion α. Ea is related to the heating rate β and the temperature by Equation (23): [31]

$$-\log \beta_1 - 0{,}4567 \frac{Ea}{RT_1} = -\log \beta_2 - 0{,}4567 \frac{Ea}{RT_2} \qquad (23)$$

According to Equation (23), a plot of $\log \beta$ versus T^{-1} gives a straight line, whose slope and intercept can be used to determine E_a at any given conversion α. Then it can calculate the pre-exponential factor A from the equation (22).

2.4 Single reaction one step model

In order to calculate the reaction order n for one step model the rate of conversion can be described by Equation (24) which is resulted from combination of Equation (7) (8) and (9).

$$\frac{d\alpha}{dt} = Ae^{-\left(\frac{Ea}{RT}\right)} * f(\alpha) = Ae^{-\left(\frac{Ea}{RT}\right)} * (1-\alpha)^n \qquad (24)$$

If the activation energy Ea is determined using Ozawa method, the reaction order n and pre-exponential factor A can be calculated by non-linear least square fitting. [19]

2.5 Model with independent parallel reactions (Three-pseudo-components model)

Alternatively, three-pseudo-components models developed by Varhegyi and co-workers [18,38,39], can be used to extract kinetic parameters from TGA data. This model may offer better fit to the experimental data, considering that plant biomass is composed of three main components. Hemicelluloses, lignin and cellulose, with different reactivity for pyrolysis and thus more than one reaction may be involved. According this model the pyrolysis rate can be determined by Equation (25).

$$\frac{d\alpha}{dt} = \sum_{i=1}^{3} \frac{d\alpha_i}{dt} = \sum_{i=1}^{3} c_i A_i \exp(-\frac{Ea_i}{RT}) f(\alpha_i) \qquad (25)$$

Depend on the reaction order n. the following kinetic equations can be used for each pseudo- --component

$$\frac{d\alpha_i}{dt} = C_i A_i \exp(-\frac{Ea_i}{RT}) * (1-\alpha_i)^{n_i}$$
$$= C_i A_i * \exp(-\frac{Ea_i}{RT}) * \exp\left\{-\frac{A_i}{\beta}\int_{T_0}^{T} \exp(-\frac{Ea_i}{RT}) dT\right\}, n_i = 1 \qquad (26)$$

$$\frac{d\alpha_i}{dt} = C_i A_i \exp(-\frac{Ea_i}{RT}) * (1-\alpha_i)^{n_i} =$$
$$= C_i A_i * \exp(-\frac{Ea_i}{RT}) * \left\{\left(\frac{(n_i-1)A_i}{\beta}\int_{T_0}^{T} \exp(-\frac{Ea_i}{RT}) dT\right) + 1\right\}^{\frac{n_i}{(1-n_i)}}, n_i \neq 1 (27)$$

The unknown parameters of the model such as activation energy E_{ai}, pre-exponential factor A_i, reaction order n_i and dimensionless factor C_i are determined by the evaluation of the experimental data by non-linear least square fitting.

3 Experimental

3.1 Equipment setup for biomass torrefaction

Fig 4 represents the experimental setup used for biomass torrefaction in this study, which includes a tubular reactor placed in an electric muffle furnace, a nitrogen gas supply system with a heating element for gas preheating, and a condenser connected to outlet of the reactor. The reactor (figure 5) made of stainless steel has been designed to fit the existing furnace, Nabertherm LH 30/12, which can be operated within a temperature range of 30-3000^{o}C, the main body of the reactor about 400mm long, consisting of two cylinders which are assembled together by a sealed mechanism on the top end as shown in Fig. 5a. The diameter of outer cylinder tube (red colour part with a closed end at the bottom) is 70mm and the inner cylinder tube (Fig. 5a green colour part with an opened end at the bottom) diameter is 50mm. A removable sample cup (Fig. 5a. blue colour part) with a fixed bed (stainless steel grind) at the bottom is mounted to the lower end of the inner cylinder as can also be seen in Fig. 2b. A thermocouple (Type K) equipped with a digital thermometer was used to monitor the samples temperature during torrefaction process, which is controlled by the furnace temperature through the control panel unit integrated to the furnace. The thermocouple is introduced into the reactor from the top as shown in Figure 4 and Fig 5, and measures temperature in the middle of the sample cup.

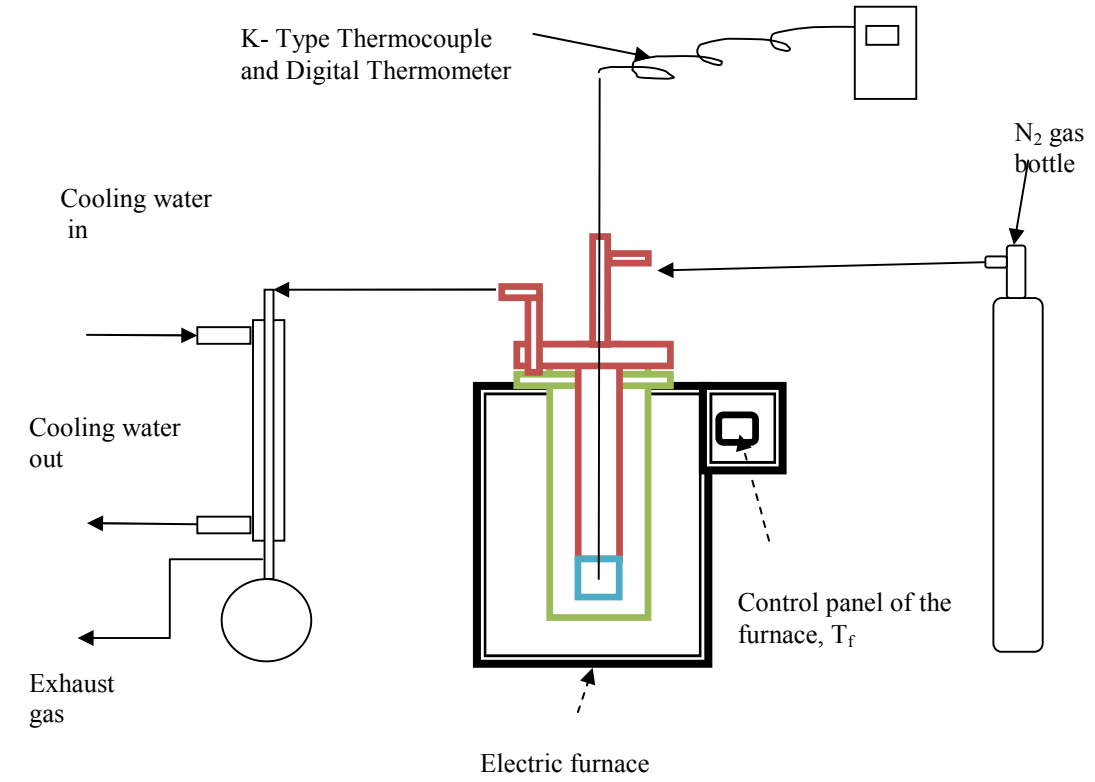

(a)

(b)

Figure 4: The experimental set-up for biomass torrefaction (a: schematic view; b: lab view)

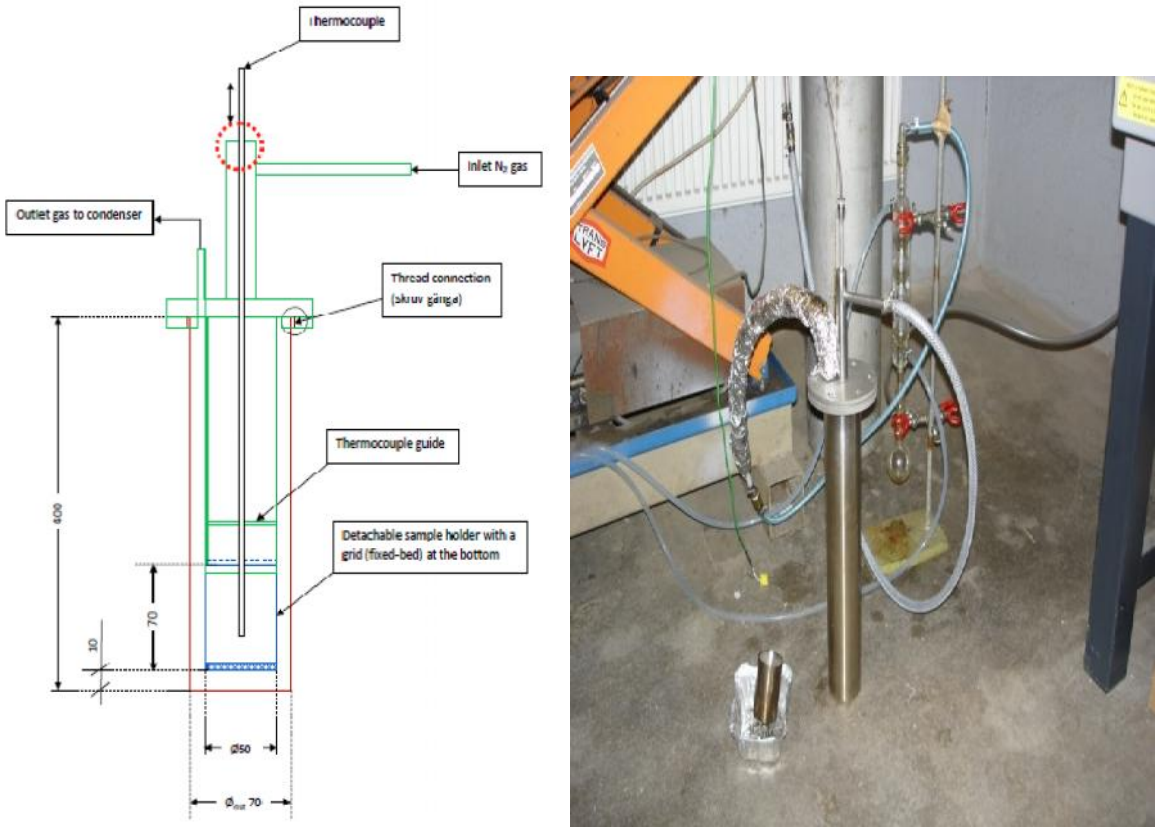

(a) (b)

Figure 5: the reactor design (a: schematic reactor view; b: lab view)

3.2. Torrefaction procedure

About 8 grams of biomass sample (pre-dried at 105^{o}C for 24 hours) was used for each torrefaction experiment. The weight of sample was first balanced and placed in the sample cup. Then the cup was mounted to the inner cylinder of the reactor. The reactor assembly completed with the outer cylinder was then connected to the inlet nitrogen gas and the condenser. Nitrogen gas (Nitrogen 4.5 from Strandmollen) was blown through the reactor at a flow rate of 5 l/min. For one hour in order to purge oxygen out of the system. Then the nitrogen flow was reduced to 0.5 l/min before placing the reactor into the furnace, which has been preheated to a set temperature. The recorded heating rate of the sample in the reactor was about 5^{o}C/min. The torrefaction reaction time of 30-35 minutes was counted from the point the reaction (sample) temperature reached 200^{o}C to the end point when the reactor was removed from the furnace for cooling in the ambient air.

During torrefaction process, volatile compounds were released from the samples, following the stream and collected in the condenser system. Non-condensable gases were released into a safe exhaust ventilation system. The solid product left in the sample cup after the torrefaction was collected and saved in an excicator for further analyses.

3.3 Instruments and analytical methods

The moisture content and ash content were determined by Swedish standard methods [5-7]. The heating value of samples was obtained by a bomb calorimeter from Parr Instrument model 6300 Oxygen, according to the Swedish standard method [8]

Untreated biomass samples was ground by a cutting-knife mill (Retsch SM 2000), integrated with a mesh sieve allowing particles smaller than 25 μm through it.

A burr grinder machine Krup's GVX2 was used for grindability analysis of torrefied biomass. After grinding, the powder of samples was sieved by sieve shaker machine (Retch SV001) with four size fraction: <0.8 mm, 0.8~1 mm, 1~1.4 mm and >1.4 mm.

A thermogravimetric analyzer (TGA) from Perkin Elmer (Pyris 1) was employed for studying thermal decomposition of torrefied biomass in nitrogen. The function of TGA was to measure and record the dynamics of samples weight loss with increasing temperature or time. The volume flow of nitrogen was set up 40 ml/min for each running. The initial mass of sample was used in a range of 6-8 mg and the temperature decomposition ranged in TGA from 25^{o}C to 600^{o}C with the heating rate at 10 K/min. 20 K/min and 40 K/min.

3.4 Material

Three types of biomass were used as feedstock for torrefaction in this study. They were Norway spruce stump (hereafter called stump – S), poplar (P) and Fuel Tree Chips (FTC) from Vattenfall AB. Some fuel properties of the three samples are presented in Table 1, as results of an approximate analysis using Swedish standard method [5-7]. The poplar sample and stump had been dried in ambient air and stored indoor for 26 months. So the moisture

contents of these samples were very low compared with the fresh Fuel Tree Chips as can be seen in Table 1.

Table 1: Approximate analysis of the material investigated

Sample	Moisture content (%)	Ash content (%)	HHV(MJ/kg)
Poplar	8.91	1.10	19.25
Fuel Tree Chips	37.86	2.49	19.39
Spruce Stump	7.06	8.14	20.55
Method	**SS 187170**	**SS 187171**	**SS 187182**

HHV= Higher heating value

3.5 Torrefaction conditions

Different torrefaction conditions were designed for the present study and presented in Table 2. The reaction temperature was at 200^{o}C. 250^{o}C and 300^{o}C and the holding time at each reaction temperature were 5 and 10 minutes, giving two values (30 and 35 minutes. respectively) of the total reaction time for each reaction temperature.

Nitrogen gas with a constant gas flow of 0.5 l/min was introduced and maintained in the reactor during the experiments.

Table 2: Different treatments of the investigated biomass at different torrefaction conditions

Temprature(^{o}C)	**200**		**250**		**300**	
Holding time	**5min**	**10min**	**5min**	**10min**	**5min**	**10min**
Sample						
Poplar	P_A5	P_A10	P_B5	P_B10	P_C5	P_C10
Fuel Tree Chips					FTC_C5	FTC_10
Stump	S_A5	S_A10	S_B5	S_B10	S_C5	S_C10

4 Results

4.1 Torrefaction solid products

Figure 6 shows solid products collected from biomass torrefaction in different conditions presented in Table 2. It is clear that torrefaction temperature had very strongly effect on the colour of the solid products. The higher the temperature, the darker the product colour was. However, the reaction time seemed to have less pronounced effect on the colour of the products. The colour of biomass torrefied at 200^{o}C was light brown. At 250^{o}C the colour became brown. At 300^{o}C the colour was dark brown. In addition, the solid product collected from biomass torrefaction at 300^{o}C was every brittle.

(a) Torrefied poplar samples

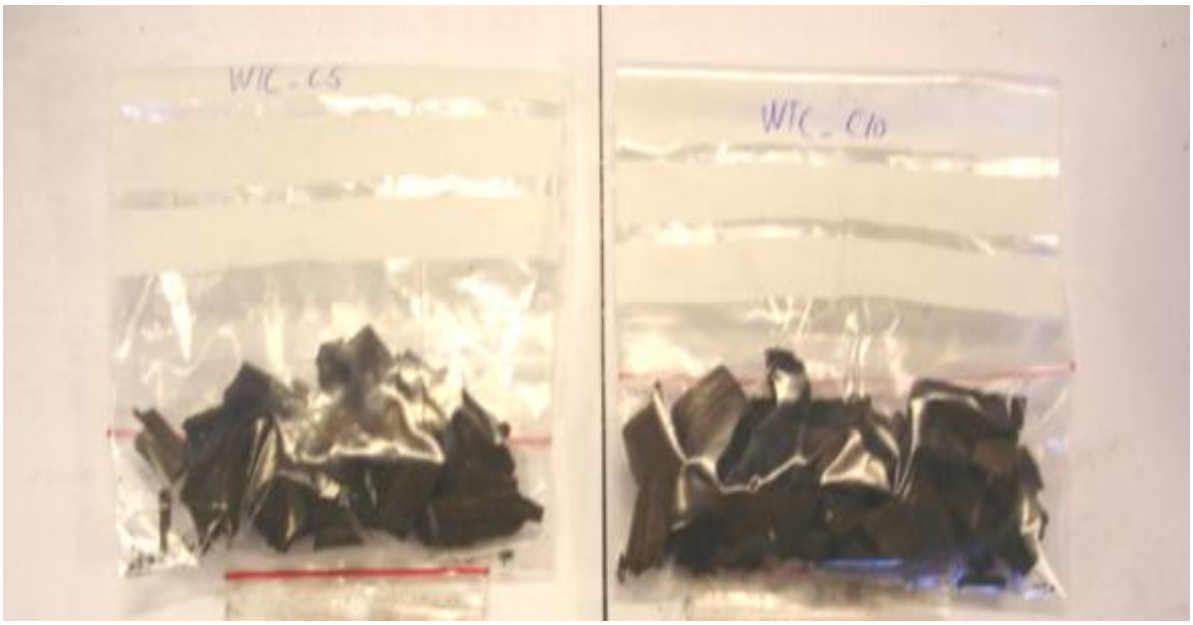

(b) Torrefied FTC samples

(c) Torrefied stump samples

Figure 6: Solid products collected from torrefaction of biomass in different conditions

4.2 Mass and energy balance

Table 3 presents the mass of solid biomass before and after torrefaction process, and the heating value of the solid products collected from the torrefaction processes. It was calculated that the mass loss of the solid by torrefaction was about 34% for the torrefaction in conditions of the highest temperature (300^{o}C) and the longest reaction time (35 minutes. corresponding to the holding time at this temperature of 10 minutes). In addition, the mass loss increased with reaction temperature and/or time. At the same reaction temperatures longer holding times resulted in more mass losses. For the same reaction time, higher reaction temperatures also resulted in more mass losses.

Table 3: Collected data for mass and energy balance calculation

Temprature(^{o}C)	**200**		**250**		**300**	
Reaction time	**30min**	**35min**	**30min**	**35min**	**30min**	**35min**
	Mass of biomass sample before torrefaction (g)					
Poplar	7.99	8.04	8.02	8.03	8.01	7.99
Fuel Tree Chips					8.00	8.02
Stump	7.99	8.02	7.98	7.99	8.01	8.02
	Mass of biomass sample after torrefaction (g)					
Poplar	7.57	7.45	7.04	6.95	4.99	4.56
Fuel Tree Chips					5.65	5.11
Stump	7.68	7.55	7.19	6.95	5.52	5.24
	HHV(MJ/kg)					
Poplar	19.05	19.10	19.72	19.82	21.65	22.12
Fuel Tree Chips					21.11	21.64
Stump	20.15	20.30	21.07	21.08	22.70	23.01
	Diemnsionless energy densification factor					
Poplar	0.98	0.99	1.02	1.03	1.12	1.15
Fuel Tree Chips					1.09	1.12
Stump	0.98	0.99	1.025	1.026	1.10	1.12

As can be seen in Table 3, the heating values of torrefied biomass increased with increasing reaction time and/or temperature. The solid collected from biomass samples torrefied at 300^{o}C for 10 minutes had the highest heating value and the heating value increases with 14% for poplar and 12% for both Fuel Tree Chips and stump comparing with the untreated biomass.

The energy densification of the torrefaction processes was calculated and the results are presented in Figure 7, which shows that the energy density of solid product (torrefied biomass)

increased with both increasing reaction time and torrefaction temperature as shown in Figure 7. The energy densification of poplar torrefied at 300^{o}C for 35 minutes increases by a factor of 1.15 and 1.12 for both FTC and stump. At the same torrefaction temperature the longer reaction time resulted in a high energy density. Comparing the energy densification of poplar with stump torrefied at the same conditions, the earlier had a higher energy density than the later.

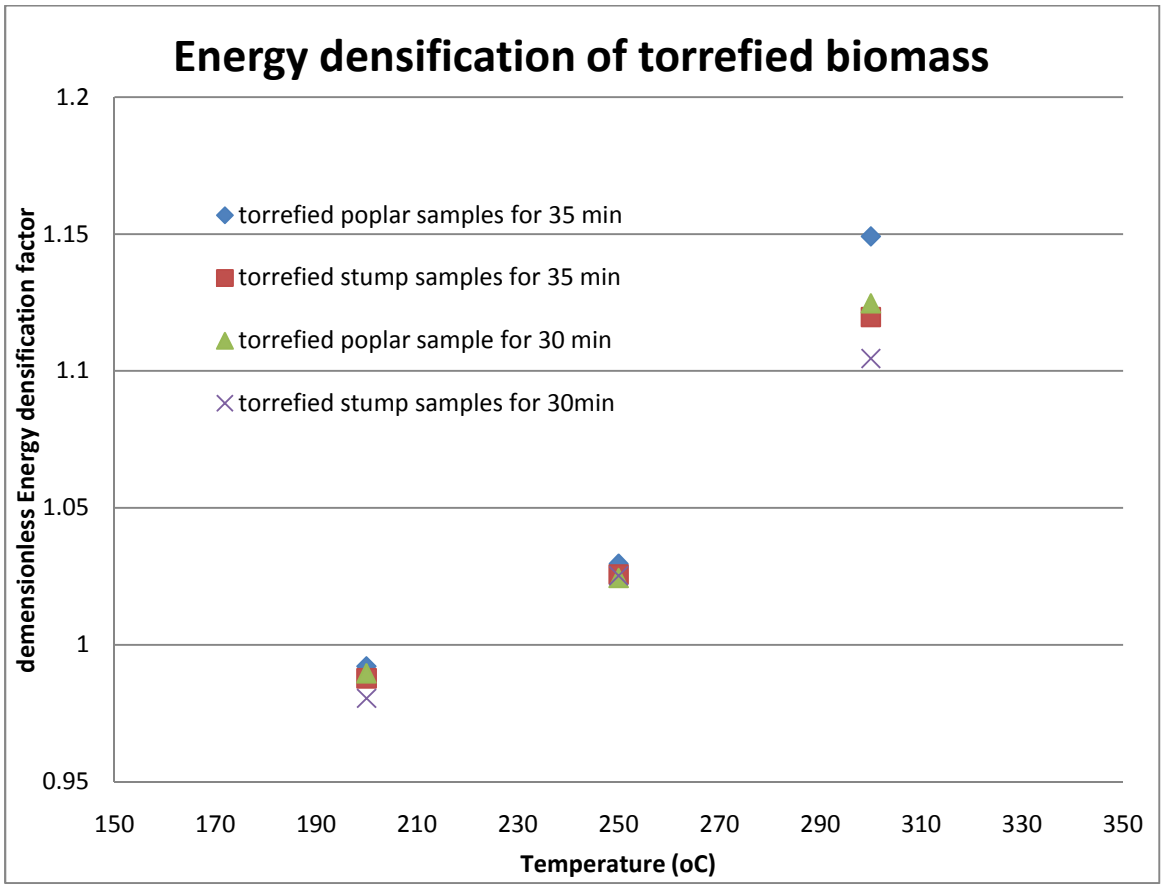

Figure 7: Energy densification of torrefied biomass against reaction temperature

4.3 Grindability

A coffee burr grinder machine, Krup's GVX2, was used to study the grindability of solid products collected from the biomass torrefaction experiments. The grinder was set at an unchanged power level for grinding the same amount, 4g, of every sample. Table 4 presents data obtained from the grindability tests, which shows that either increases reaction temperature or reaction time resulted in reduce grinding time or energy in other words. However, the effect of reaction temperature was much more pronounced than that of the

reaction time. In addition, among the three biomass types (torrefied at 300°C), the grinding time of the stump was the longest, followed by poplar then the fuel tree chip. This observation can be probably explained by the higher lignin content in the stump than in poplar and the fact that the Fuel Tree Chips might contain softwood with relatively low lignin content.

Table 4: Time/energy saving during comminution of torrefied biomass

Sample ID	Grinding time. S
P_B5 (250°C. 30min)	75
P_B10 (250°C. 35min)	72
P_C5 (300°C. 30min)	15
P_C10 (300°C. 35min)	12
FTC_C5 (300°C. 30min)	18
FTC_C10 (300°C. 35min)	15
S_B5 (250°C. 30min)	92
S_B10 (250°C. 35min)	90
S_C5 (300°C. 30min)	40
S_C10 (300°C. 35min)	30

For further evaluation of the grindability for the solid products, the powder samples collected from the grinding step were sieved and classified in four size fractions: <0.8 mm. 0.8~1 mm. 1~1.4 mm and >1.4 mm. Figure 8 shows the particle size distribution by mass fraction for the tests.

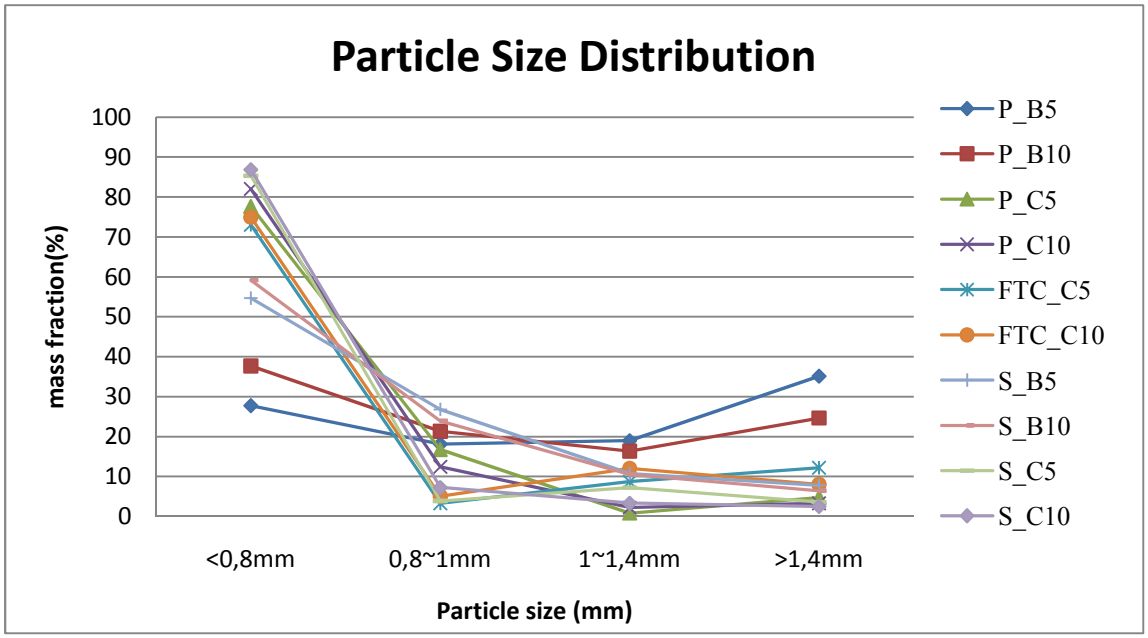

Figure 8: Particle size distributions of torrefied biomass ground by a coffee grinder

From Figure 8 it can be seen that more than 70% of the mass for all biomasses torrefied at 300^{o}C with different reaction time were gone through the 0.8 mm sieve. Less than 60% of the stump torrefied at 250^{o}C and 40% of the poplar torrefied at 250^{o}C pass through the 0.8 mm sieve. At the same reaction temperature, the longer the reaction time, the more improved grindability of the torrefied biomass was.

4.4 Non-isothermal decomposition of biomass in nitrogen

4.4.1 TGA and DTG curves of untreated biomass

Non-isothermal decomposition of the three untreated biomass samples was investigated in nitrogen of a mass flow rate of 40 ml/min and at three heating rates of 10, 20, and 40 K/min, using the TGA described earlier. Data collected from this investigation is shown in Figure 9 in the form of weight loss plotted against temperature, TGA curves, from which the weight loss rates can be extracted and presented as DTG (differential thermogravimetry) curves.

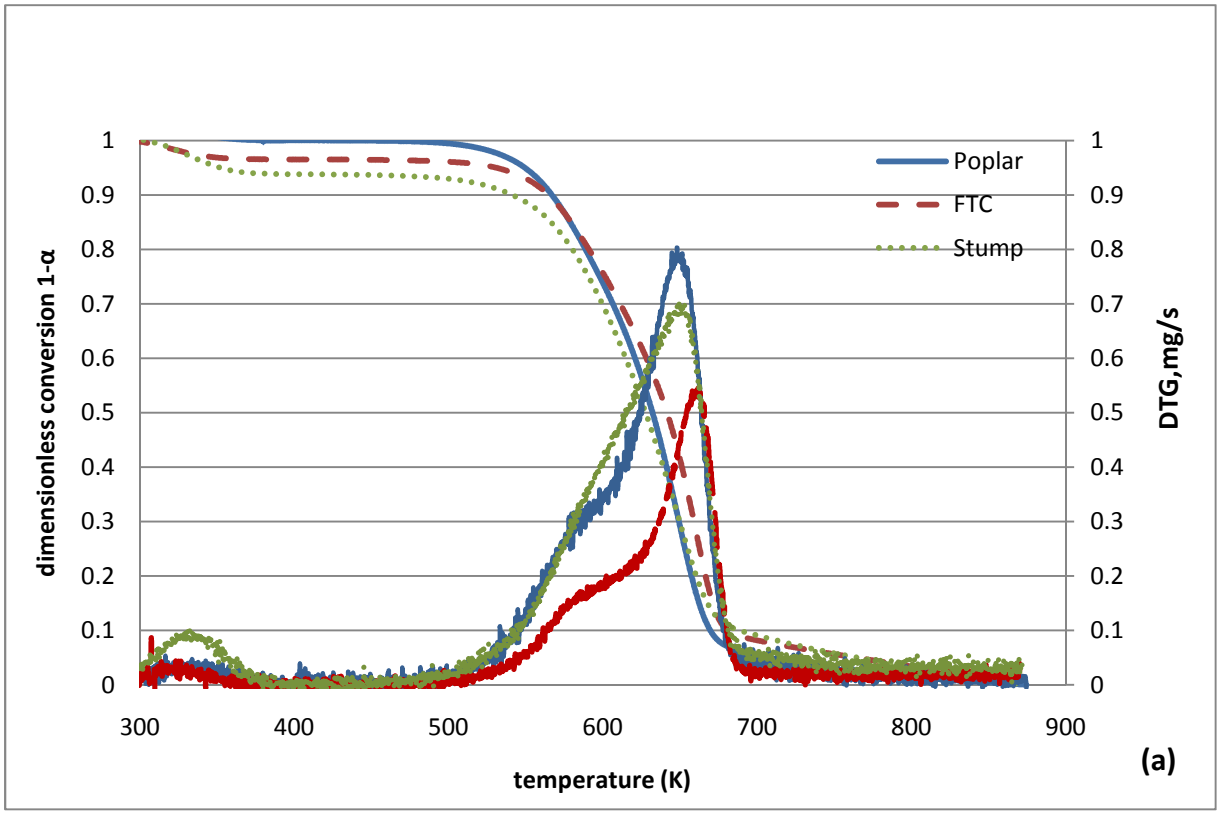
dimensionless conversion 1-α
DTG,mg/s
temperature (K)
Poplar
FTC
Stump
(a)

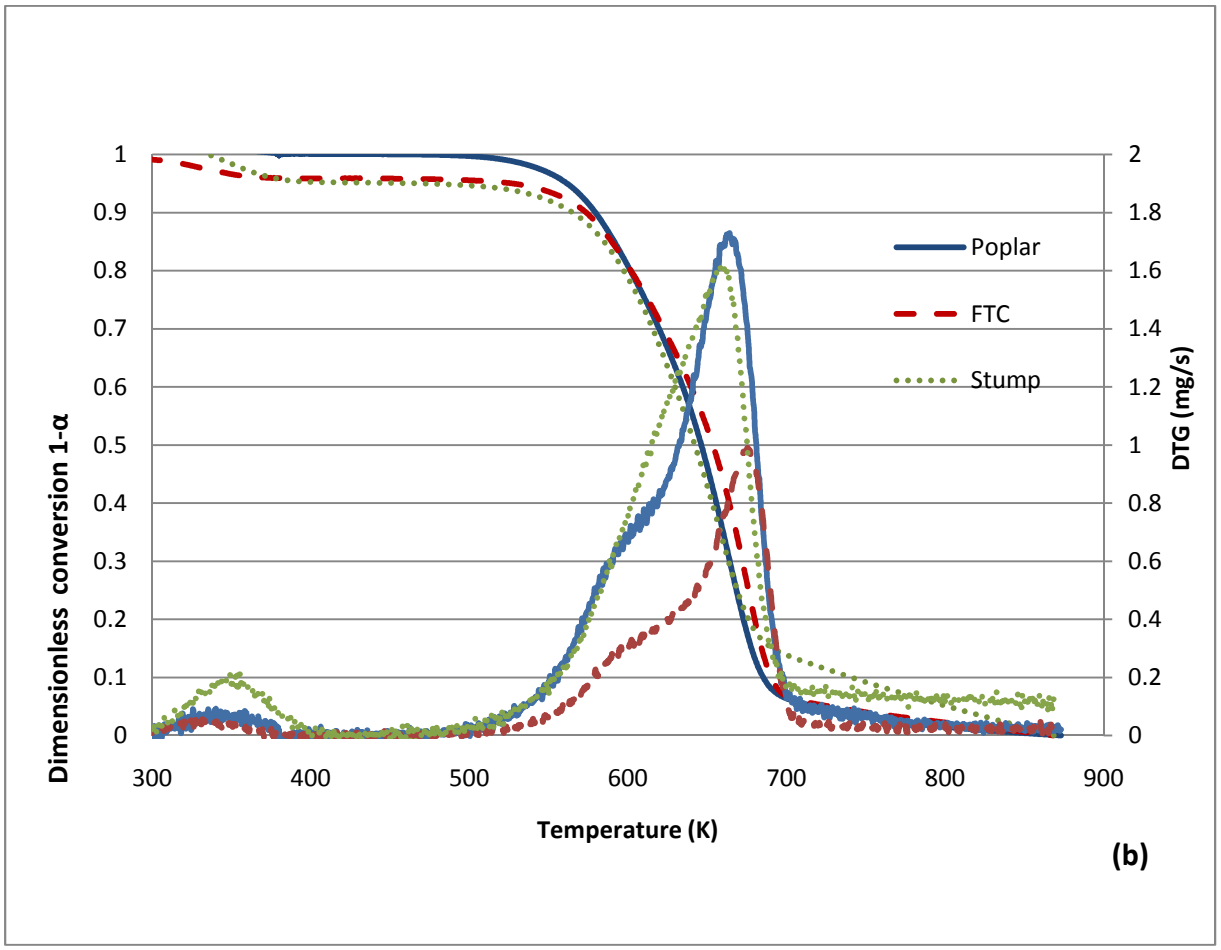
Dimensionless conversion 1-α
DTG (mg/s)
Temperature (K)
Poplar
FTC
Stump
(b)

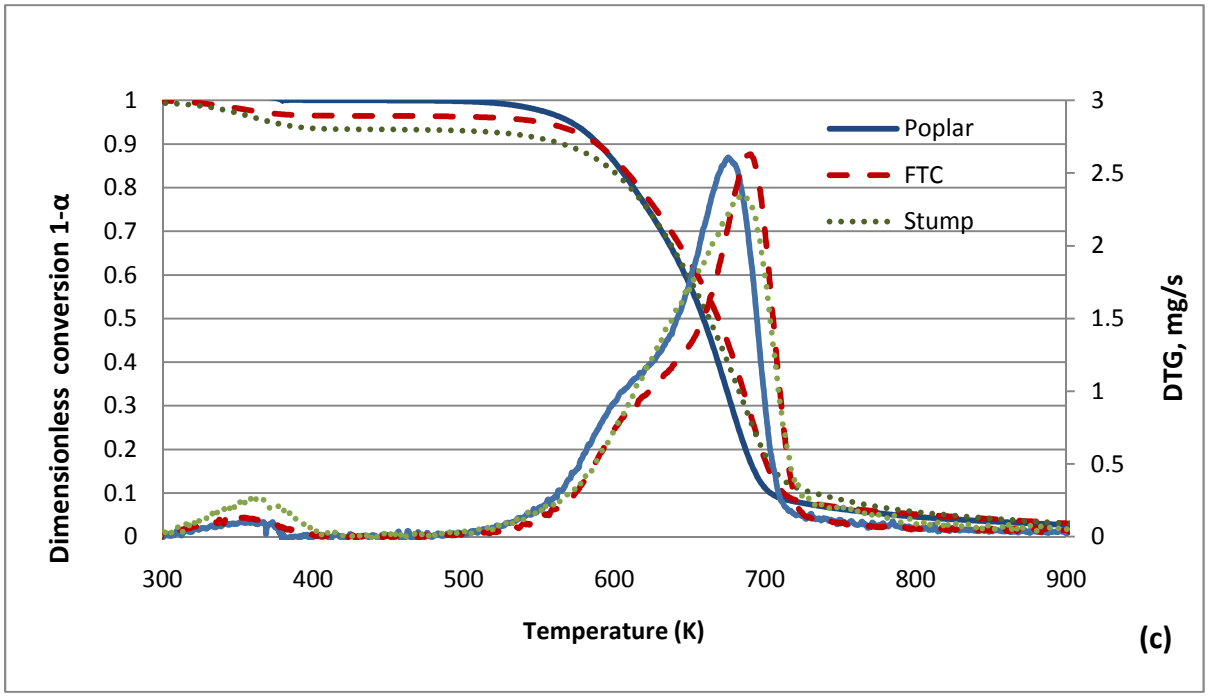

Figure 9: TGA and DTG curves of three different untreated biomasses at different heating rate with nitrogen gas flow 40ml/min (a: 10K/min; b: 20K/min; c: 40K/min)

As can be seen in Figure 9, there are two peaks for each DTG curve. The first tiny peak occurred at 400 K, corresponding to the drying step. The second peak, being the main weight loss step, started at temperature of around 500 K, responsible for the thermal decomposition of biomass. The shoulder at the lower temperature side of the main peak is believed to represent the decomposition of hemicelluloses [27,28,29]. This shoulder seemed missing for the stump, which indicates that stump biomass contained less hemicelluloses than the other biomass fuel types under investigation.

At the heating rate of 10 K/min, Figure 9(a), the maximum decomposition rates was about 0.79 mg/s. 0.56 mg/s and 0.70 mg/s, which were observed to occur at 651 K, 661 K and 649 K for poplar, FTC and stump, respectively. Comparing the DTG curves of the three biomasses one can see that poplar had relatively higher values of maximum pyrolysis rate and FTC had relatively lower values of maximum pyrolysis rate.

When the heating rate increased to 40 K/min, Figure 9(c), the value of maximum pyrolysis rate of all three samples increased to 2.61mg/s, 2.38 mg/s and 2.62 mg/s and the maximum point rates of decomposition occurred at 675 K, 690 K and 685 K for poplar, FTC and stump respectively. Again, comparing the DTG curves of the three biomasses at heating 40K/min one can see that the FTC had relatively higher values of maximum pyrolysis rate and stump

has relatively lower values. The maximum pyrolysis rate of FTC increased significant by increasing the heating rate.

4.4.2 Influence of heating rate on the data collected from TGA

The data presented in the previous section was rearranged, Figure 10, for an analysis of effects of heating rate on the data collected from the TGA. As can be seen in Figure 10, TGA- and DTG-curves of individual untreated biomass at different heating rates look quite similar with some common features. In general, higher heating rates gave higher conversion or weight loss rates. In addition, when the heating rate increases, the TGA-curves shifted toward the right and the peaks of DTG curves are slightly shifted towards higher temperatures.

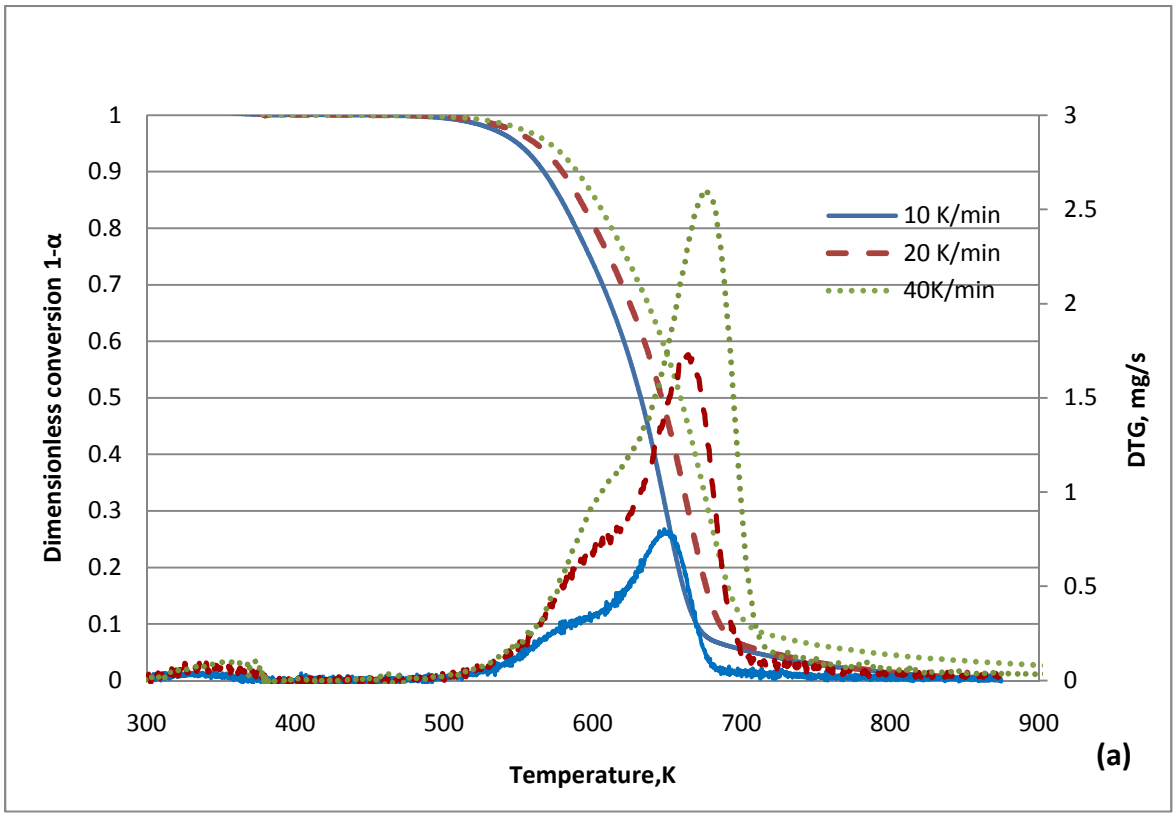

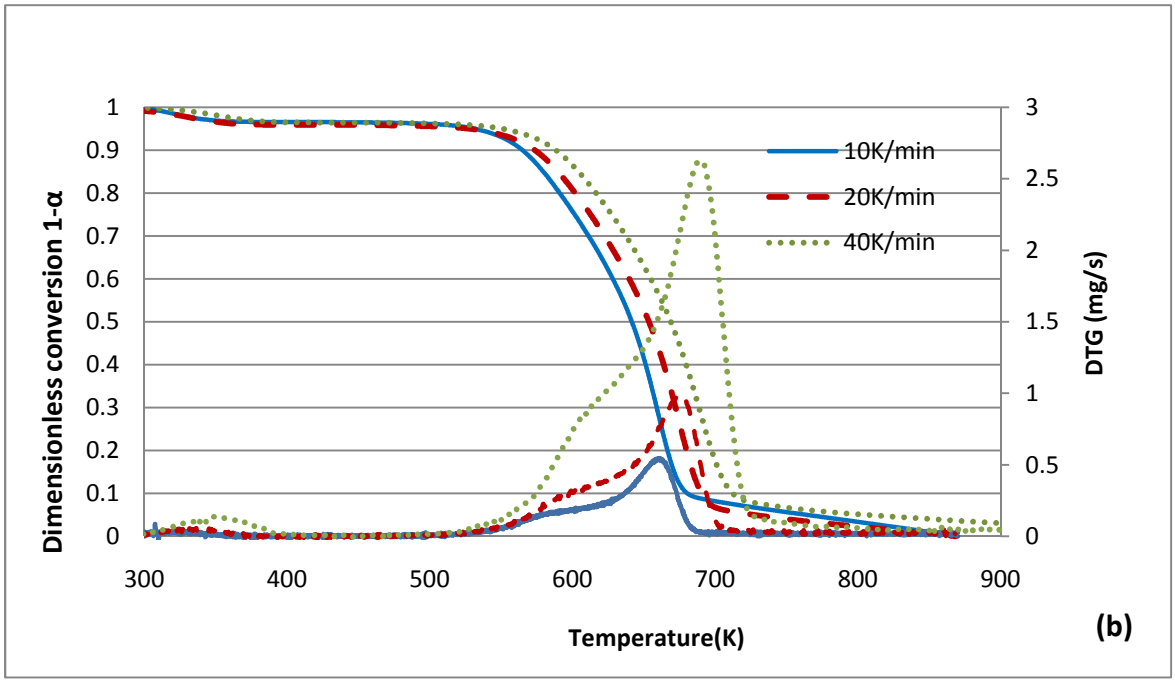

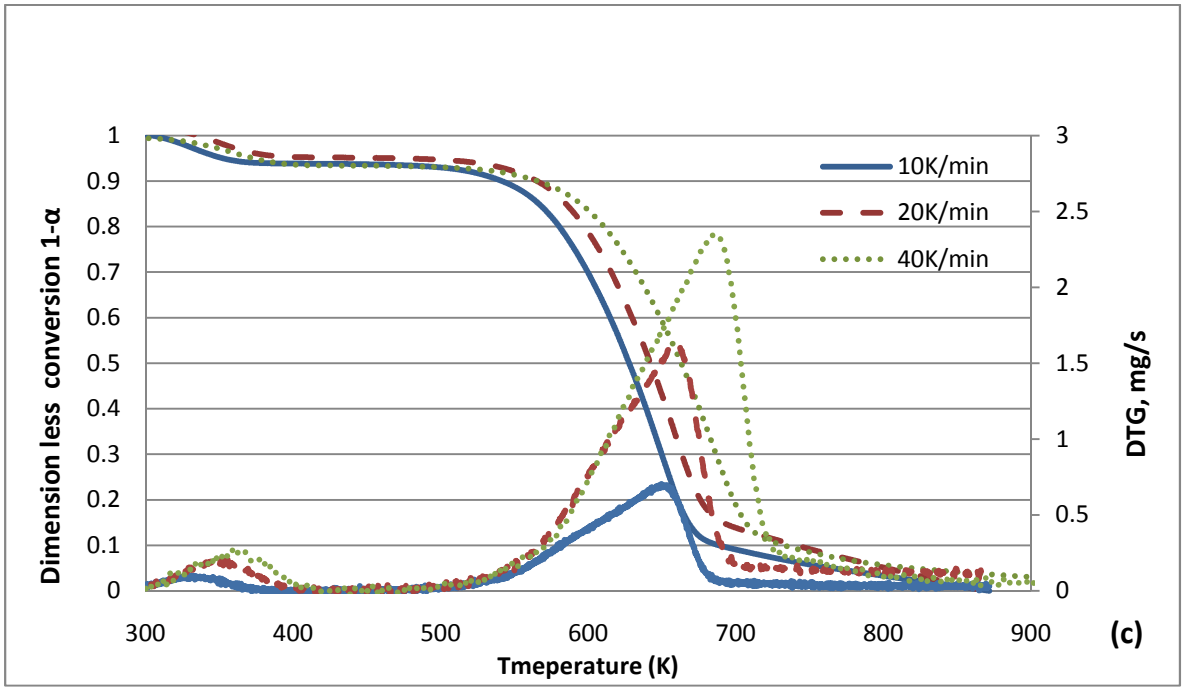

Figure 10: TGA and DTG curves of different untreated biomasses at heating rates 10K/min, 20K/min and 40K/min with nitrogen gas flow 40ml/min (a: poplar; b: FTC; c: stump)

4.4.3 Effect of torrefaction temperature

TGA and DTG curves collected at the heating rate of 40 K/min. for untreated and torrefied stump samples are showed in Figure 11. Clearly, untreated biomass was more reactive than its torrefaction products. In addition, the TGA curves of torrefied samples shifted towards the right with increasing torrefaction temperature, giving the DTG peaks shifting slightly away

from the left to the right as well, but the peak height decreases with increasing torrefaction temperature, except for the sample torrefied at 300 C.

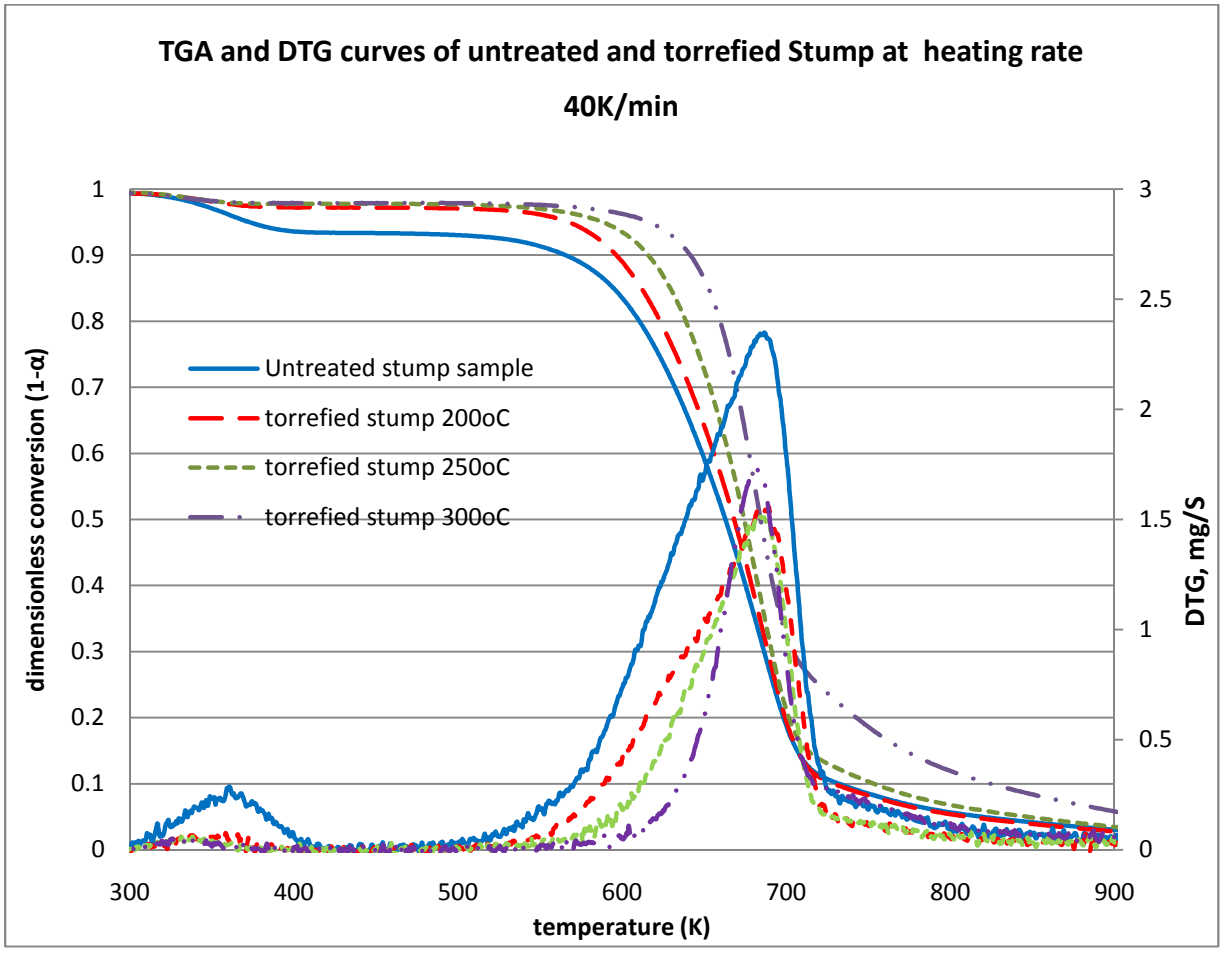

Figure 11: TGA and DTG curves of untreated and torrefied stump samples at the heating rate of 40 K/min in nitrogen of a gas flow rate of 40 ml/min

In order to have a better understanding of physical changes of biomass sample during torrefaction samples of untreated stump and stump torrefied at different temperatures were examined by means of a scanning electro-microscopy (SEM). Figure 12 presents SEM pictures of untreated (a) and torrefied (b and c) stump samples. Increasing number of the openings on the surface of the examined samples (Fig. 12a and 12b) can be attributed to the way gas products released during torrefaction broke the biomass structure in order to escape outward. In addition, the biomass structure was broken more severely with increasing torrefaction temperature (Fig. 12b and 12c)

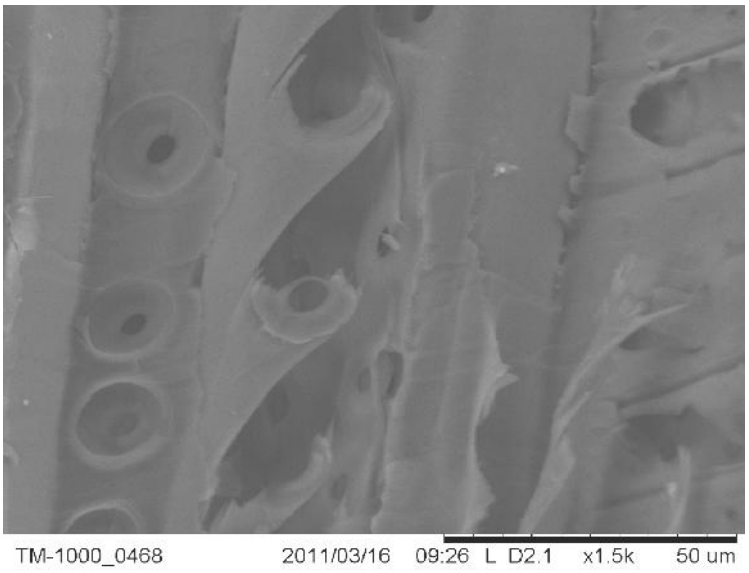

(a)

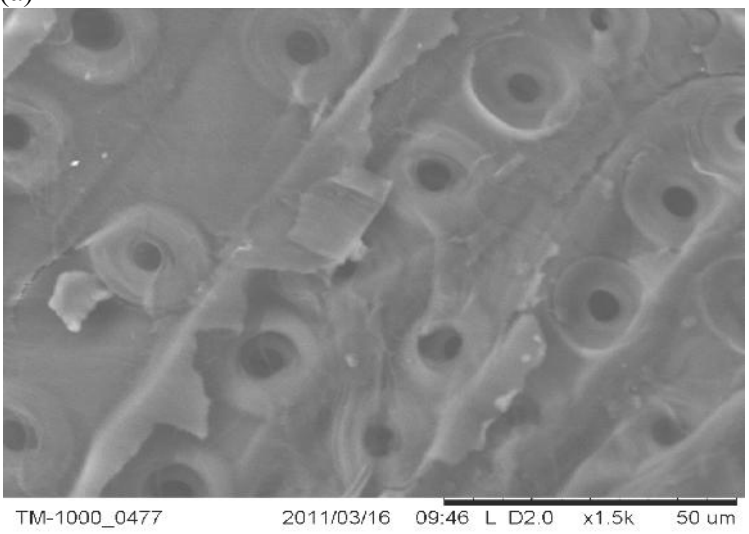

(b)

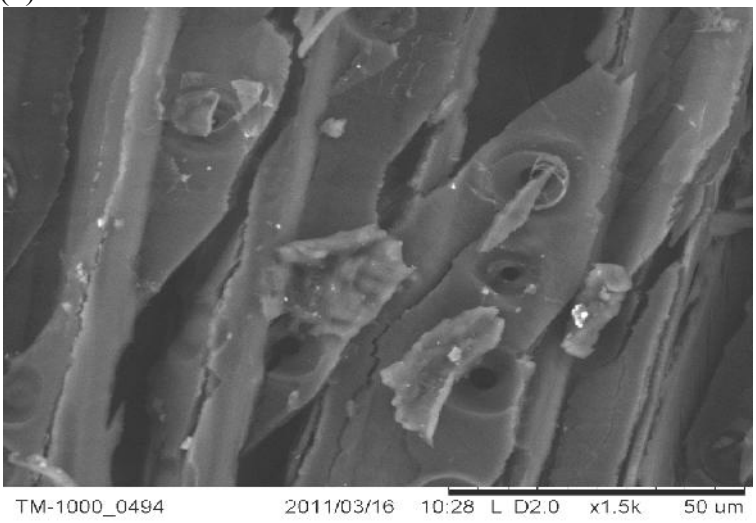

(c)

Figure 12. SEM pictures of untreated stump sample and torrefied stump samples (a: Untreated stump sample; b: Stump torrefied at 250^{o}C for 10min; c: Stump torrefied at 300^{o}C for 10min)

4.5 Kinetic parameters determination by Ozawa method

Ozawa method allows determining kinetic parameters such as activation energy (E_a), utilizing Arrhenius equation. By constructing plots of $\log\beta$ versus T^{-1}, which give straight lines, whose slopes and intercepts can be used to calculate E_a at different conversion α. The exponential factor A at different conversion α could also be calculated using Equation (7).

Figure 13 represents graphically the determination of activation energy and pre-exponential factor by Ozawa method for untreated biomass samples under investigation. The same range of the conversion α from 0.14 to 0.81 was used for all the samples.

For the poplar, the activation energy was found to be in between 127 and 167 kJ/mol, and pre-exponential factor varied between 1.82E+11 and 1.45E+13. The average activation energy and pre-exponential factor are 153kJ/mol and 6.06E+12.

For the FTC the activation energy was observed to be within the range between 154 and 173 kJ/mol, and the pre- exponential factor varies was from 3.07E+12 to 7.33E+13. The average activation energy was 166kJ/mol and the average pre-exponential factor was 3.69E+13.

For the stump the activation energy varied from 125 to 133kJ/mol and the average value of activation energy was 129kJ/mol. The pre-exponential factor was found in between 1.39E+10 and 2.39E+11 and the average value was 6.59E+10.

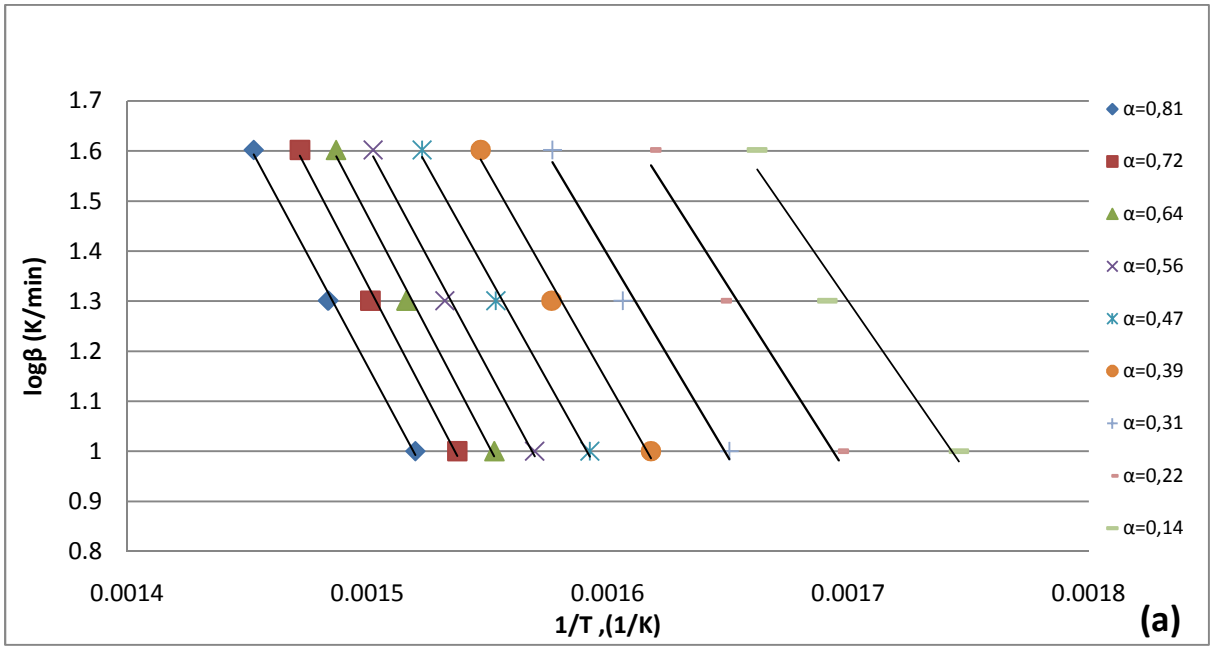

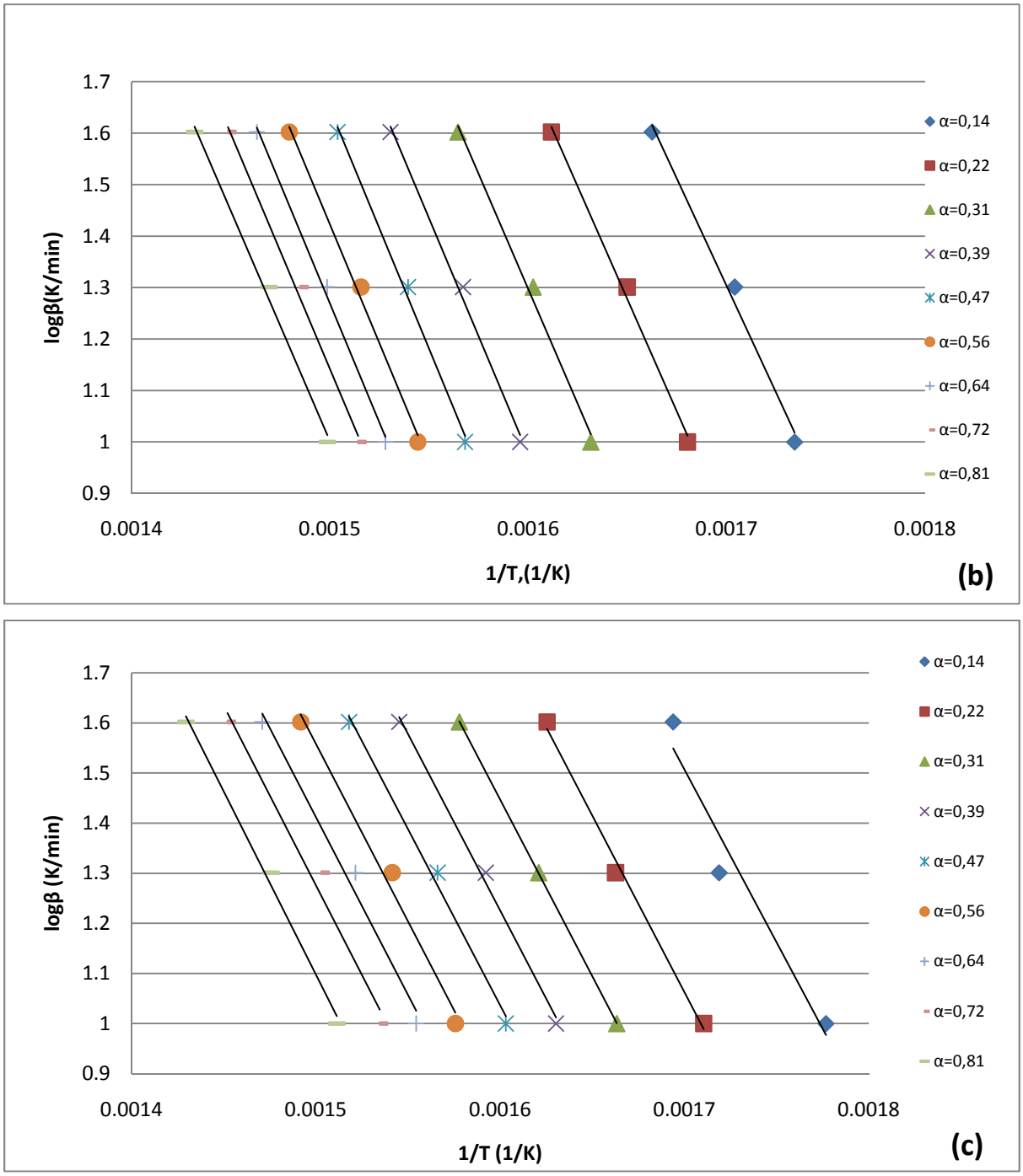

Figure 13: Determination of activation energy by Ozawa method for untreated biomass samples (a: poplar; b: FTC; c: stump)

Results from the determination of activation energy and pre-exponential factors by Ozawa method are numerically summarized in Table 5. From this table, one can see that the FTC had relative higher values of activation energy and pre-exponential factor than the others. Among the three types of biomass, stump had lowest values of activation energy and pre-exponential factor.

Table 5: Numerical summary of activation energy and pre-exponential factor - Ozawa method

	Poplar		FTC		Stump	
α	**Ea**	**A**	**Ea**	**A**	**Ea**	**A**
0.14	127	1.82E+11	154	4.80E+13	125	2.39E+11
0.22	138	7.71E+11	158	3.51E+13	128	1.48E+11
0.31	147	2.39E+12	167	6.79E+13	128	7.02E+10
0.39	154	4.67E+12	171	7.33E+13	128	4.24E+10
0.47	157	5.05E+12	173	6.48E+13	128	2.67E+10
0.56	163	1.05E+13	171	2.73E+13	129	2.10E+10
0.64	166	1.45E+13	168	1.08E+13	129	1.56E+10
0.72	167	1.24E+13	166	5.50E+12	130	1.39E+10
0.81	163	3.99E+12	166	3.07E+12	133	1.47E+10

4.6 Kinetic models for non-isothermal decomposition of biomass

4.6.1 One-step model

At the fist instance, one-step model was employed for simulation of non-isothermal decomposition of biomass, from which the reaction order n and pre-exponential factor A were determined by searching for the best fit between the experimental data and simulated results using non-linear regression analysis. Table 6 represents results from this simulation study, including the value of σ^2 (least square).

Table 6: Results from one-step modelling

Poplar				
heating rate K/min	**Ea(KJ/mol)**	**A(1/s)**	**one single step (n≠1)**	**σ^2**
10	153	3.19E+12	2.61	4.39E-04
20	153	3.20E+12	2.55	1.69E-03
40	153	5.21E+12	3.33	7.01E-03
Stump				
heating rate K/min	**Ea(KJ/mol)**	**A(1/s)**	**one single step (n≠1)**	**σ^2**
10	129	3.01E+10	2.93	3.28E-04
20	129	5.56E+10	3.34	1.55E-03
40	129	3.64E+10	3.27	3.22E-03

4.6.2 Three-pseudo-components model

Three-pseudo-components model with reaction order n=1 and n≠1 was also used to for the simulation study in the present work and the graphical presentation of the fitting between the

simulated results and the experimental data is given in Appendix 7.8.9.10. Tables 7 and 8 represent a numerical summary of the kinetic data (A in s^{-1}, Ea in kJ/mol^{-1}) extracted from the simulation for poplar and stump, respectively. The dimensionless fitting value C is also calculated by least square fitting method.

Table 7: Kinetic parameters extracted from three-pseudo-component modelling for poplar (A in s^{-1}. Ea in kJ/mol^{-1})

Heating rate	**10K/min**							
n=1	**Ea**	**A**	**C**	**n≠1**	**Ea**	**A**	**C**	**n**
hemicelluloses	107	1.98E+09	0.14	**hemicelluloses**	114	1.74E+09	0.73	8.78
cellulose	199	8.27E+15	0.35	**cellulose**	198	8.27E+15	0.36	1.21
lignin	51	1.17E+04	0.02	**lignin**	85	2.01E+07	0.07	2.68
Heating rate	**20K/min**							
n=1	**Ea**	**A**	**C**	**n≠1**	**Ea**	**A**	**C**	**n**
hemicelluloses	107	2.49E+09	0.15	**hemicelluloses**	112	1.71E+09	0.61	6.61
cellulose	185	5.49E+14	0.34	**cellulose**	171	5.09E+13	0.34	1.08
lignin	48	9.91E+03	0.02	**lignin**	82	2.15E+07	0.09	2.30
Heating rate	**40K/min**							
n=1	**Ea**	**A**	**C**	**n≠1**	**Ea**	**A**	**C**	**n**
hemicelluloses	108	9.32E+08	0.56	**hemicelluloses**	105	1.01E+09	0.30	2.85
cellulose	181	3.17E+14	0.33	**cellulose**	176	1.28E+14	0.33	1.00
lignin	52	3.69E+04	0.02	**lignin**	80	2.86E+07	0.06	3.62

Table 8: the Kinetic parameters extracted from three-pseudo-component modelling for stump (A in s^{-1}. Ea in kJ/mol^{-1})

Heating rate	**10K/min**							
n=1	**Ea**	**A**	**C**	**n≠1**	**Ea**	**A**	**C**	**n**
hemicelluloses	77	1.23E+06	0.26	**hemicelluloses**	77	1.27E+06	0.26	1.04
cellulose	181	2.86E+14	0.27	**cellulose**	185	5.59E+14	0.27	1.02
lignin	50	6.67E+03	0.02	**lignin**	83	1.82E+07	0.08	3.97
Heating rate	**20K/min**							
n=1	**Ea**	**A**	**C**	**n≠1**	**Ea**	**A**	**C**	**n**
hemicelluloses	84	6.38E+06	0.27	**hemicelluloses**	81	4.04E+06	0.28	1.01
cellulose	170	5.38E+13	0.27	**cellulose**	173	8.91E+13	0.27	1.02
lignin	42	2.18E+03	0.02	**lignin**	84	1.65E+07	0.12	8.07
Heating rate	**40K/min**							
n=1	**Ea**	**A**	**C**	**n≠1**	**Ea**	**A**	**C**	**n**
hemicelluloses	78	2.31E+06	0.27	**hemicelluloses**	77	1.98E+06	0.27	1.01
cellulose	172	5.38E+13	0.25	**cellulose**	180	1.98E+14	0.27	1.19
lignin	50	2.03E+04	0.03	**lignin**	84	2.78E+07	0.08	2.61

4.6.3 Comparison of simulation of thermal decomposition of different biomasses by different models

Figure 14 presents a comparison of results from simulation of thermal decomposition of different biomass using different models. In all cases, the single-step model appears to be poorly predicting the process. Whereas, the thermal decomposition of the untreated poplar and stump, as well as torrefied stump are well described by three-pseudo-component model with both n=1 or n≠1. In general, three-pseudo-component model with n≠1 resulted in better fits that n=1 but the difference is small.

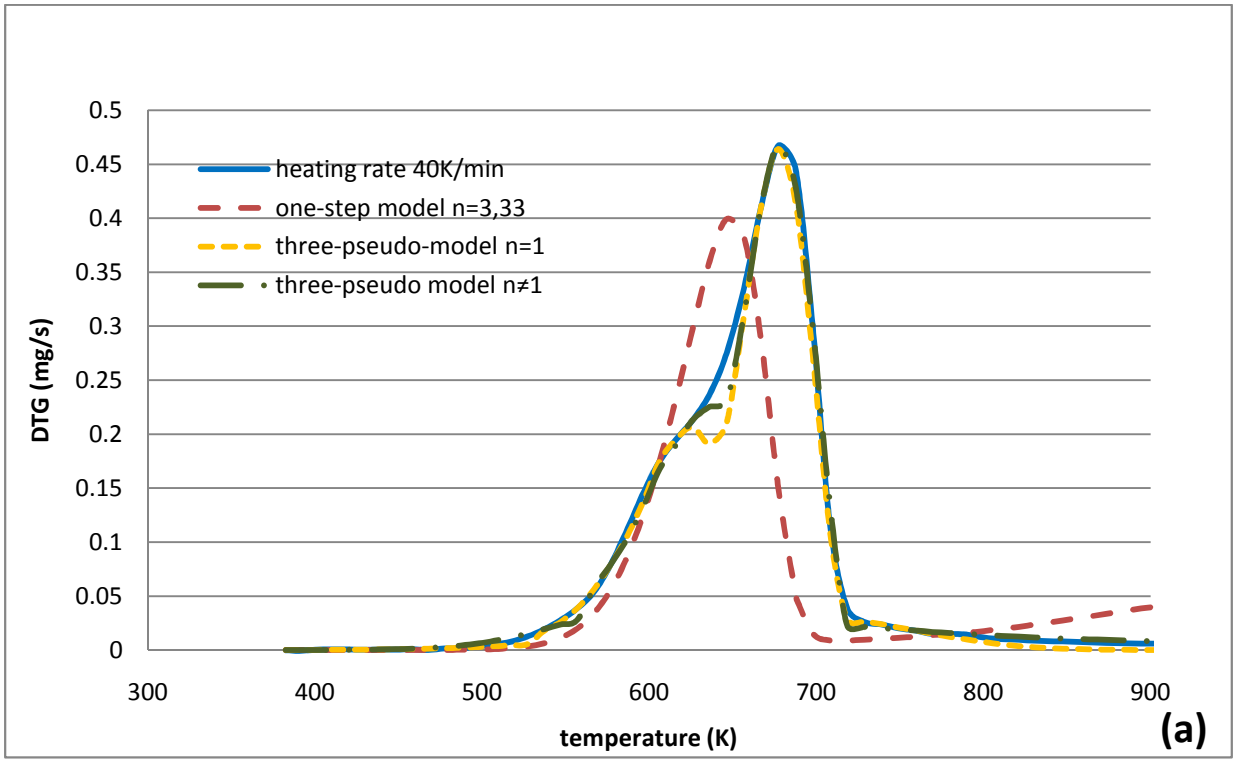

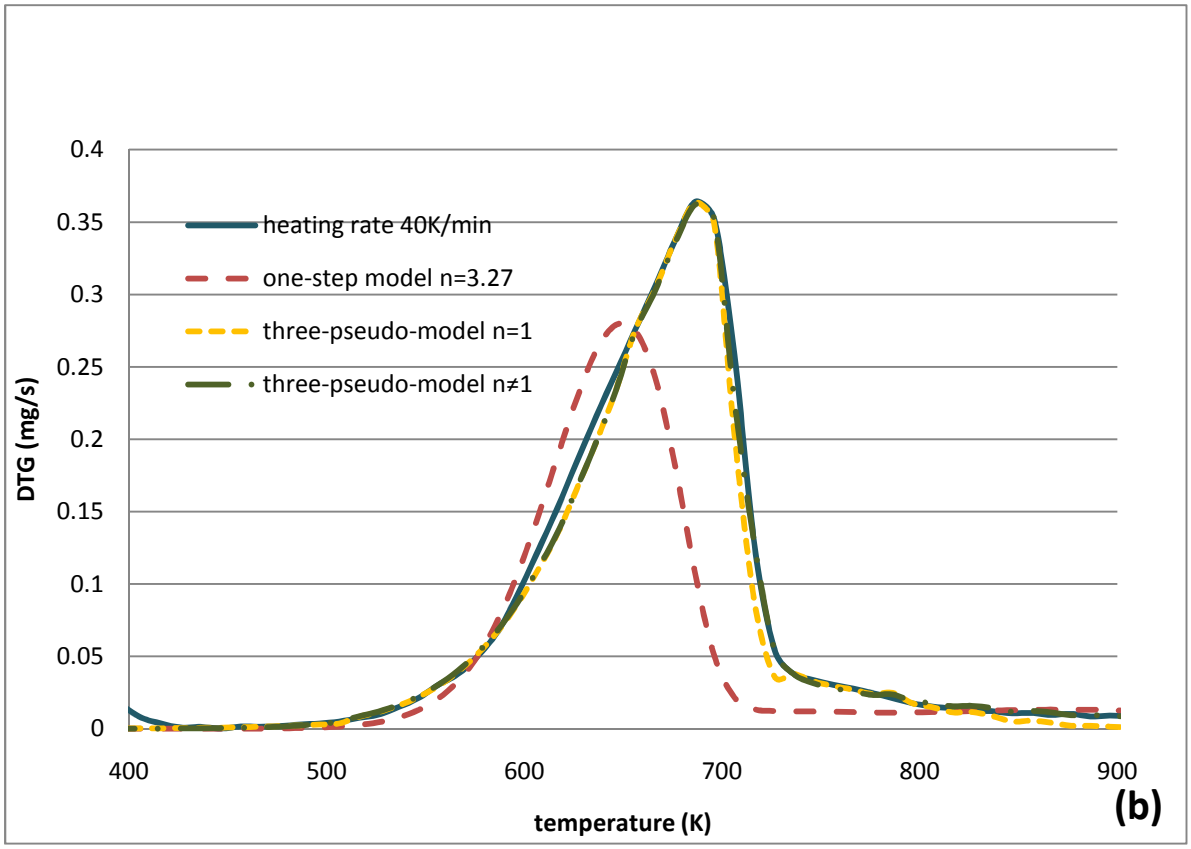

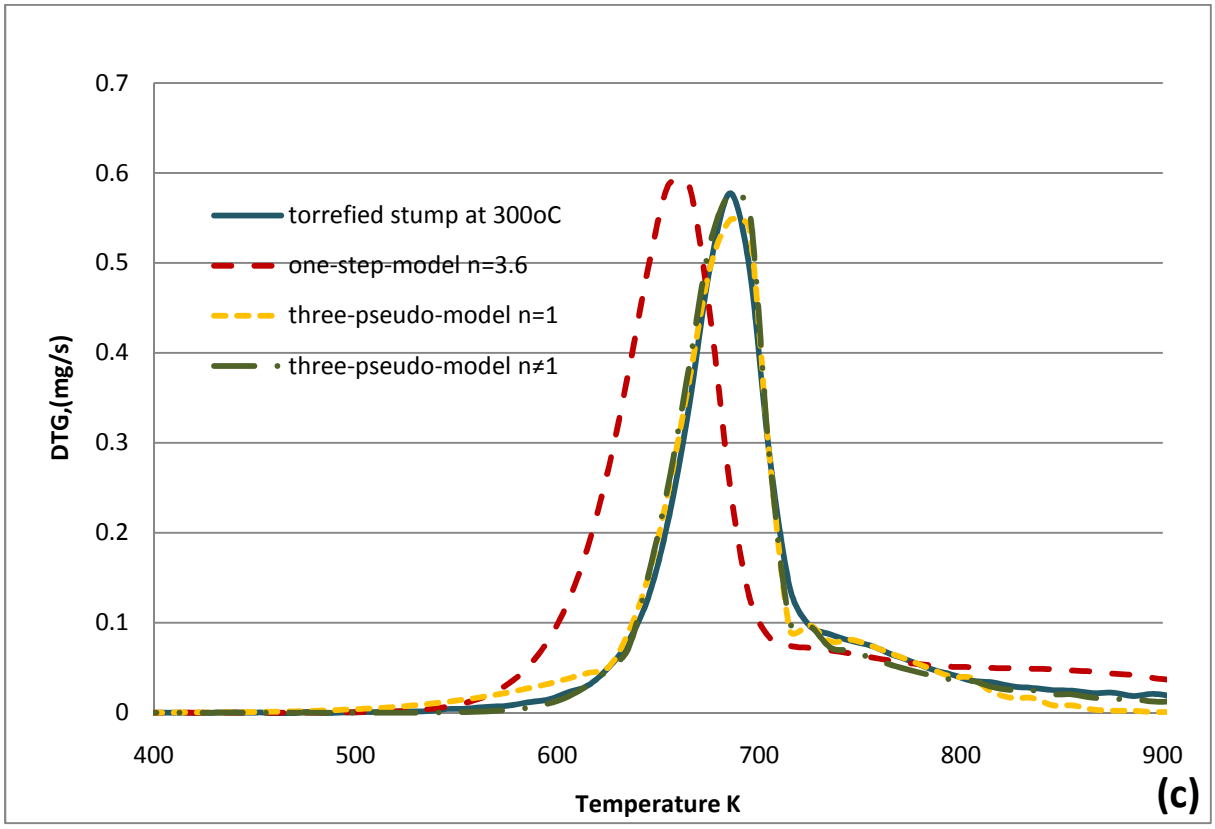

Figure 14: comparison of simulation of pyrolysis of untreated and torrefied biomass by different models at heating rate 40K/min (a: untreated poplar; b: untreated stump; c: 300^{o}C torrefied stump)

Table 9 summarizes results of best fitting value for unknown model parameters by non least square fitting method. The result of σ^2 also presents the one-step model is not appropriate to simulate the biomass thermal decomposition, even if for torrefied biomass. The three-pseudo-components model with $n \neq 1$ gives the better simulated curve than n=1.

Table 9: Kinetic data obtained by different models

Poplar at heating rate 40K/min					**Stump at heating rate 40K/min**					**300oC torrefied Stump at heating rate 40K/min**				
one-step model					**one-step model**					**one-step model**				
Ea	**A**	**n**	**σ^2**		**Ea**	**A**	**n**	**σ^2**		**Ea**	**A**	**n**	**σ^2**	
153	5.21E+12	3.33	7.01E-03		129	3.64E+10	3.27	3.22E-03		136	8.32E+10	3.6	1.00E-02	
three-pseudo-model n=1					**three-pseudo-model n=1**					**three-pseudo-model n=1**				
Ea	**A**	**C**	**σ^2**		**Ea**	**A**	**C**	**σ^2**		**Ea**	**A**	**C**	**σ^2**	
108	9.32E+08	0.56	2.27E-05		78	2.31E+06	0.27	5.74E-06		199	5.80E+15	0.38	1.85E-04	
181	3.17E+14	0.33			172	5.38E+13	0.25			58	7.94E+04	0.06		
52	3.69E+04	0.02			50	2.03E+04	0.03							
three-pseudo-model n≠1					**three-pseudo-model n≠1**					**three-pseudo-model n≠1**				
Ea	**A**	**C**	**n**	**σ^2**	**Ea**	**A**	**C**	**n**	**σ^2**	**Ea**	**A**	**C**	**n**	**σ^2**
105	1.01E+09	0.30	2.85	1.49E-05	77	1.98E+06	0.27	1.01	3.90E-06	205	1.56E+16	0.40	1.01	1.59E-04
176	1.28E+14	0.33	1.00		180	1.98E+14	0.27	1.19		184	6.77E+14	0.21	3.9	
80	2.86E+07	0.06	3.62		84	2.78E+07	0.08	2.61						

5 Concluding remarks

A reactor has been developed to use with the existing muffle furnace for studying the process of biomass torrefaction for fuel upgrading. It has been demonstrated that the reactor can be used for torrefying of biomass in nitrogen. The produced solid torrefied biomass, collected from the torrefaction of stump, poplar and Fuel tree chips have been characterized to investigate improvements in energy density, grindability, and thermal reactivity.

The result showed that the biomass torrefied at 300^{o}C for 35 minutes gave the highest heating value. The heating value of poplar torrefied at this condition increases with 14% compared with untreated poplar. For both stump and FTC the heating values increase was 12%.

Both torrefaction temperature and reaction time had strong effects on the torrefaction process. At the same torrefaction temperature, the longer reaction time, the better fuel quality the solid product had. Temperature had stronger effect in the same trend, giving higher fuel quality of the solid product at higher temperatures for the same reaction time. However, too long reaction time and/or too higher torrefaction temperature would decrease the amount of solid products, which is the main product of the torrefaction process.

TG analyses of the three biomass types have been performed in nitrogen. The results showed that the DTG curves of stump have a less pronounced shoulder compared with the other two samples, which indicates that stump has less hemicelluloses than the two other biomass types.

Ozawa method was employed to determine activation energy of thermal decomposition of the three biomasses in nitrogen. The results showed the FTC has a relatively higher average activation energy (166kJ/mol) and pre-exponential factor (3.69E+13). The average activation energy for stump and poplar were 129kJ/mol and 153kJ/mol and the average pre-exponential factor were 6.59E+10 for stump and 6.06E+12 for poplar. The activation energy and pre-exponential factor varies at different conversions.

Different kinetic models, including one step and three-pseudo-component models, were tested for the thermal decomposition of the biomasses. The first mentioned appears to be unsuitable to simulate the pyrolysis of both untreated and torrefied biomass, considering the poor fittings from the regression analysis and the resulted unrealistically high reaction order. The three-

pseudo-component model (n=1 or n≠1) appears to be suitable for simulating the behaviour of biomass during thermal decomposition. The best fittings were observed for the model with n ≠1.

This is a preliminary study of torrefaction of stump for use as fuel. Further research and developments are needed to improve the operation of the reactor. Better gas flow controllers, higher heating rates, possibilities to monitor oxygen concentration in the reactor and chemical compositions of gas products released from process are recommended.

6 Acknowledgement

This work was carried out at the Bioenergy, Department of Energy and Technology, Swedish University of Agriculture Sciences, under supervision of Dr. Khanh-Quang Tran, whose academic supports and scientific guidance are gratefully acknowledged. Whenever I hade technical and theoretical problems during this project, my supervisor always encouraged me, actively gave me good advices, and discussed with me to solve the problems.

I would like to thank Professor Tord Johansson for approving my research proposal and allowing me to carry out the work at the Bioenergy lab.

I would also like to thank Dr. Gulaim Seisenbaeva for her kind collaboration and supports in performing TG and SEM analyses and data collection.

Special thanks are due to Dr. Raida Jirjis, Dr. Almir Karacic, Erik Anerud and Anders Eriksson for providing with biomass samples and making the facilities available.

I thank all the administrative and technical staff at Energy and Technology, SLU, who helped me during the project. Special thanks are due to Sven Smårs and Dick Gustafsson for practical supports.

7 References

[1] Energiläget i siffror 2010 Energy in Sweden– facts and figures 2010. 2010

[2] Bergman P.C.A., Boersma A.R., Kiel J.H.A., Prins.M.J., Ptasinski K.J., Janssen F.J.J.G., 2005. ECN Torrefaction for entrained-flow gasification of biomass. ECN-C--05-067

[3] Drift A.van der, Boerrigter H., Coda B., Cieplik M.K., Hemmes K., 2004. ENTRAINED FLOW GASIFICATION OF BIOMASS--Ash behaviour, feeding issues, and system analyses. ECN-C--04-039

[4] Koukious, E.G., Mavrokoukoulakis, J. and Abatzoglou, N., 1982. Energy densification of biomass, Proc. 1st. National Conf. On Soft Energy Forms, Thessaloniki

[5] SS 18 71 70. SIS 1997, Swedish Standard. Biofuels-Determination of moisture content

[6] SS 18 71 71. SIS 1984, Swedish Standard. Biofuels-Determination of ash content

[7] SS 18 71 82. SIS 1990, Swedish Standard. Solid material fuels-Determination of the gross or calorific heating value by bomb calorimetric method, and calculation of the net or effective heating value

[8] Anerud E. 2010. Stump as a fuel- the influence of harvesting technique and storage method on fuel quality of Norway spruce. Licentiate thesis SLU ISSN 1654-9406

[9] Strömberg B., 2005, .Bränslehandboken- handbok av fuel. VÄRMEFORSK Service AB, ISSN 0282-3772

[10] Karacic A., post doctor, Swedish University of Agricultural Sciences.
Department of Energy and Technology

[11] Eriksson A, Civilingenjör, Swedish University of Agricultural Sciences. Department of Energy and Technology

[12] Phanphanich M. Mani S. 2010. Impact of torrefaction on the grindability and fuel characteristics of forest biomass. Bioresour. Technol.doi:10.1016/j.biortech 2010.08.028

[13] Uslu A. Faaj A.P.C.. Bergman P.C.A.. 2008. Pre-treatment technologies. and their effect on international bioenergy supply chain logistics. Techno-economic evaluation of torrefaction. fast pyrolysis and pelletisation Elsevier ltd. All rights reserved doi: 10.1016/j.energy.2008.03.007

[14] Prins M.J..Ptasinski K.J.. Janssen F.J.J.G.. 2006. More efficient biomass gasification via torrefaction. Elsevier Ltd. Doi:10.1016/j.energy.2006.03.008

[15] Evan E. David A. 1998. Biomass cofiring: status. prospects 1996. Fuel processing technology 54 (1-3)

[16] David.A. 2000. Biomass cofiring: the technology. the experience. the combustion consequences. Biomass and bioenergy 19(6) 365-384

[17]Bergman PCA. Combined torrefaction and pelletisation: the top process. Petten. the Netherlands: ECN 2005

[18] J. Deng. G-J Wang. J-h Kuang. Y-l Zhang. Y-h Luo. pretreatment og agricultural residues for co-gasification via torrefaction. J.Anal. Appl. Pyrolysis 86(2009) 331-337

[19] Song Hu. Andreas Jess. Minhou Xu. Kinetic study of Chinese biomass slow pyrolysis: comparison of different Kinetic models

[20] Wei-Hsin C. Po-Chih K. 2010. A study on torrefaction of various biomass materials and its impact on lignocellulosic structure simulated by a thermogravimetry. Energy 35 2580-2586

[21]Lukas G. Zuzana K. L'uduovit. Tatranske M. 2009 May 25-29. Kinetic study of wood chips decomposition by TGA. Slovakia.

[22] Karacic A. 2005. Production and Ecological Aspects of Short Rotation Poplars in Sweden Acta Universitatis Agriculturae Sueciae: 13

[23] Simon P. 2004. Isoconversional methods: fundamentals. meaning and application. Journal of Thermal Analysis and calroimetry. Vol 76 123-132.

[24] Vlaev* L.T.. Markosvska I.G.. Lyubchev L.A.. 2003. Non-Isothermal Kinetics of pyrolysis of rice husk. Thermochimica Acta 406 1-7.222

[25] Arias B. Pevida C. Fermoso J. Plaza M.G.. Rubiera F. Pis J.J. 2008. Influence of torrefaction on the grindability and reactivity of woody biomass Elsevier doi:10.1016

[26] Bridge T.G.. Jones J.M.. Williams A.. Waldron D.J.. 2010. An investigation of the grindability of two torrefied energy crops. Elsevier 3911-3918.

[27] Müller-hagedor M. Bockhorn H. Krebs L. Müller U. 2003. A comparative kinetic study on the pyrolysis of three different wood species. J. Anal. Pyrol. p. 231-249

[28] Fisher T. Hajaligol M. Waymack B. Kellogg D. 2003. Pyrolysis behavior and kinetics of biomass derived material. J. Anal Appl. Pyrol. 62 p. 331-349

[29] Wang G. Li W. Li B. Chen H. 2008. TG study on pyrolysis of biomass and its three components under syngas. Fuel 87 p. 552-558

[30]Vamvuka. D. Kakaras.E. Kastanaki.E. 2003. Pyrolysis characteristics and kinetics of biomass residual mixture with lignite. Fuel 82. 1949-1960.

[31] Ozawa T. 1965. Bull.chem.Soc Jpn. 38 1881.

[32]Ozawa T. 1970. J. Therm.Anal. 2. 301.

[33]Ozawa T. 1975. J. Therm.Anal. 7. 601

[34]Ozawa T. 1976. J. Therm.Anal. 9. 217.

[35] Flynn J.H. 1982. The isoconversional method for determination of energy of activation at constant heating rates—corrections for the Dolye approximation. J. Thermal Anal. 17.

[36] Doyle. C. D. 1962. Estimating isothermal life from thermogravimetric data. Journal of Applied Polymer Science. 6: 639–642. doi: 10.1002/app.070062406

[37]Blasi D. 2008. Modeling chemical and physical processes of wood and biomass pyrolysis. Progress in energy and Combustion Science. 23(1):p. 47-90

[38] Mészáros E. Várhegyi G. and Jakab E. 2004. Thermoagravimetric and reaction Kinetic Analysis of Biomass samples from an energy plantation. Energy & Fueks 18 p. 497-507

[39] Várhegyi G. Bobály B. Jakab E. 2011. Thermogravimetric study of biomass Pyrolysis Kinetics. A distributed Activation energy model with predication tests. Energy & Fuel 25. p. 24-32

8 Appendix

Appendix 1

Weight loss curves of poplar samples at heating rate 10K/min from TGA

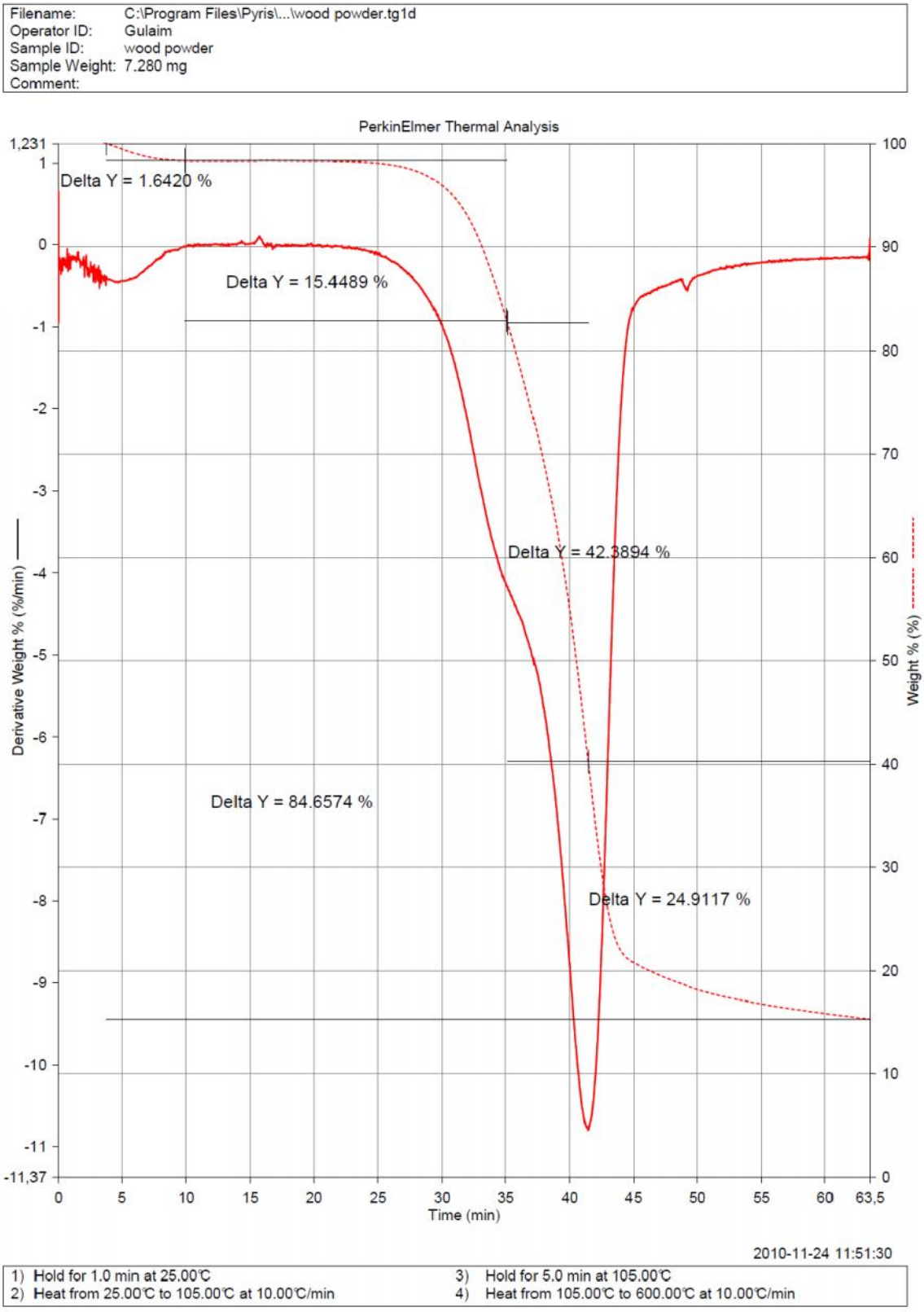

Weight loss curves of poplar samples at heating rate 20K/min from TGA

Filename:	C:\Program Files\Pyr...\wood powder_20.tg1d
Operator ID:	Gulaim
Sample ID:	wood powder_20
Sample Weight:	8.101 mg
Comment:	

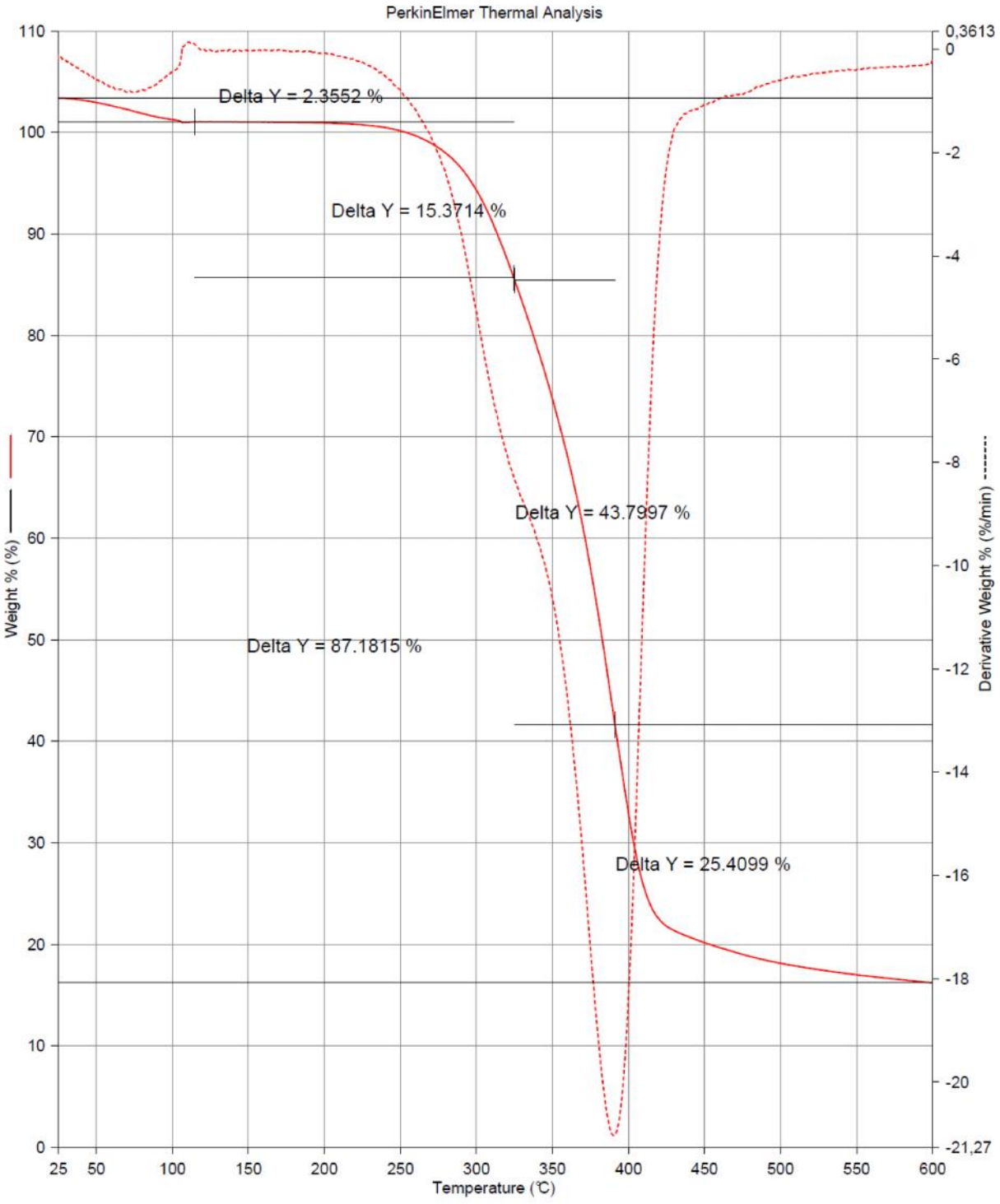

1) Hold for 1.0 min at 25.00°C
2) Heat from 25.00°C to 105.00°C at 20.00°C/min
3) Hold for 5.0 min at 105.00°C
4) Heat from 105.00°C to 600.00°C at 20.00°C/min

Weight loss curves of poplar samples at heating rate 40K/min from TGA

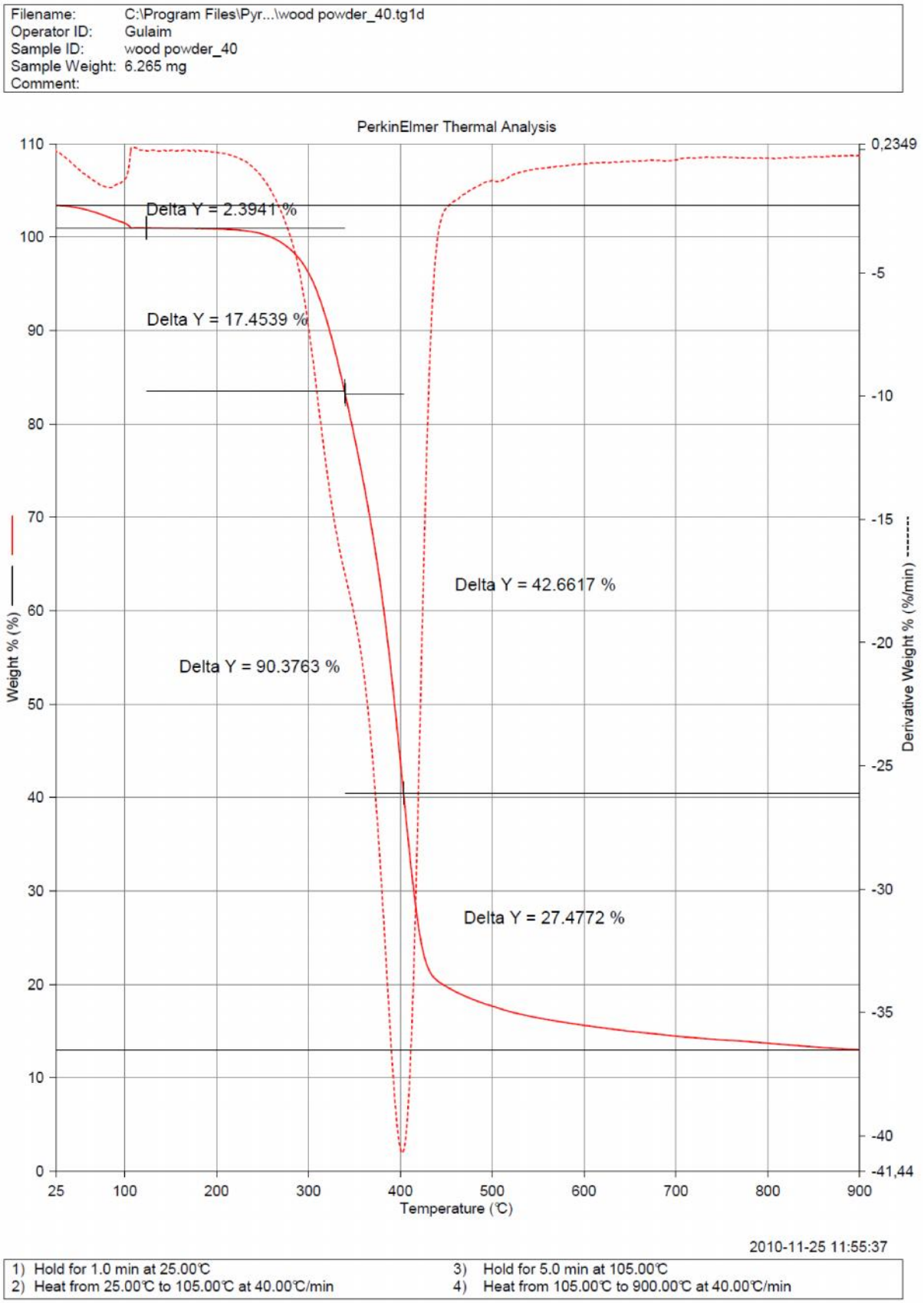

Appendix 2

Weight loss curves of FTC samples at heating rate 10K/min from TGA

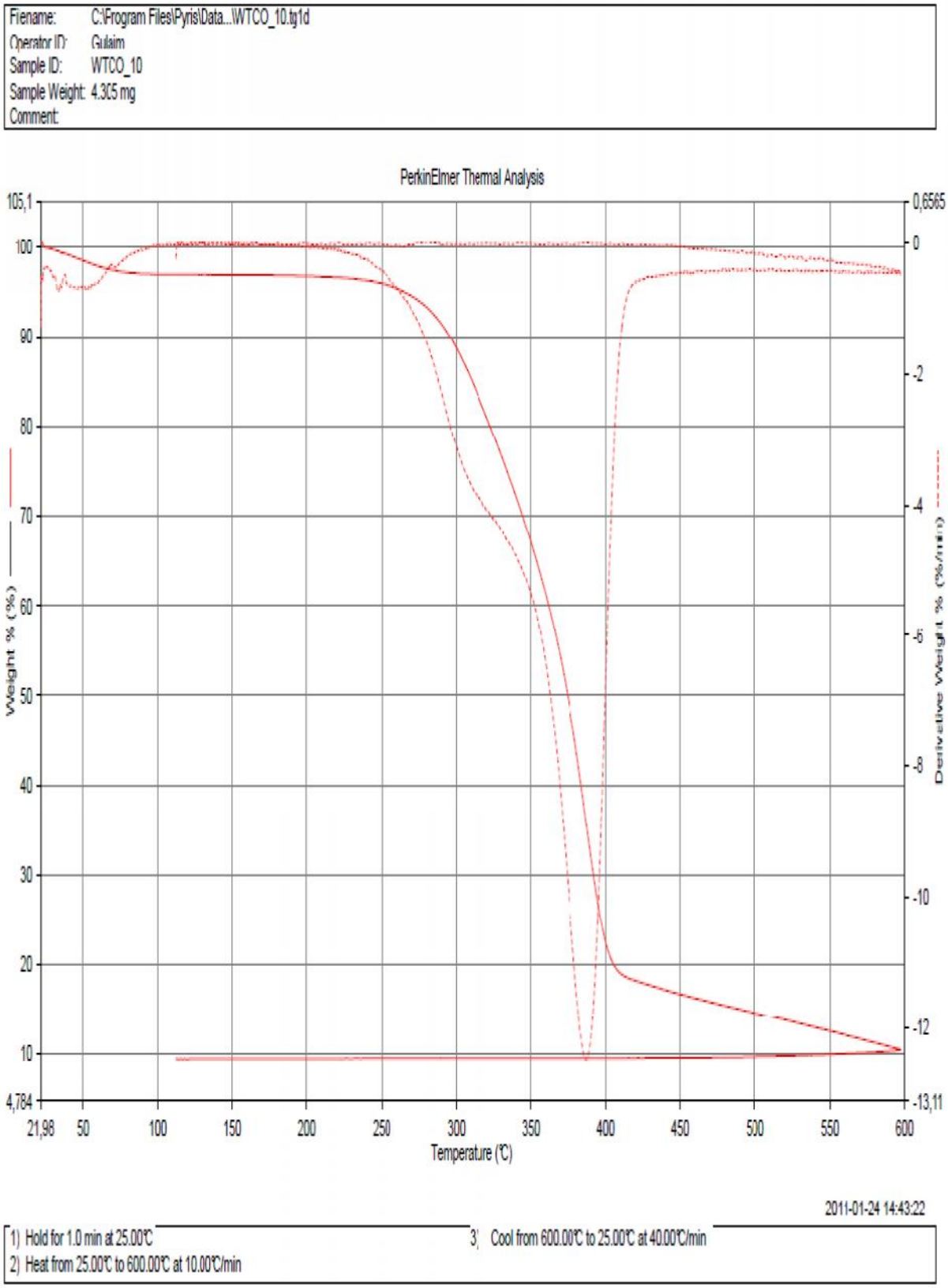

Weight loss curves of FTC samples at heating rate 20K/min from TGA

Filename:	C:\Program Files\Pyris\Data...\WTCO_20.tg1d
Operator ID:	Gulaim
Sample ID:	WTCO_20
Sample Weight:	4.190 mg
Comment:	

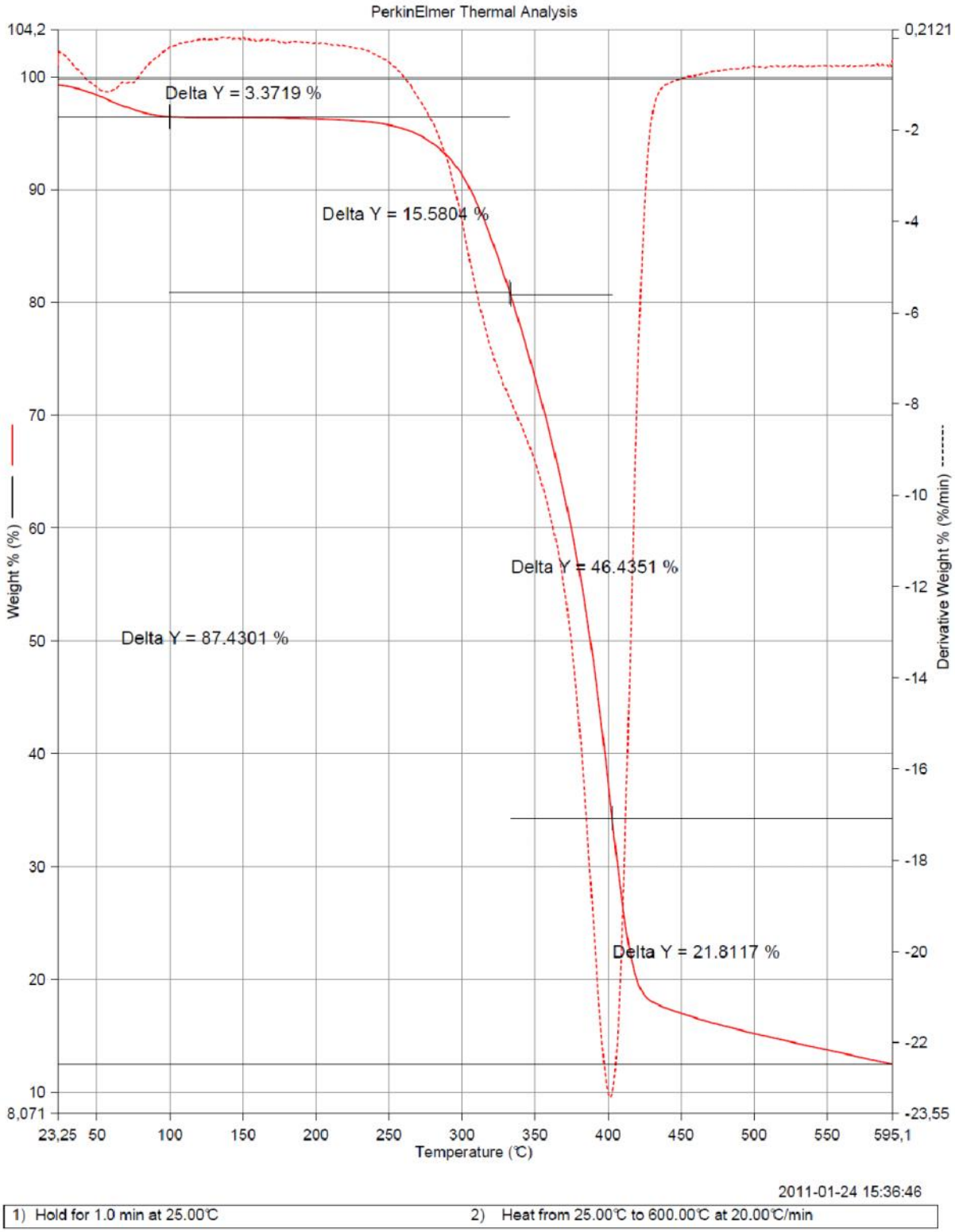

1) Hold for 1.0 min at 25.00°C	2) Heat from 25.00°C to 600.00°C at 20.00°C/min

Weight loss curves of FTC samples at heating rate 40K/min from TGA

Filename:	C:\Program Files\Pyris\Data...\WTCO_40.tg1d
Operator ID:	Gulaim
Sample ID:	WTCO_40
Sample Weight:	6.121 mg
Comment:	

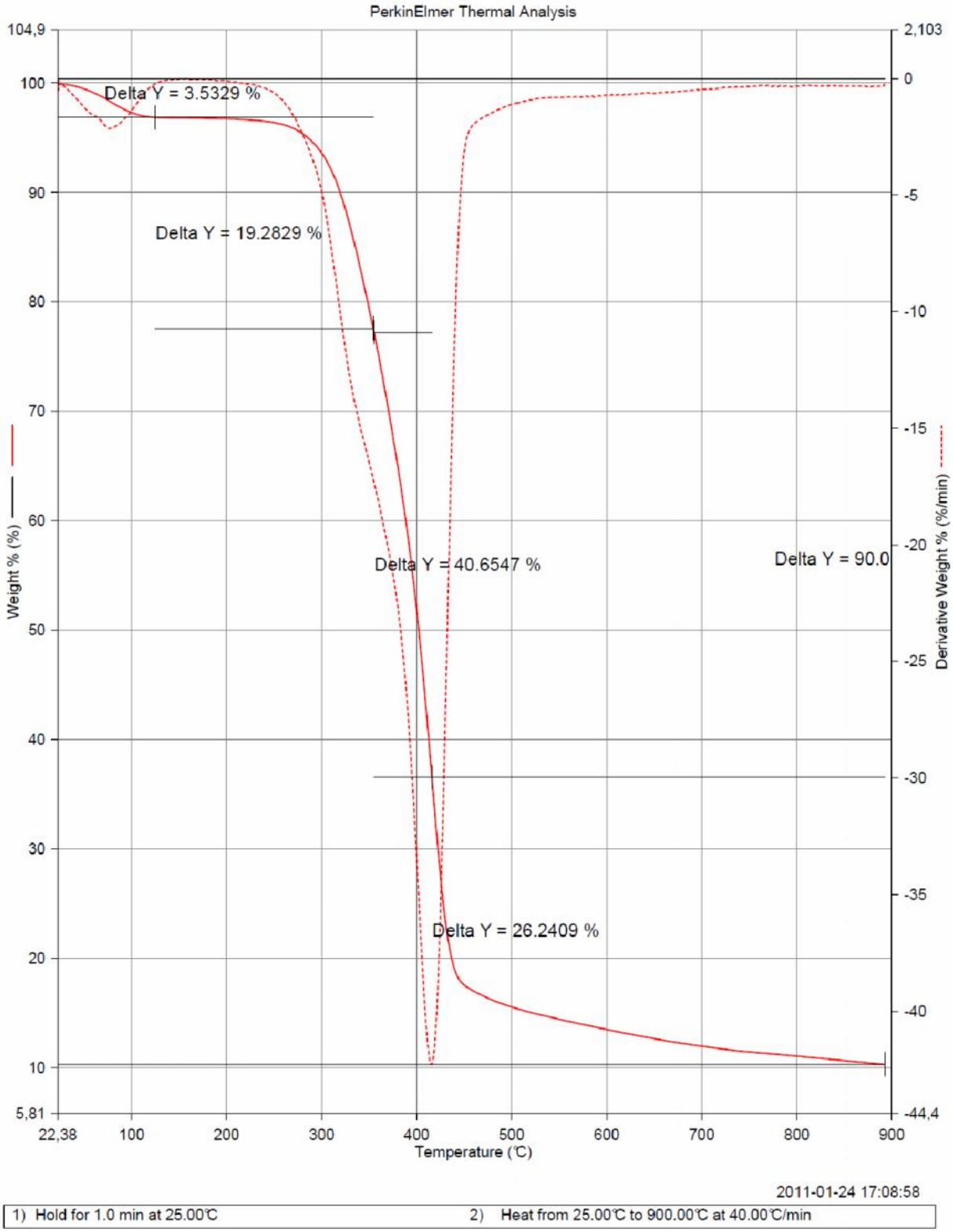

Appendix 3

Weight loss curves of stump samples at heating rate 10K/min from TGA

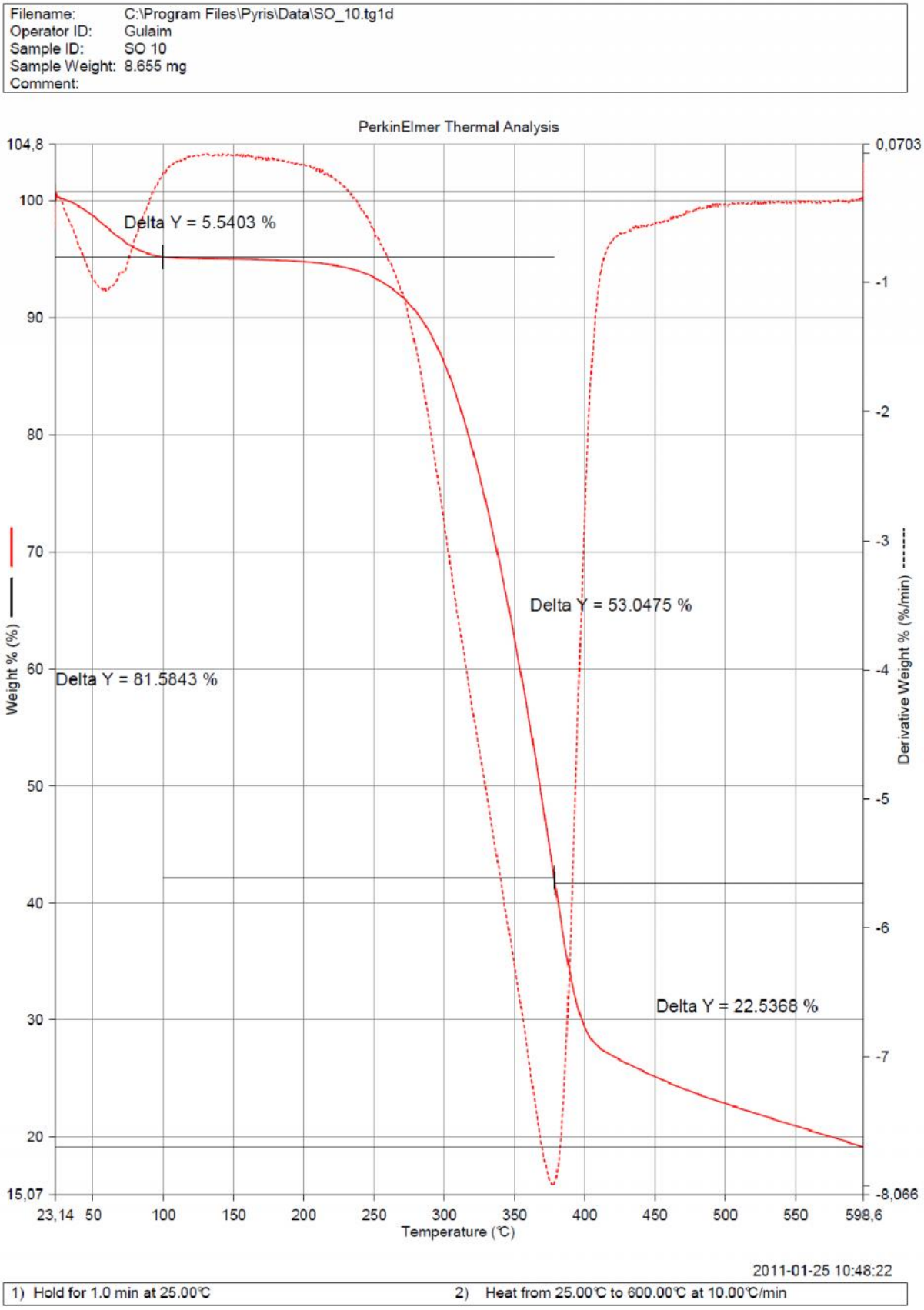

Weight loss curves of stump samples at heating rate 20K/min from TGA

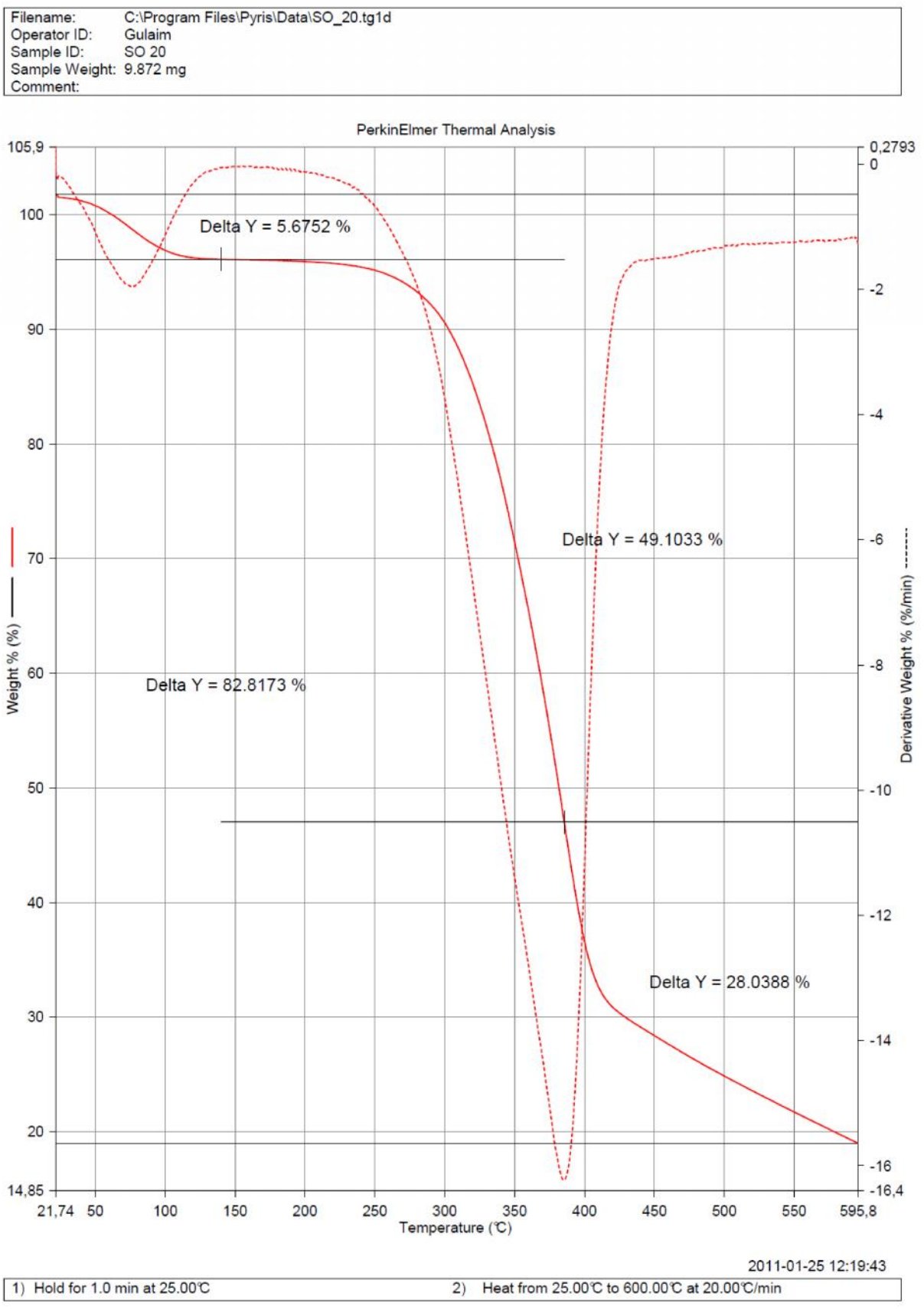

Weight loss curves of stump samples at heating rate 40K/min from TGA

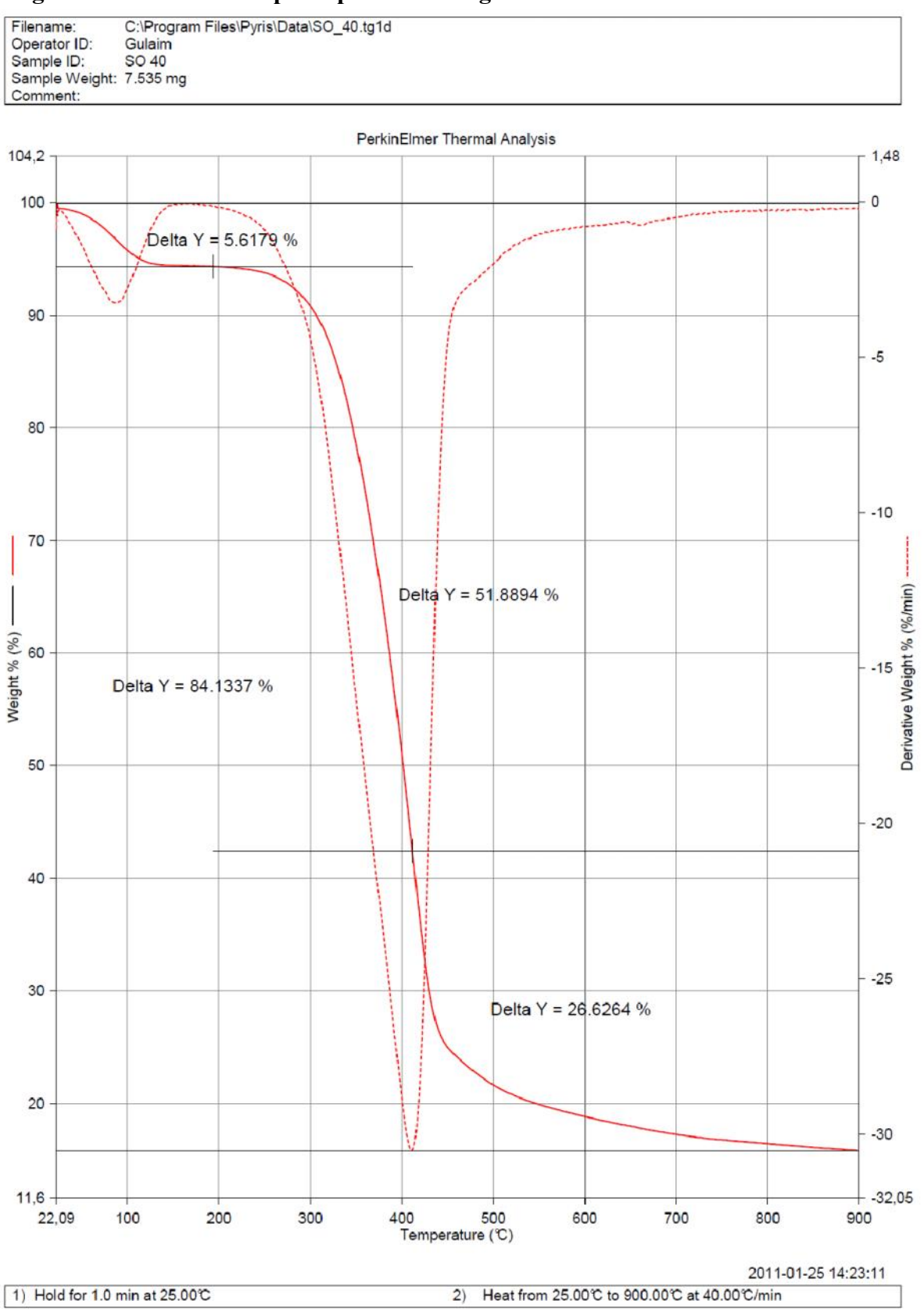

Appendix 4

Weight loss curves of untreated stump samples at heating rate 40K/min from TGA

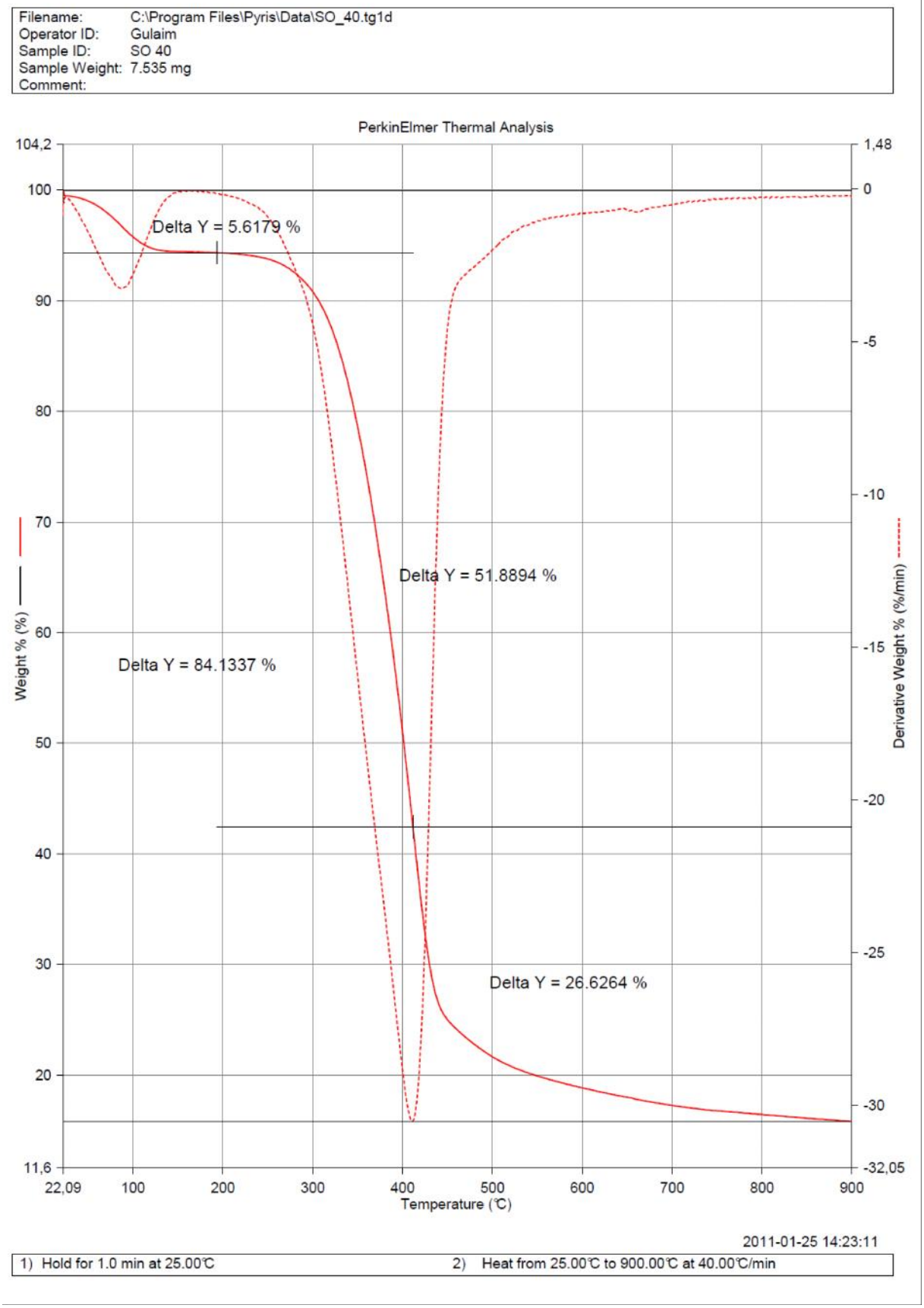

Weight loss curves of torrefied stump samples at 200°C for 10min with heating rate 40K/min from TGA

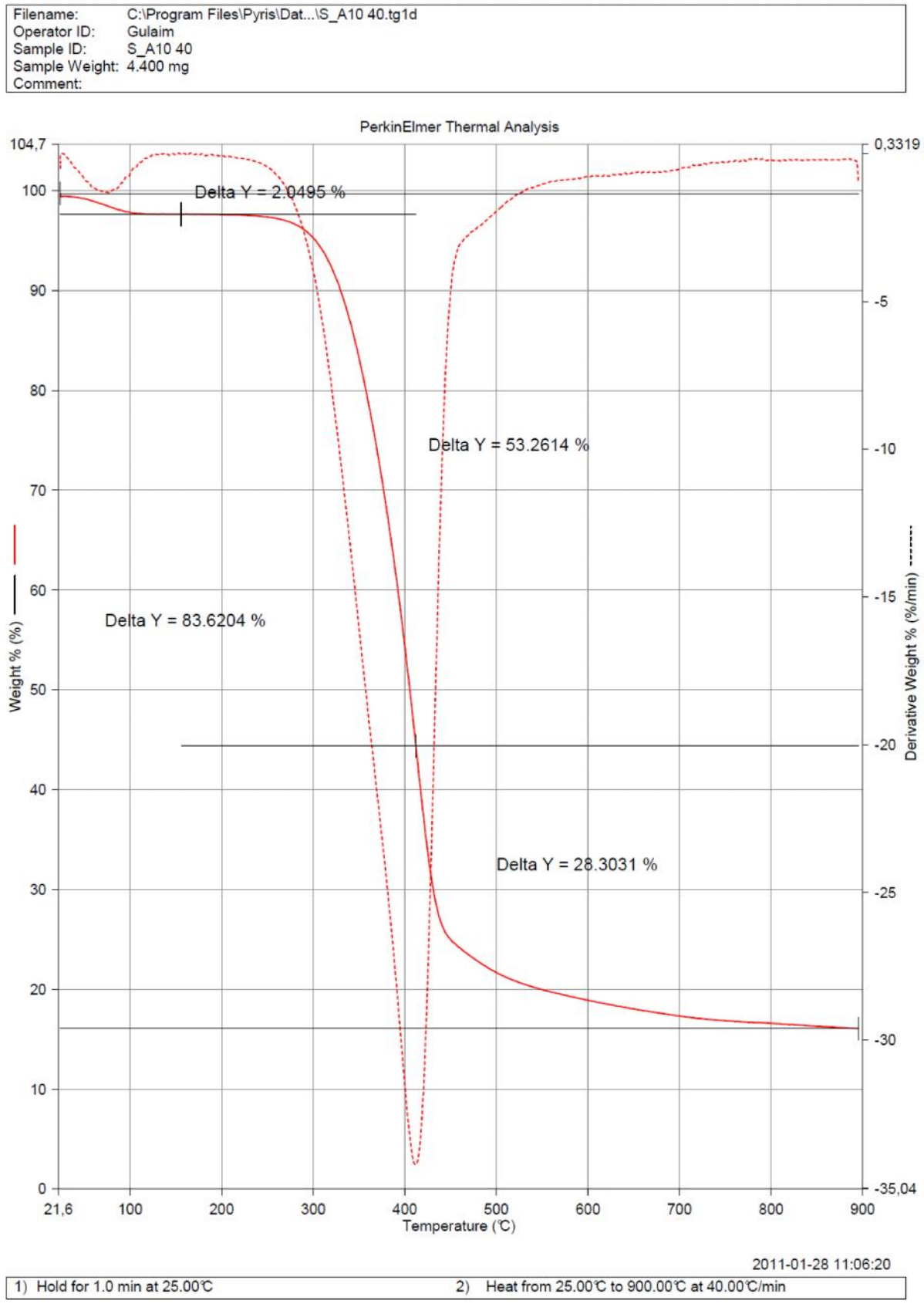

Weight loss curves of torrefied stump samples at 250°C for 10min with heating rate 40K/min from TGA

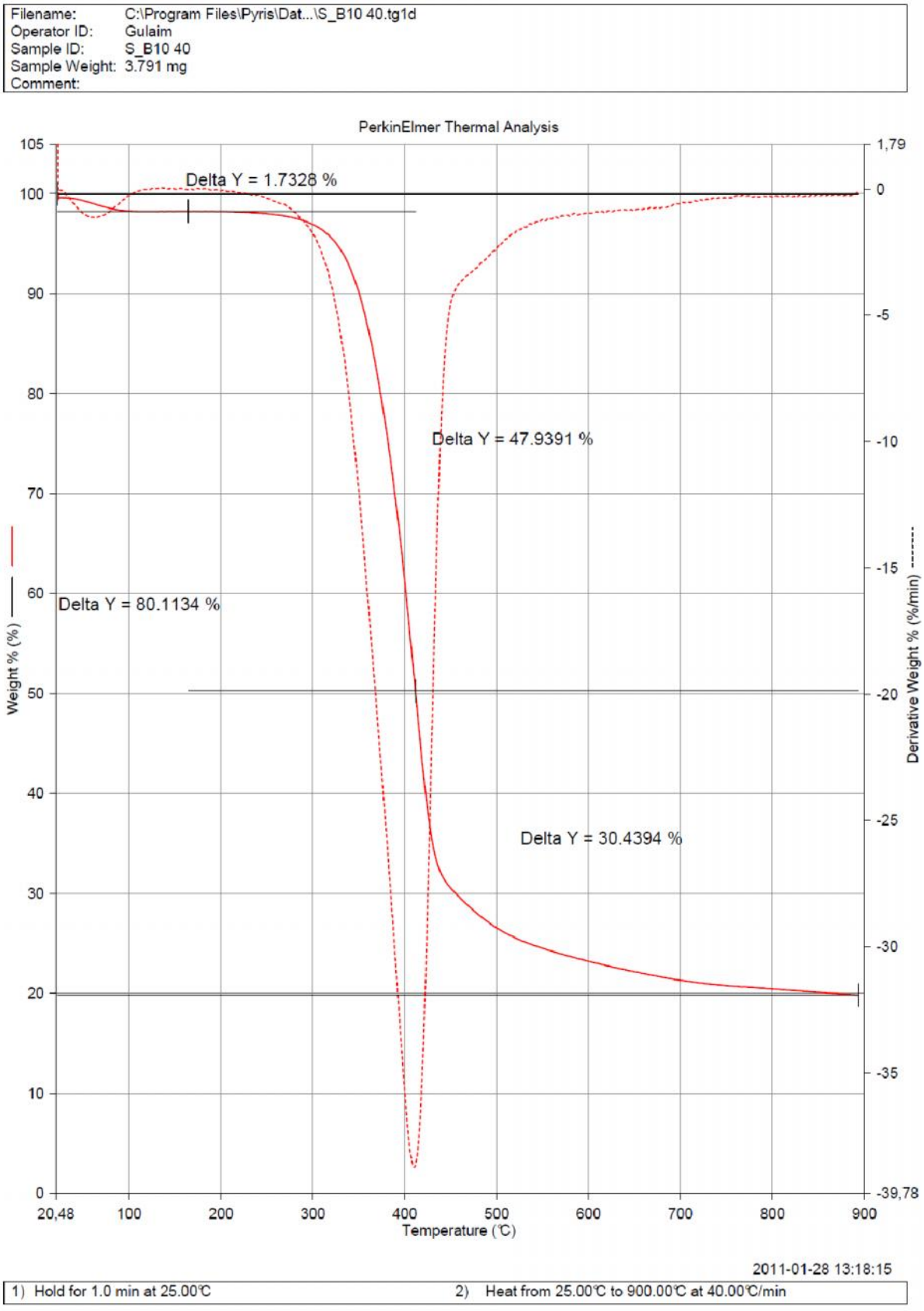

Weight loss curves of torrefied stump samples at 300°C for 10min with heating rate 40K/min from TGA

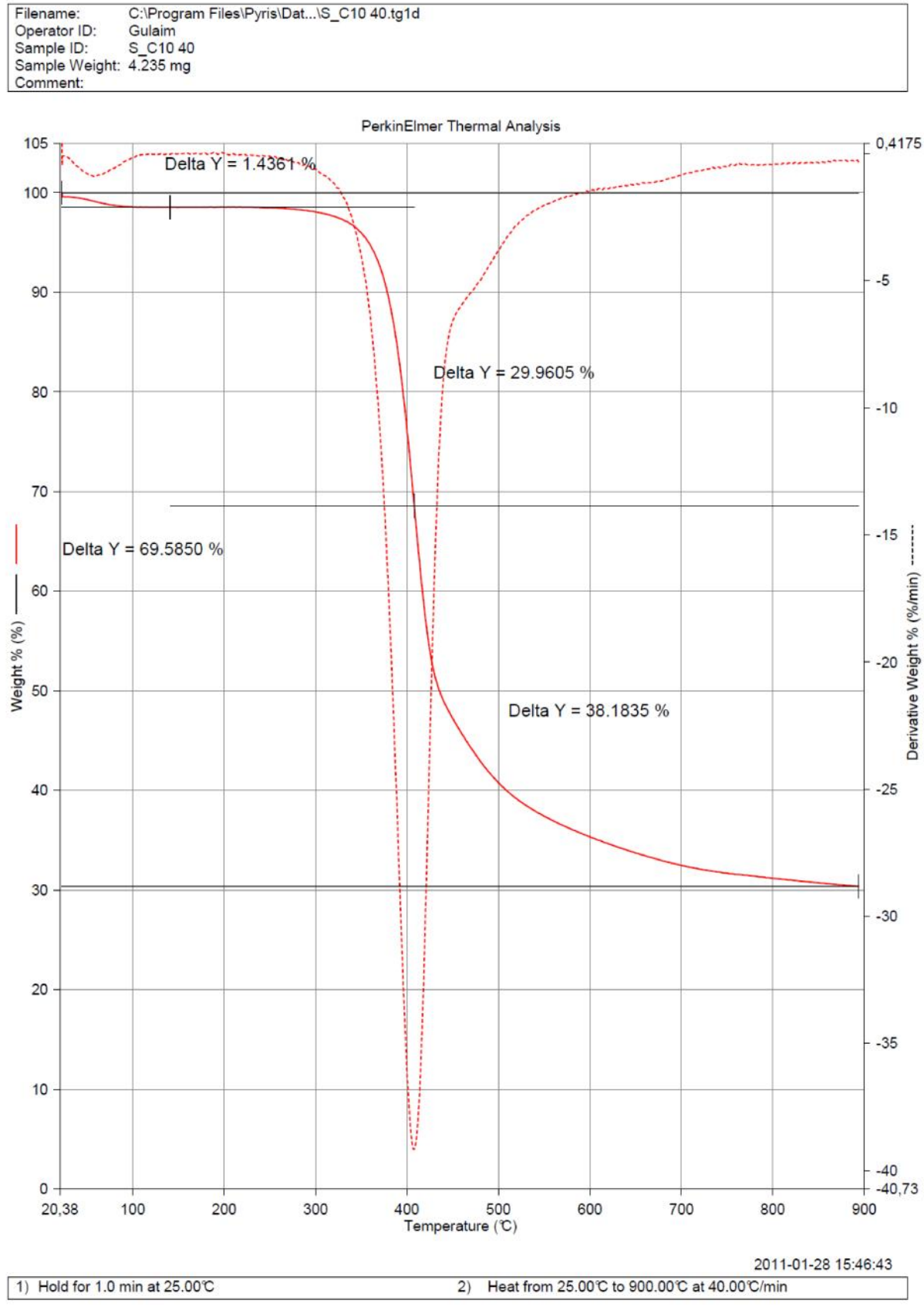

Appendix 5

Single reaction one step model for untreated poplar sample at heating rate 10K/min. 20K/min and 40K/min

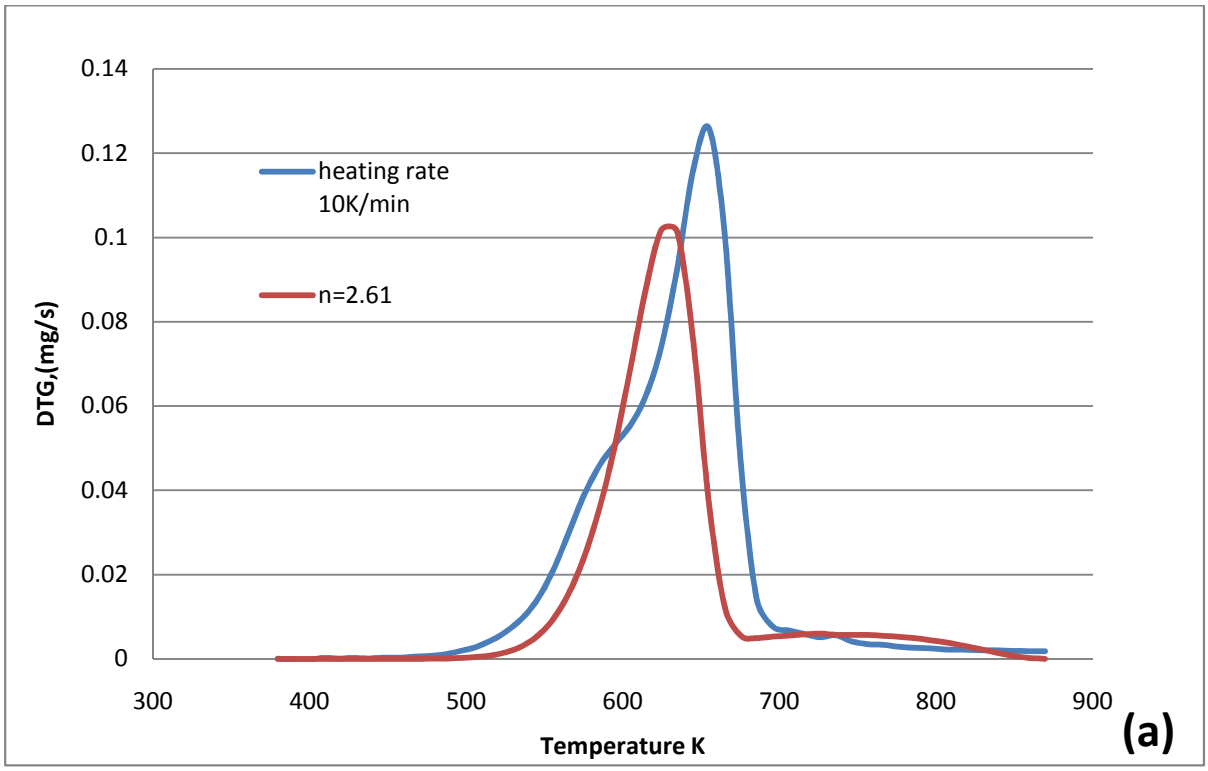

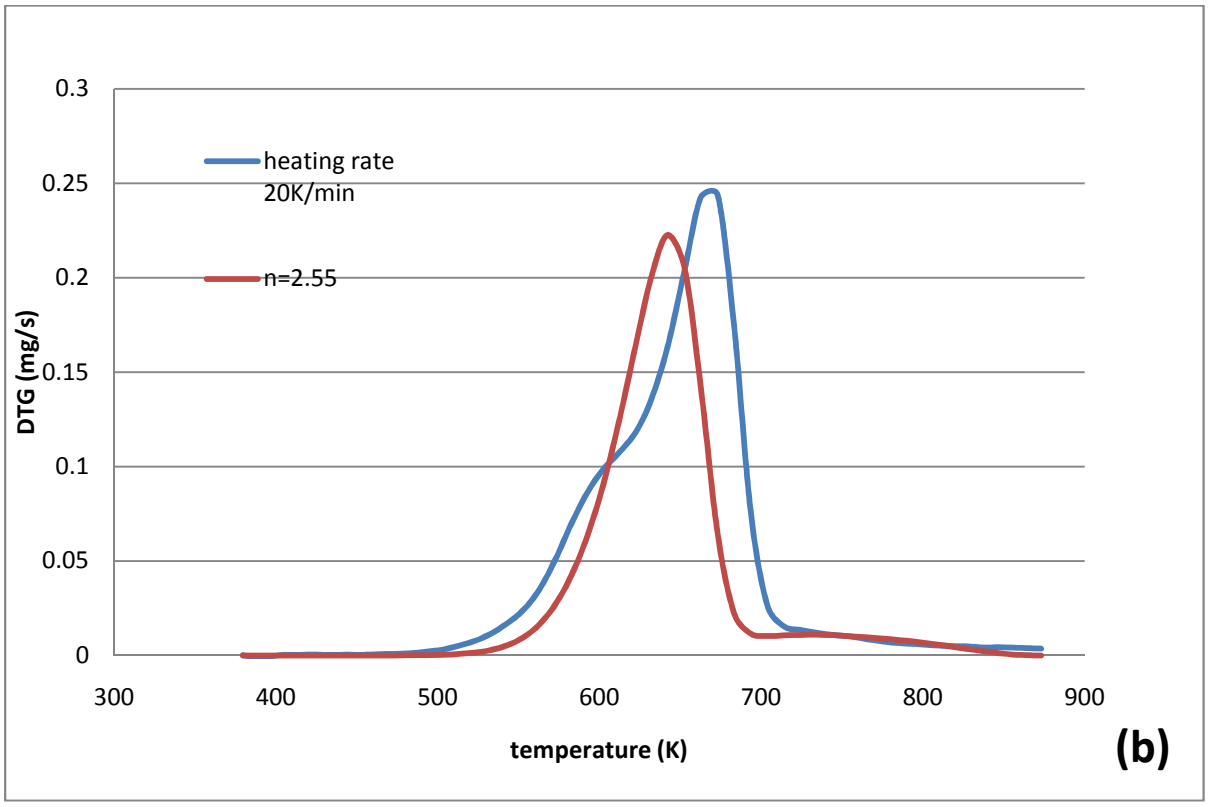

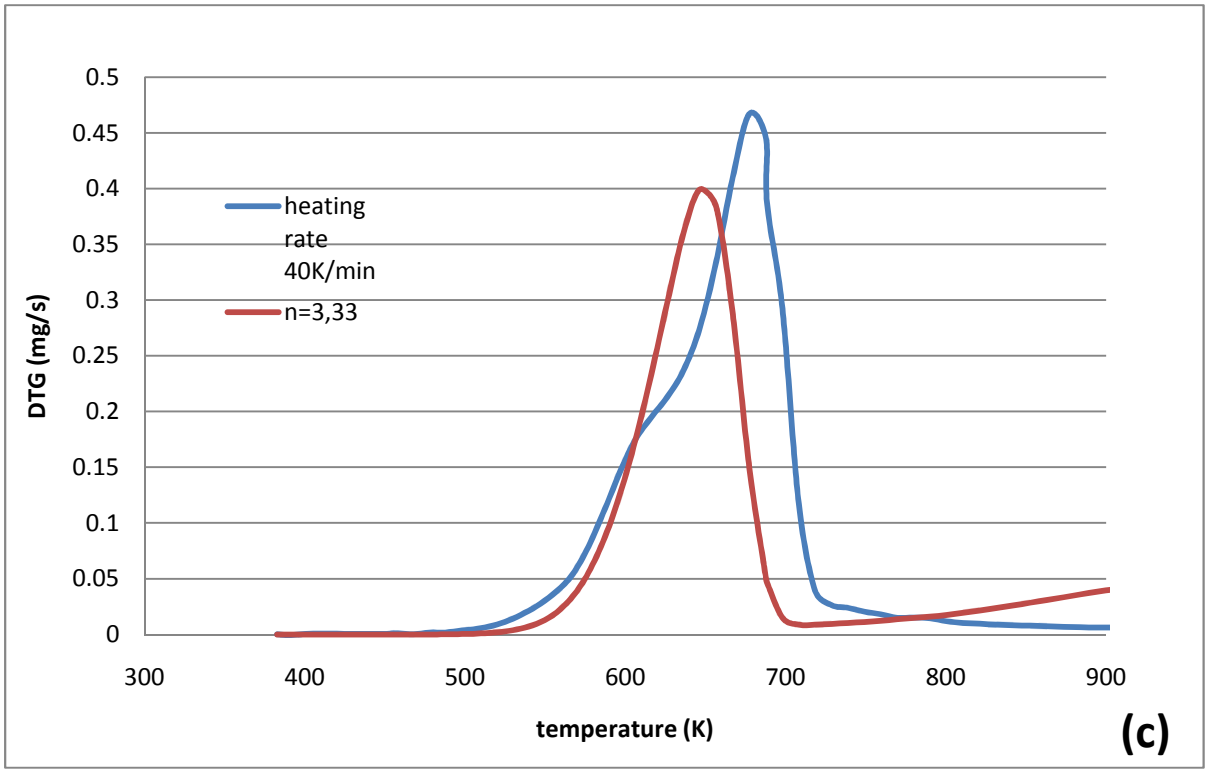

Figure 15: DTG simulation results by a one-step model of poplar pyrolysis at different heating rate (a: 10K/min; b: 20K/min; c: 40K/min)

Appendix 6

Single reaction one step model for untreated stump sample at heating rate 10K/min. 20K/min and 40K/min

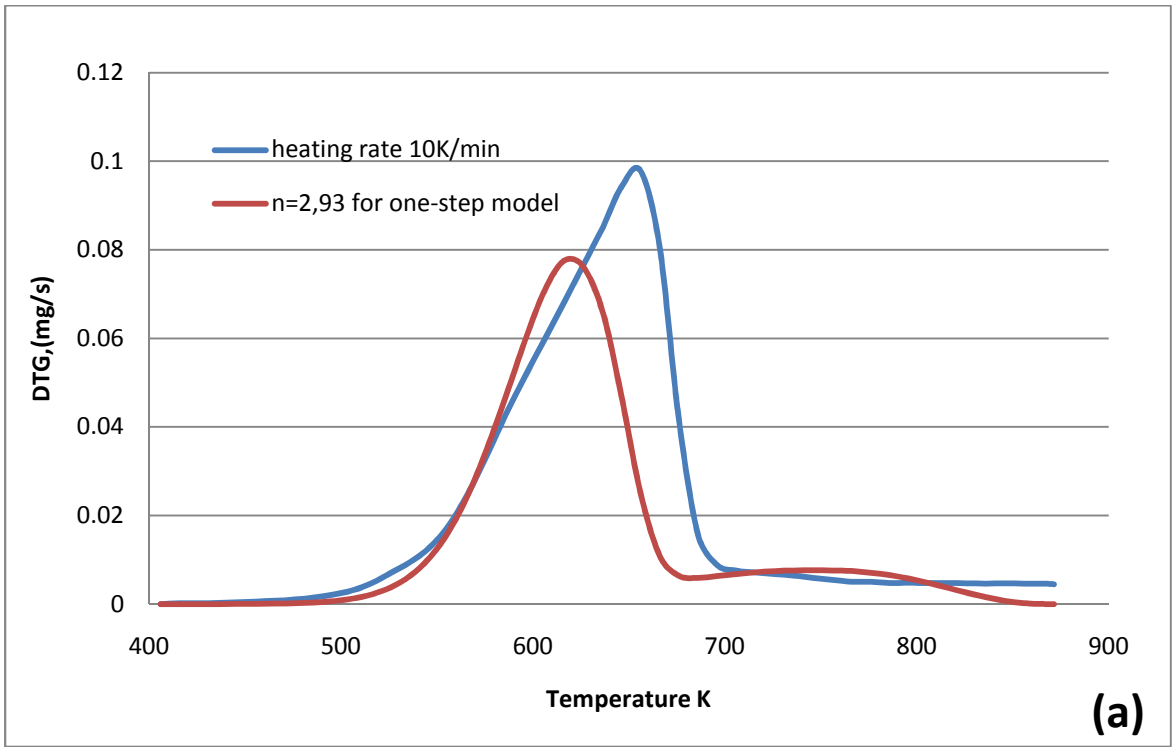

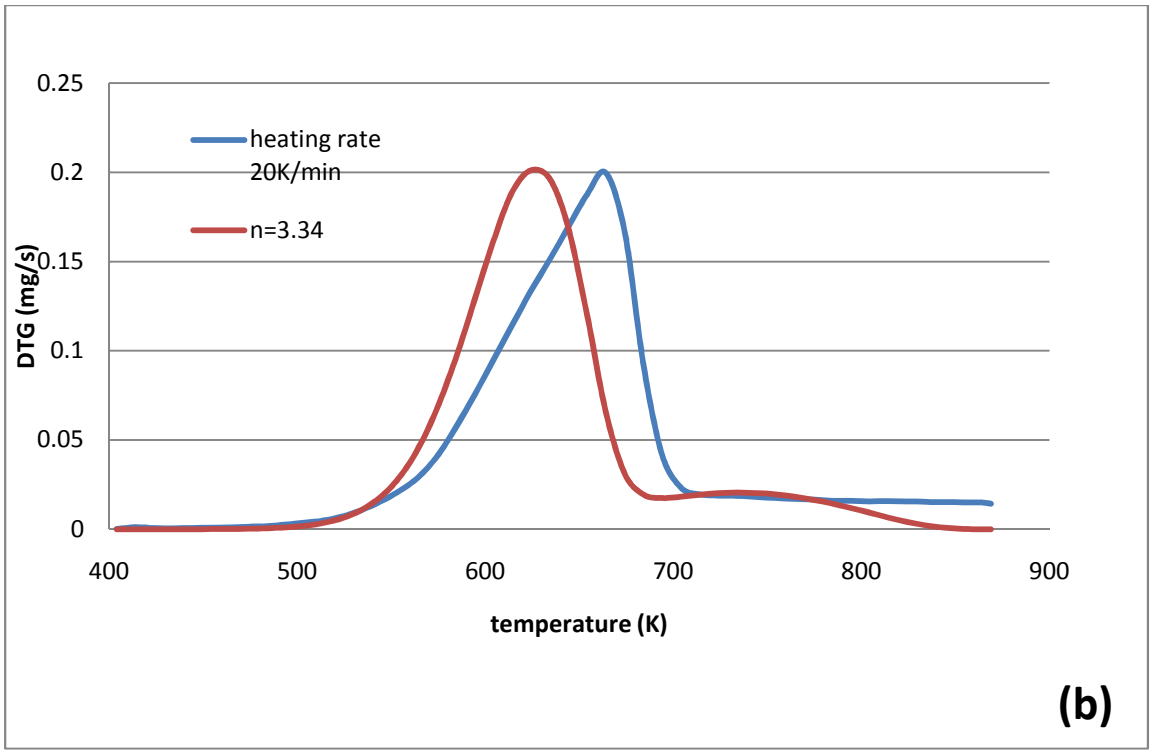

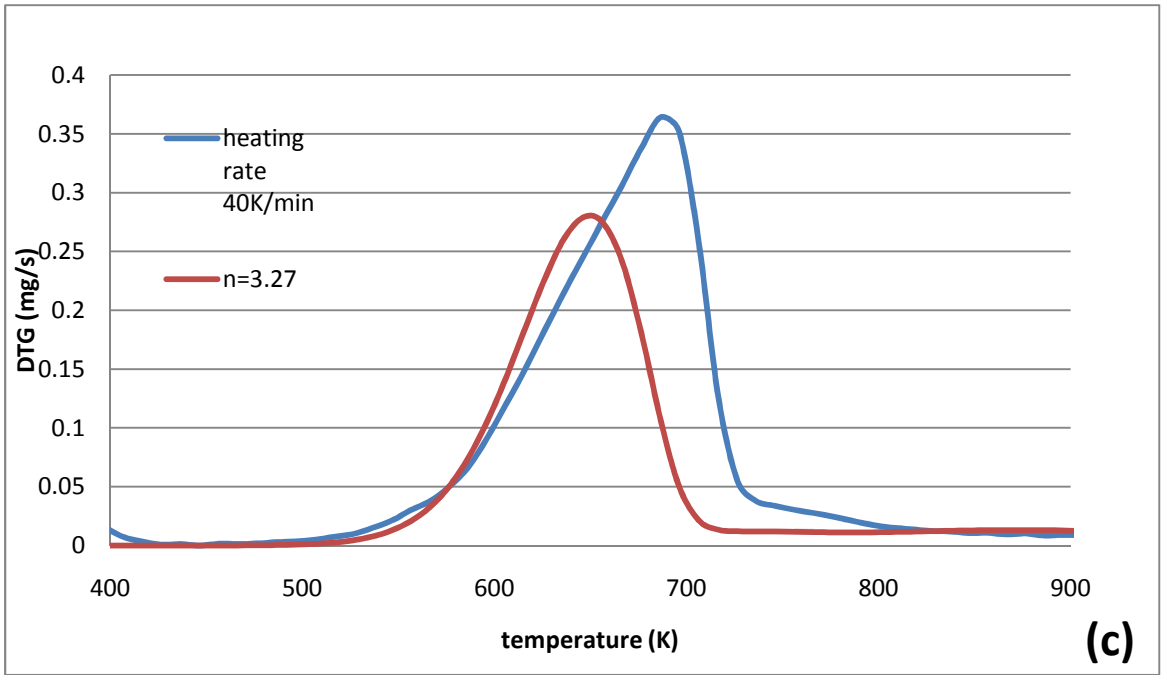

Figure 16: DTG simulation results by a one-step model of stump pyrolysis at different heating rate (a:10K/min; b: 20K/min; c: 40K/min)

Appendix 7

Three-pseudo-components model (n=1) for untreated poplar sample at heating rate 10K/min. 20K/min and 40K/min

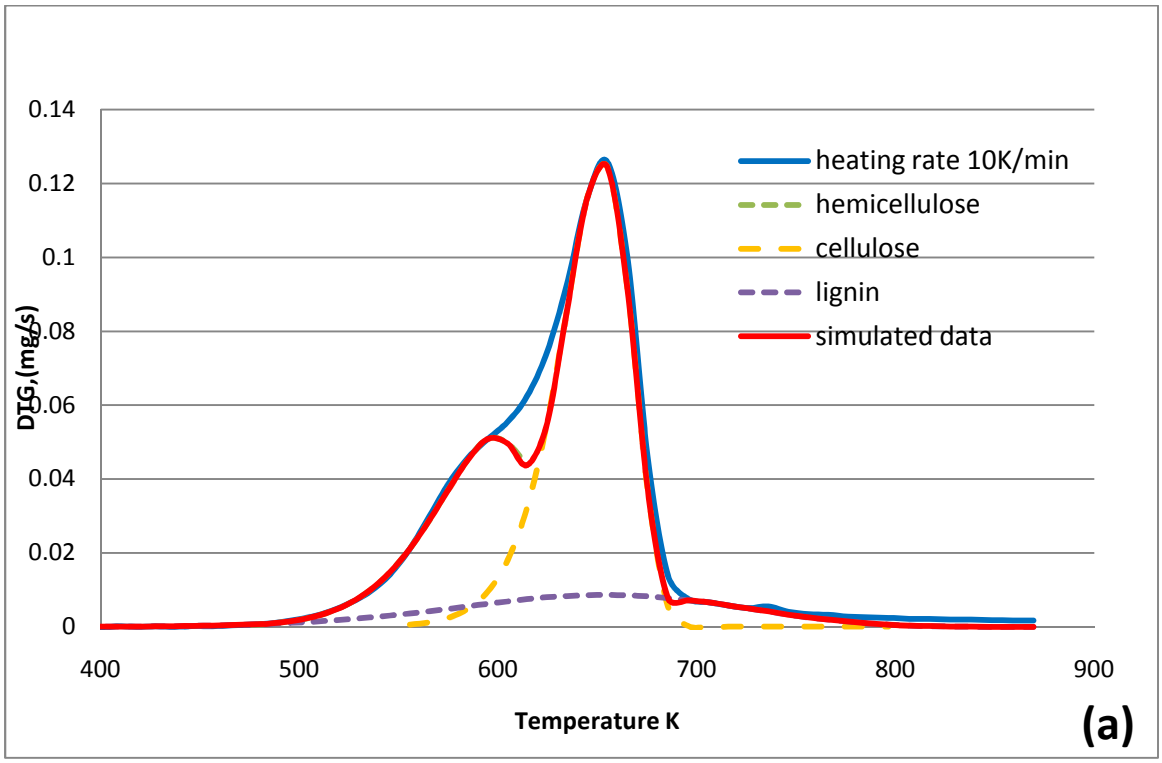

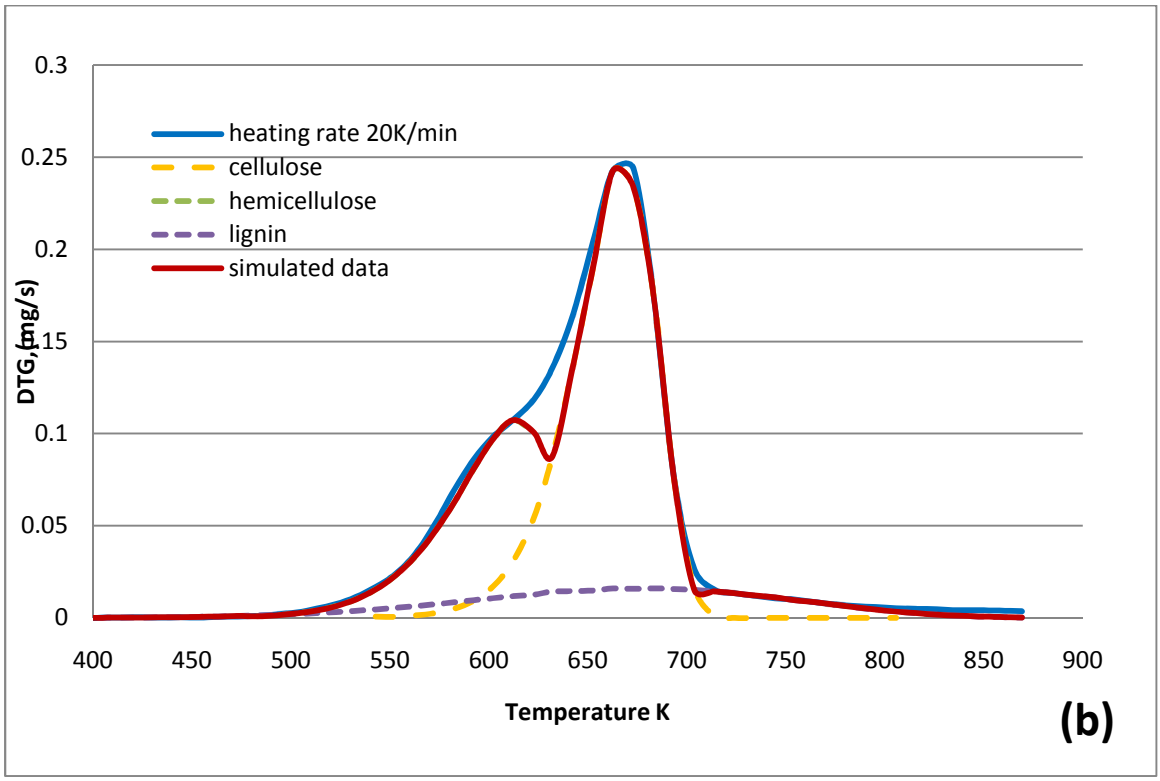

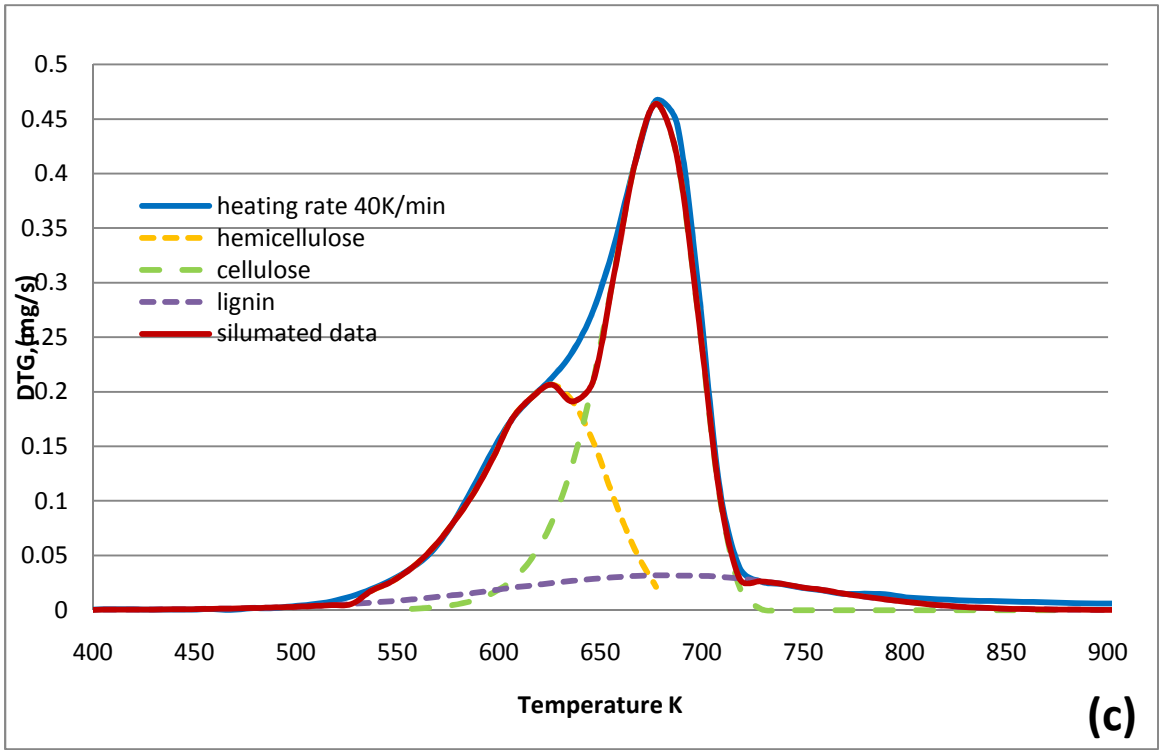

Figure 17: DTG simulation results by three-pseudo-component (n=1) of poplar pyrolysis at different heating rate (a: 10K/min; b: 20K/min; c: 40K/min)

Appendix 8

Three-pseudo-components model (n=1) for untreated stump sample at heating rate 10K/min. 20K/min and 40K/min

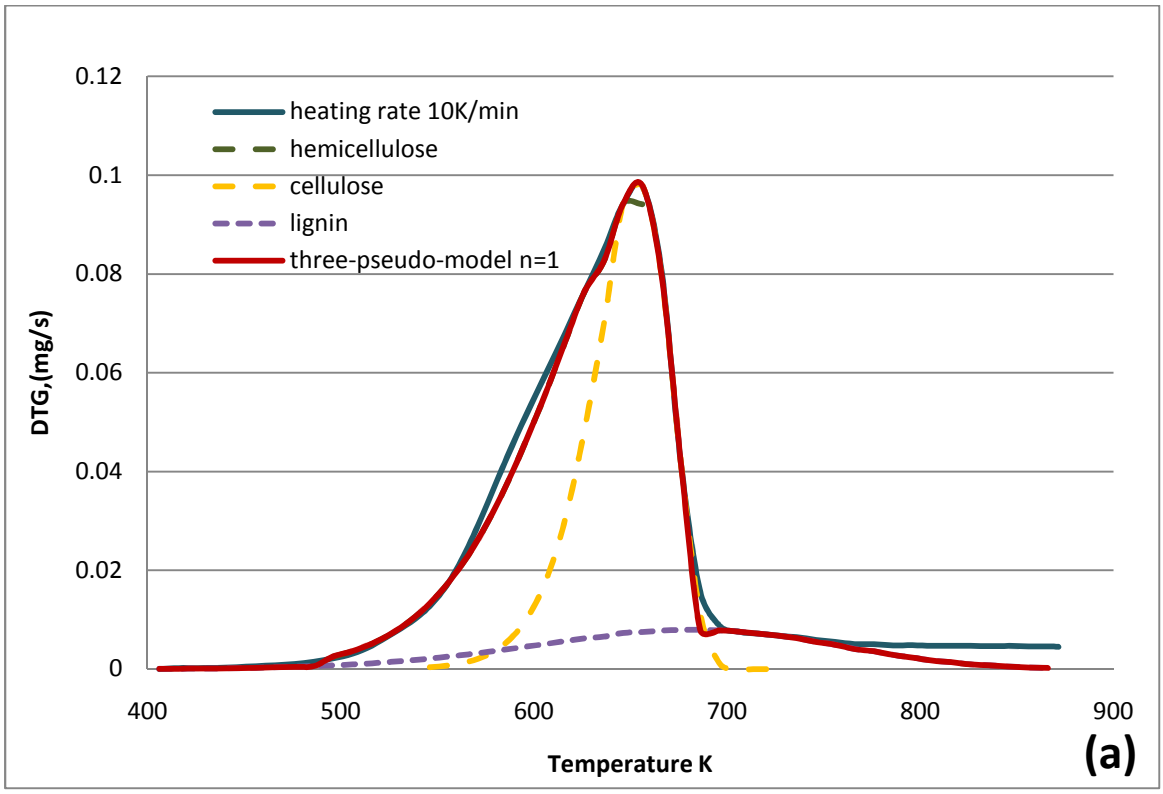

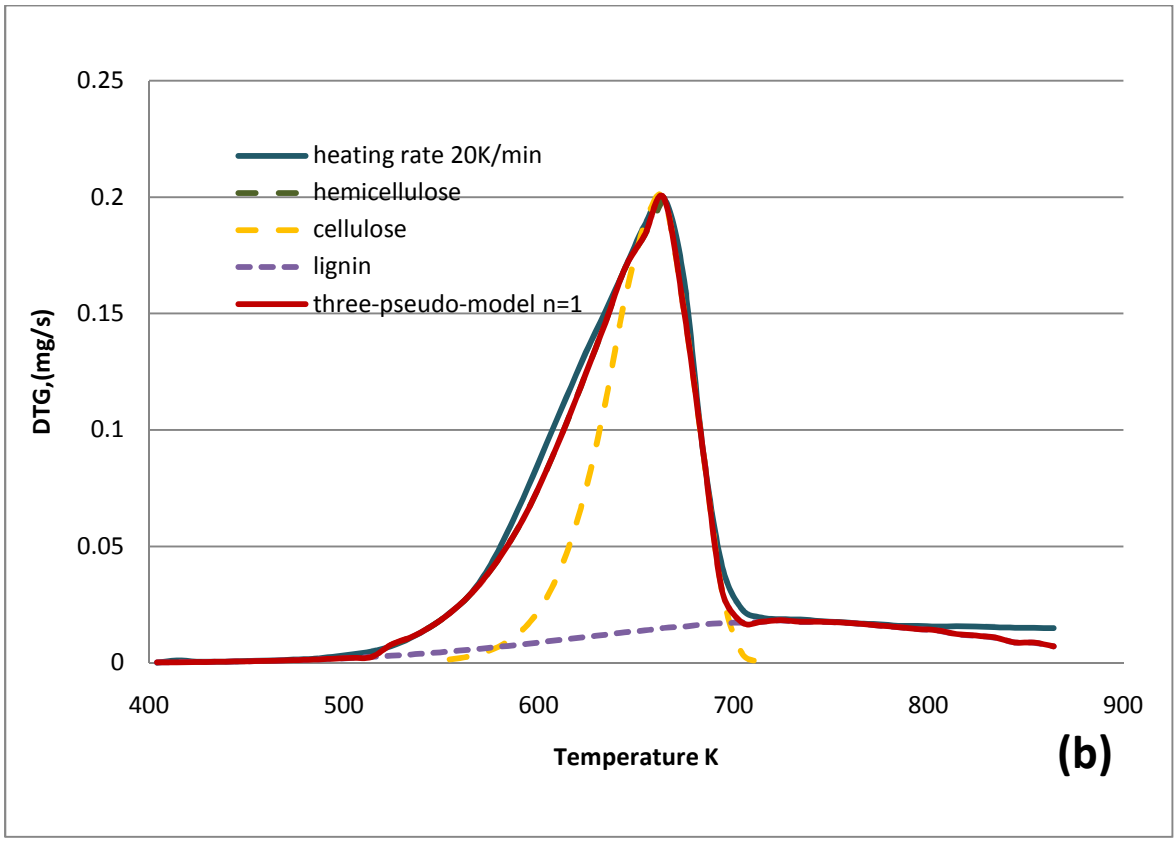

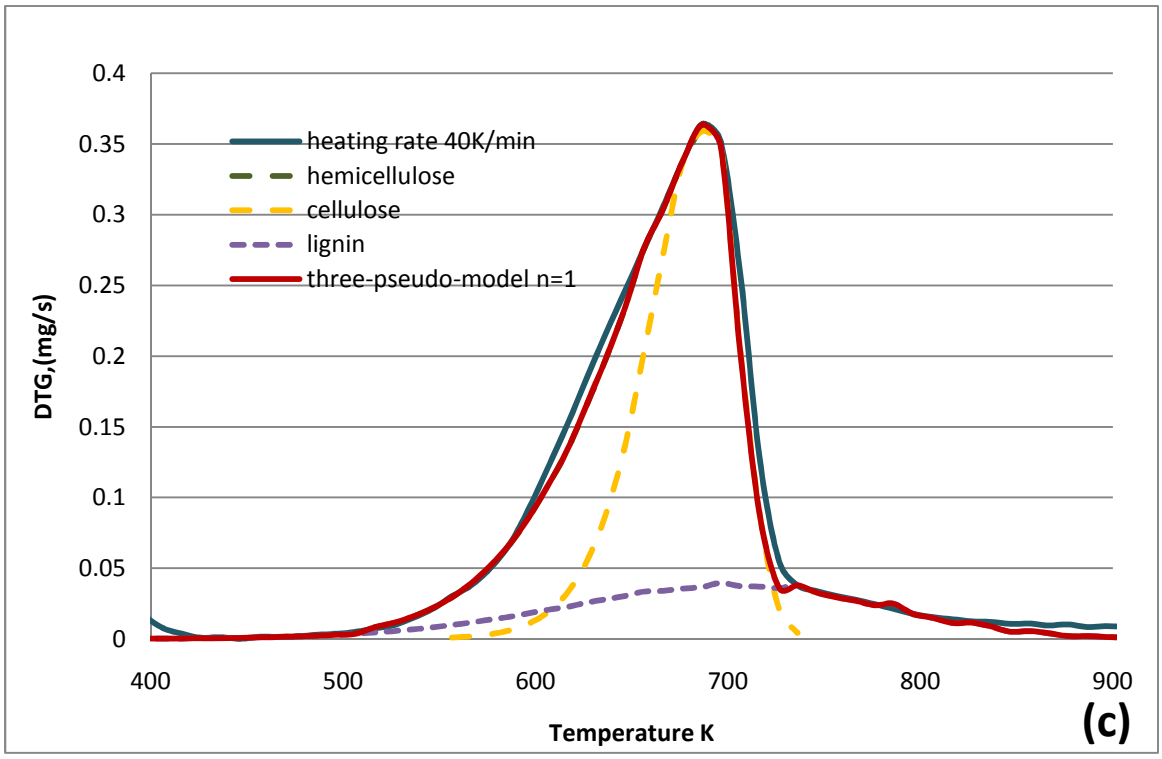

Figure 18: DTG simulation results by three-pseudo-component (n=1) of stump pyrolysis at different heating rate (a: 10K/min; b: 20K/min; c: 40K/min)

Appendix 9

Three-pseudo-components model (n≠1) for untreated poplar sample at heating rate 10K/min. 20K/min and 40K/min

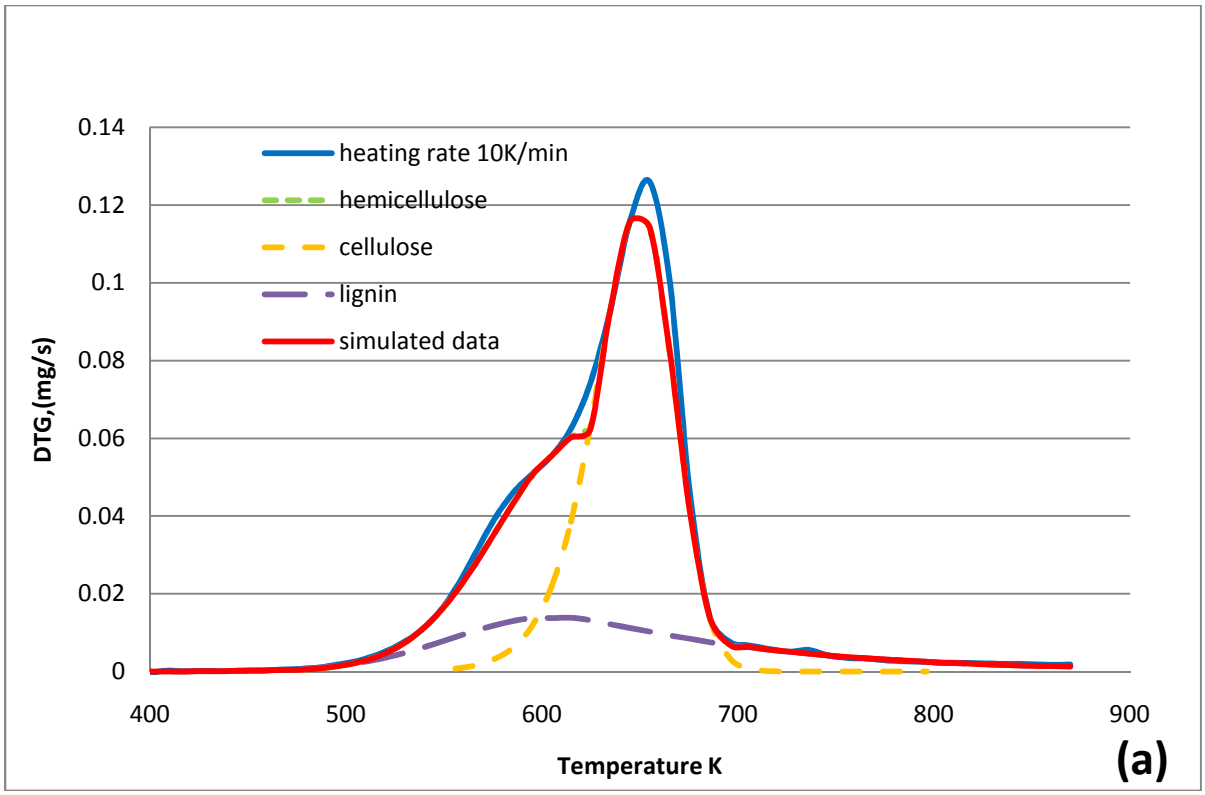

(a)

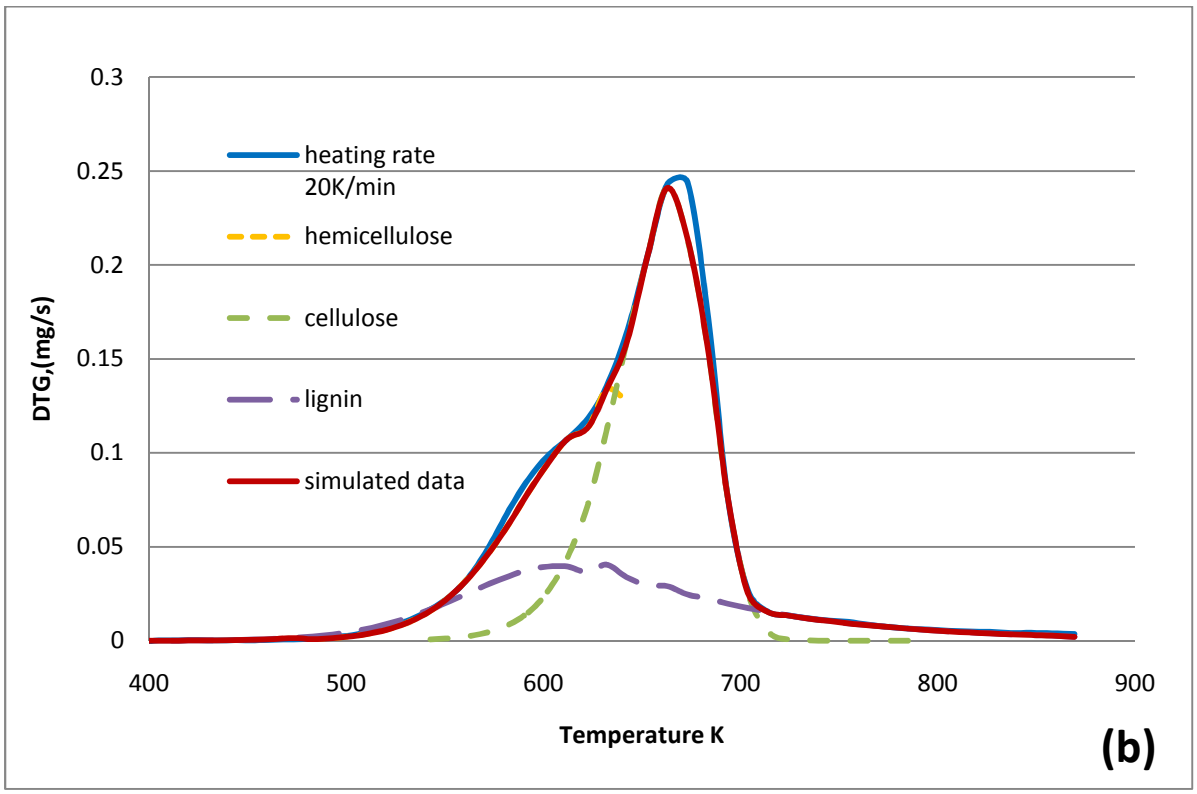

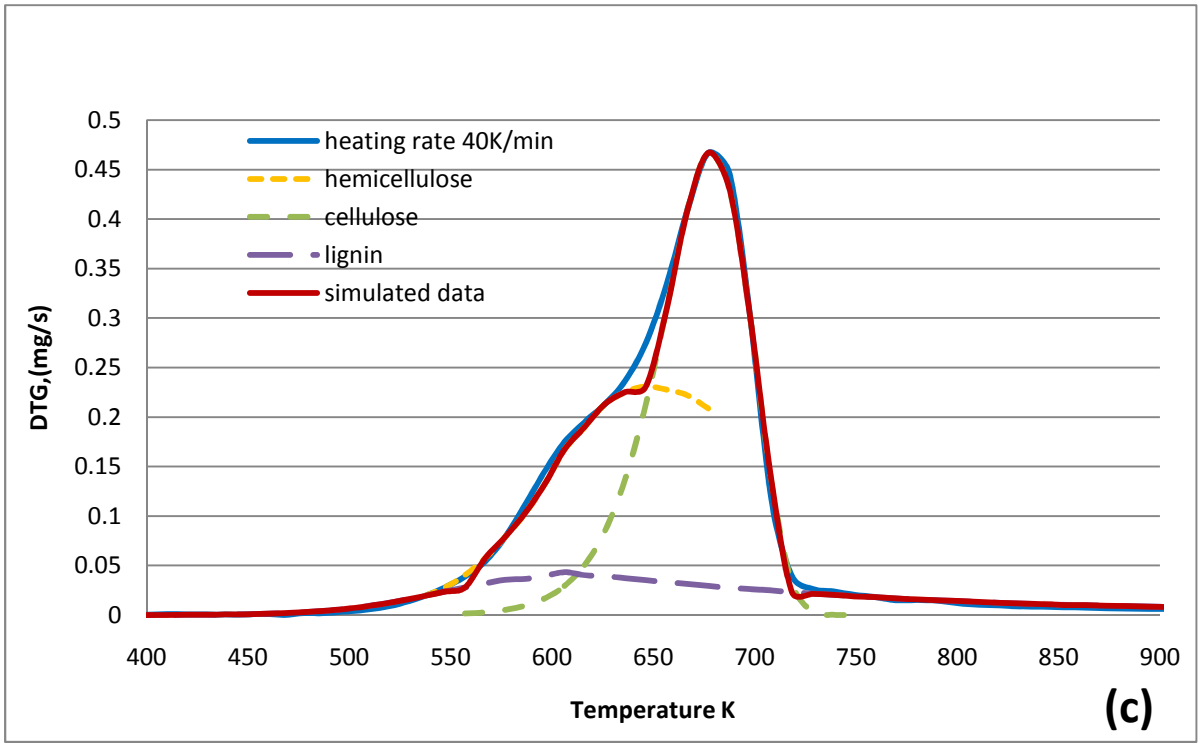

Figure 19: DTG simulation results by three-pseudo-component ($n \neq 1$) of poplar pyrolysis at different heating rate (a: 10K/min; b: 20K/min; c: 40K/min)

Appendix 10

Three-pseudo-components model (n≠1) for untreated stump sample at heating rate 10K/min. 20K/min and 40K/min

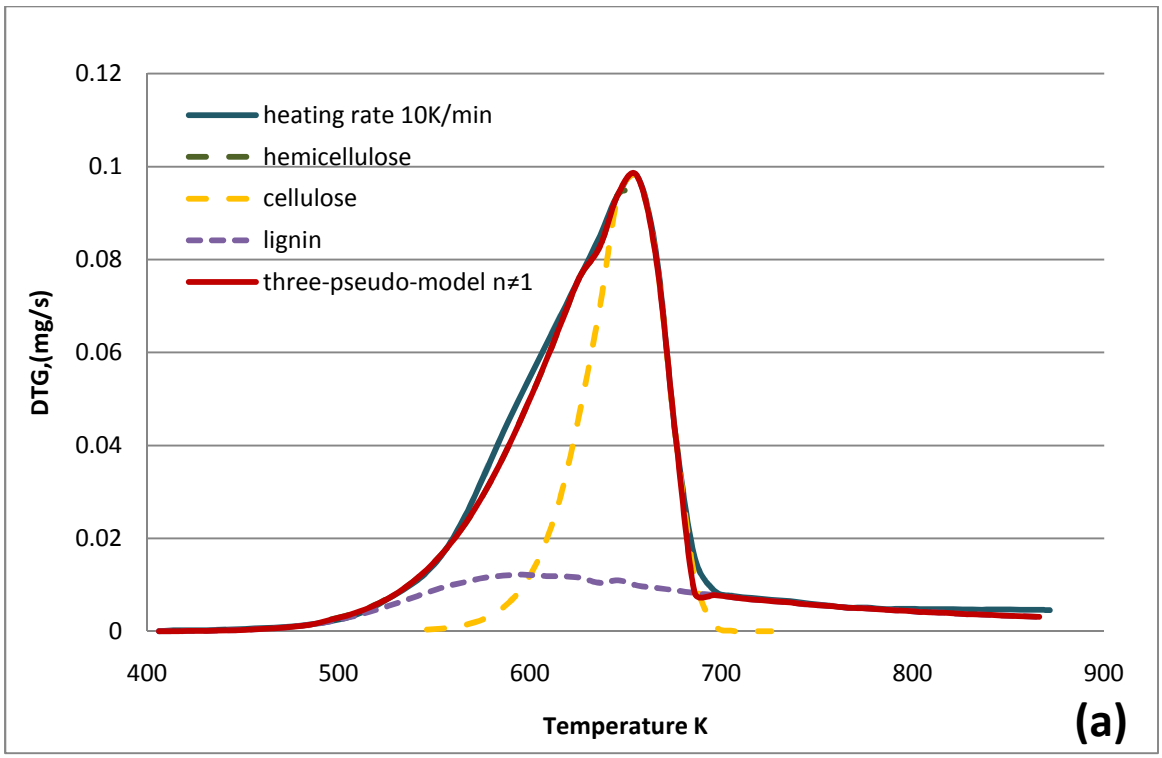

(a)

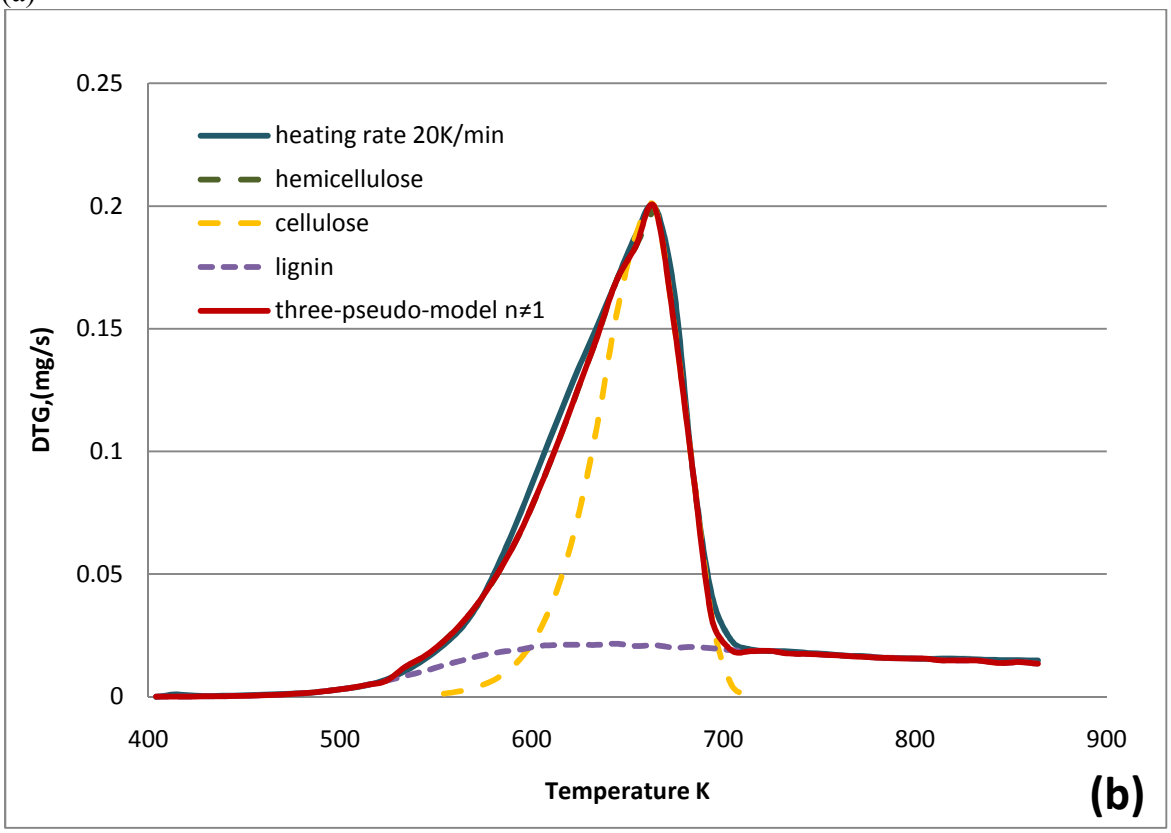

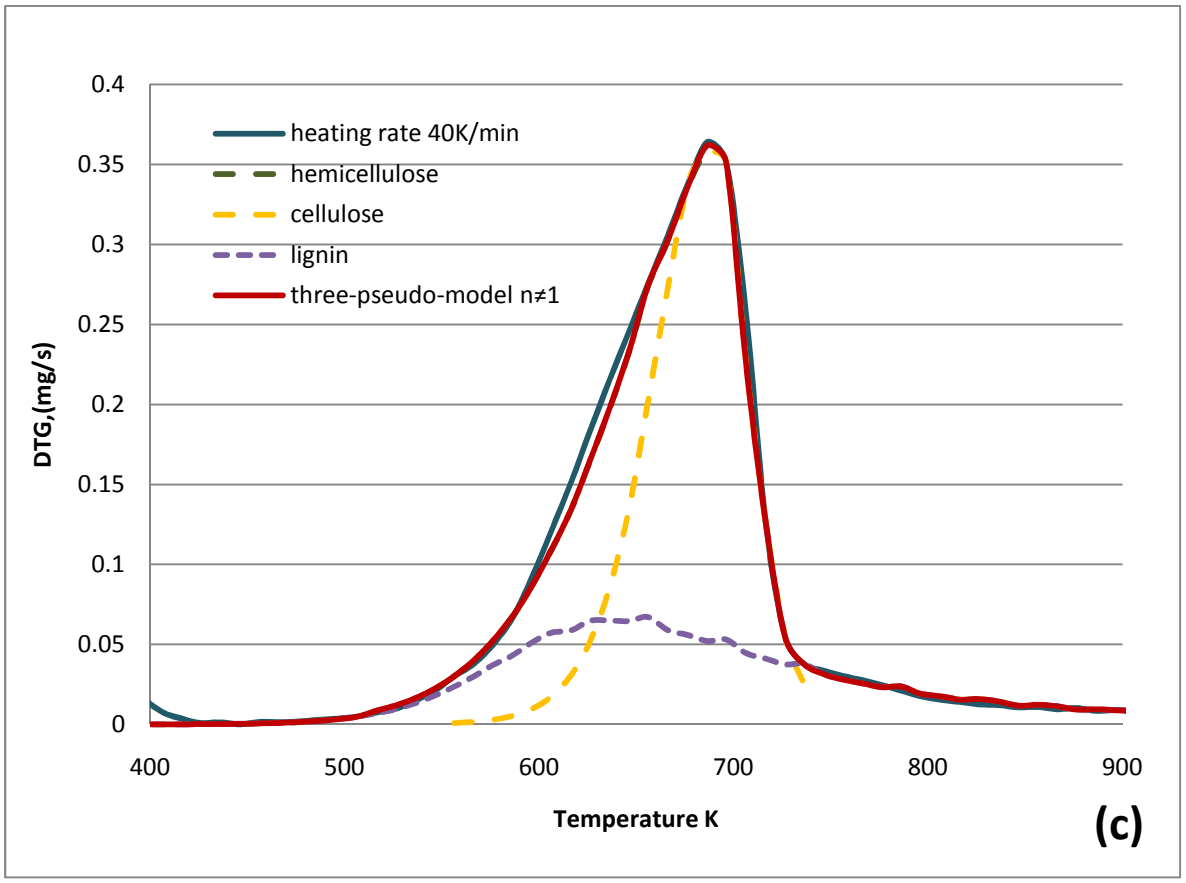

Figure 20: DTG simulation results by three-pseudo-component (n≠1) of stump pyrolysis at different heating rate (a:10K/min; b: 20K/min; c: 40K/min)

Appendix 11

Single reaction one step model for torrefied stump samples at 300°C at heating rate 40K/min

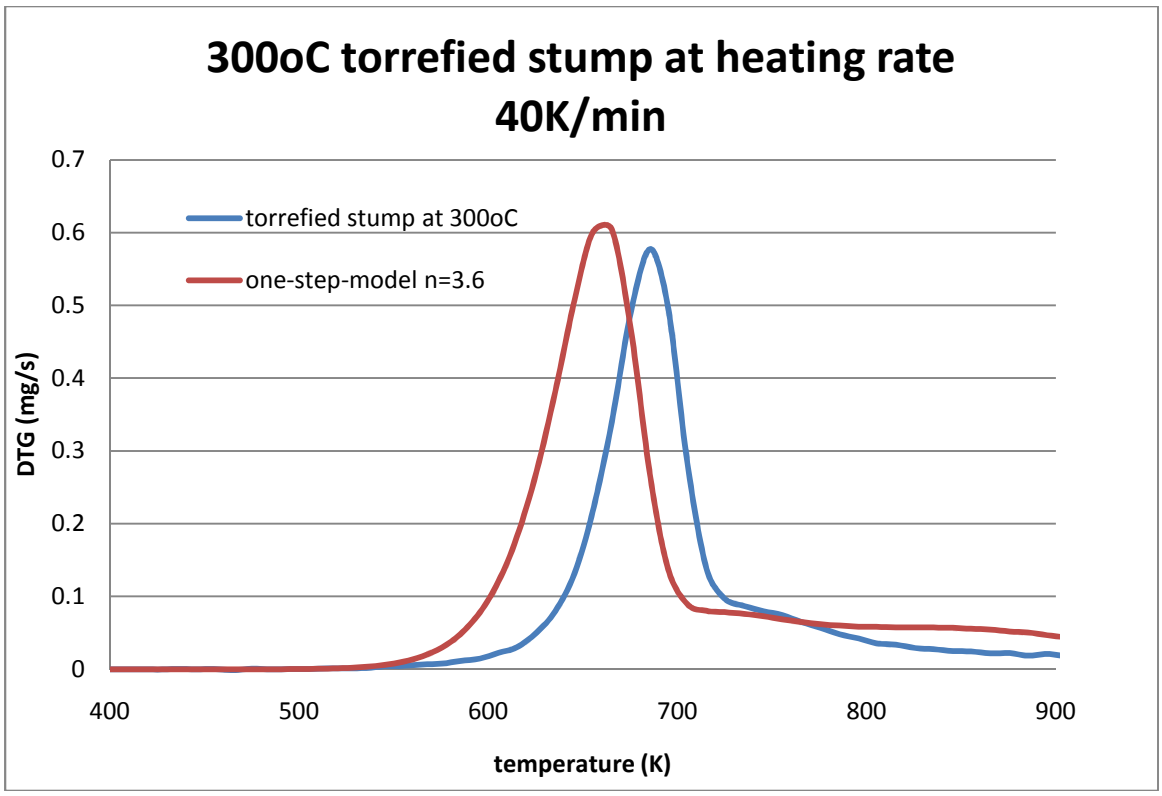

(a)

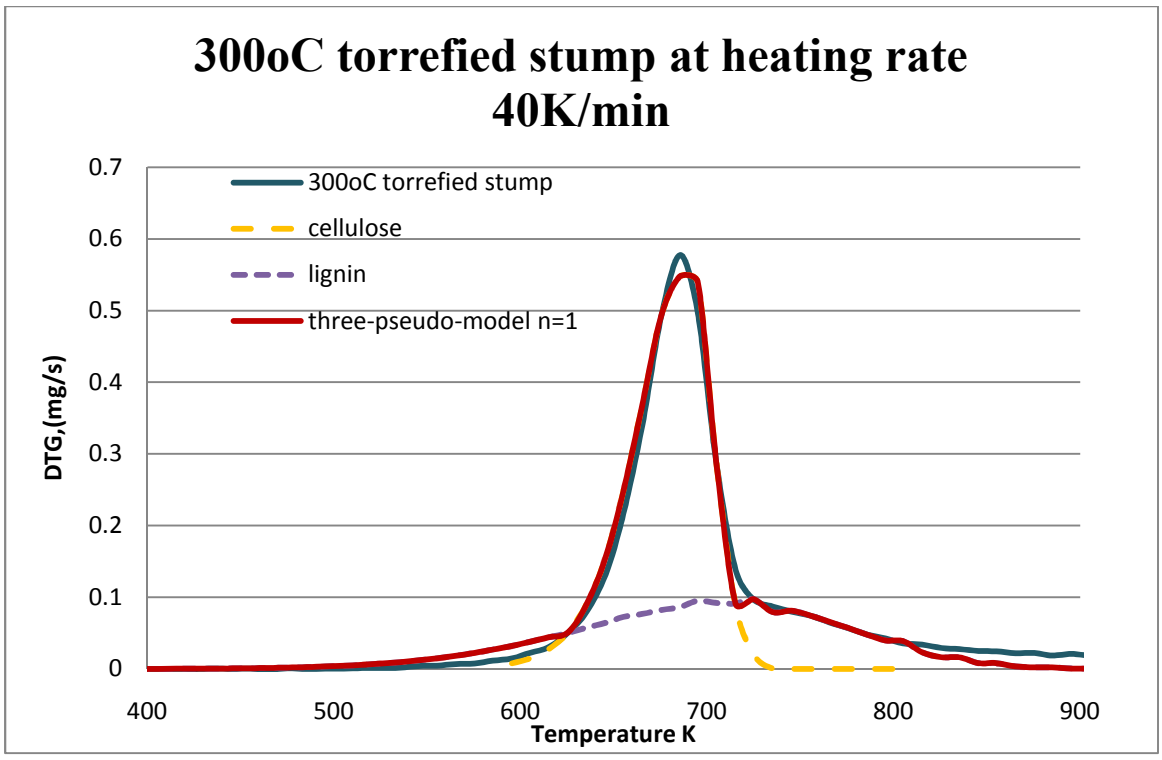

(b)

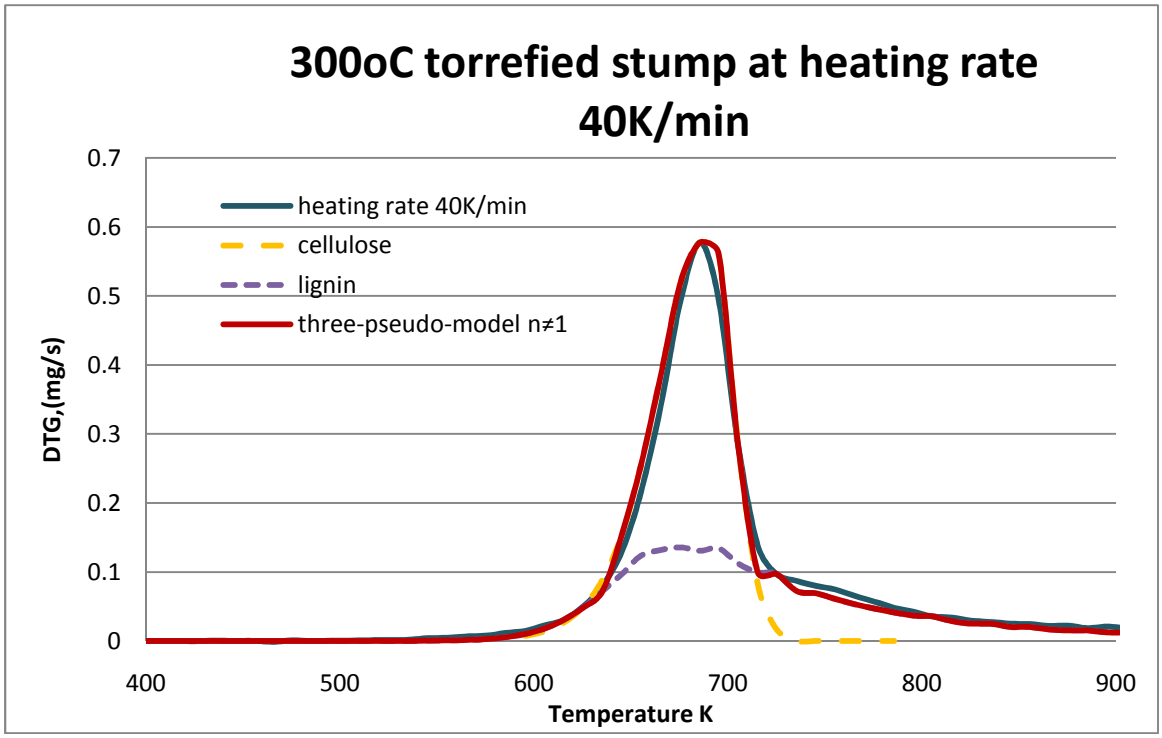

(c)

Figure 21:
(a) DTG simulation results by a one-step model of 300°C torrefied stump pyrolysis at heating rate 40K/min
(b) DTG simulation results by three-pseudo-component (n=1) of 300oC torrefied stump pyrolysis at heating rate 40K/min
(c) DTG simulation results by three-pseudo-component (n≠1) of 300oC torrefied stump pyrolysis at heating rate 40K/min

SLU
Institutionen för energi och teknik
Box 7032
750 07 UPPSALA
Tel. 018-67 10 00
pdf.fil: www.slu.se/energiochteknik

SLU
Department of Energy and Technology
P. O. Box 7032
SE-750 07 UPPSALA
SWEDEN
Phone +46 18 671000